5-fluorouracil chemotherapy-induced cardiotoxicity: studies from clinic to culture

by

Stephen Thomas Hammond

B.S., Wingate University, 2014
M.S., Eastern Michigan University, 2017

AN ABSTRACT OF A DISSERTATION

submitted in partial fulfillment of the requirements for the degree

DOCTOR OF PHILOSOPHY

Department of Kinesiology
College of Health and Human Sciences

KANSAS STATE UNIVERSITY
Manhattan, Kansas

2023

Abstract

5-fluorouracil (5FU) chemotherapy has remained a key component of numerous cancer treatment regimens since its inception in 1957. Despite high treatment efficacy and association with improved survival outcomes, 5-FU treatment can elicit a varying degree of symptomatic and/or asymptomatic cardiotoxicity, occurring in up to 30% of treated patients. Onset of these maladies often prompts deviation from preferred treatment regimens and can negatively influence patient survival outcomes. To date, the mechanisms responsible for 5-FU cardiotoxicity remain poorly understood, with the most prominent theory suggesting a direct effect of the drug on the vascular endothelium/and or smooth muscle. Therefore, the primary aim of the present dissertation was to take a 'clinic to culture' approach to better understanding how 5-FU chemotherapy impacts the cardiovascular system with special emphasis on the vasculature. In chapter 2, we demonstrate reductions in cutaneous microvascular reactivity—presumably via endothelium dependent mechanisms—in patients undergoing treatment for cancer with 5-FU based regimens. Given alterations in endothelial function are a precursor to long-term vascular sequela such as vascular calcification, this led us to hypothesize that 5-FU exposure may predispose aortic smooth muscle cells to the development of calcium deposition in chapter 3. To test this hypothesis, we collected aortic smooth muscle cells from rats treated with a clinically relevant dose of 5-FU or volume matched saline. We found that cells derived from 5-FU treated animals developed a greater degree of calcium deposition when stimulated with a calcification inducing media than cells treated with normal growth media. Interestingly, this finding was not reciprocated in cells derived from saline treated animals. Follow-up experiments in which cells from saline treated animals were cultured with an in vitro dose of 5-FU had higher concentrations of calcium than untreated cells. Findings from this study highlight the need for

more data on the potential long-term vascular consequences of 5-FU chemotherapy. In chapter 4, we sought to test the efficacy of acute exercise as a modality to prevent 5-FU cardiotoxicity. We hypothesized that acute exercise prior to treatment with a clinically based 5-FU infusion would prevent the development of cardiovascular maladaptation in rats. We found that sedentary rats treated with 5-FU presented with an increase in aortic pulse wave velocity—an established marker of aortic stiffness—over the course of the two-hour infusion. Importantly, this finding was not apparent in control groups treated with volume matched saline, or the exercise preconditioned 5-FU group, suggesting potential utility of exercise preconditioning in the prevention of 5-FU-induced vascular changes. Reverse phase protein analysis identified differential expression of several proteins involved in focal adhesion and/or cytoskeletal regulation pathways in aortic lysate from 5-FU treated rats, offering an exciting direction for future investigation into the mechanisms of 5-FU cardiotoxicity. Taken together, the findings presented in this dissertation provide new insight into the effects of 5-FU on the vasculature as well as offer a potential modality to alleviate some of the off-target cardiovascular side effects associated with 5-FU. It is our hope that our group and others can continue to build upon these findings to help ensure patients can continue to receive this efficacious treatment without increased risk to short and/or long-term cardiovascular wellbeing.

5-fluorouracil chemotherapy-induced cardiotoxicity: studies from clinic to culture

by

Stephen Thomas Hammond

B.S., Wingate University, 2014
M.S., Eastern Michigan University, 2017

A DISSERTATION

submitted in partial fulfillment of the requirements for the degree

DOCTOR OF PHILOSOPHY

Department of Kinesiology
College of Health and Human Sciences

KANSAS STATE UNIVERSITY
Manhattan, Kansas

2023

Approved by:

Major Professor
Carl J. Ade

Copyright

Abstract

5-fluorouracil (5FU) chemotherapy has remained a key component of numerous cancer treatment regimens since its inception in 1957. Despite high treatment efficacy and association with improved survival outcomes, 5-FU treatment can elicit a varying degree of symptomatic and/or asymptomatic cardiotoxicity, occurring in up to 30% of treated patients. Onset of these maladies often prompts deviation from preferred treatment regimens and can negatively influence patient survival outcomes. To date, the mechanisms responsible for 5-FU cardiotoxicity remain poorly understood, with the most prominent theory suggesting a direct effect of the drug on the vascular endothelium/and or smooth muscle. Therefore, the primary aim of the present dissertation was to take a 'clinic to culture' approach to better understanding how 5-FU chemotherapy impacts the cardiovascular system with special emphasis on the vasculature. In chapter 2, we demonstrate reductions in cutaneous microvascular reactivity—presumably via endothelium dependent mechanisms—in patients undergoing treatment for cancer with 5-FU based regimens. Given alterations in endothelial function are a precursor to long-term vascular sequela such as vascular calcification, this led us to hypothesize that 5-FU exposure may predispose aortic smooth muscle cells to the development of calcium deposition in chapter 3. To test this hypothesis, we collected aortic smooth muscle cells from rats treated with a clinically relevant dose of 5-FU or volume matched saline. We found that cells derived from 5-FU treated animals developed a greater degree of calcium deposition when stimulated with a calcification inducing media than cells treated with normal growth media. Interestingly, this finding was not reciprocated in cells derived from saline treated animals. Follow-up experiments in which cells from saline treated animals were cultured with an in vitro dose of 5-FU had higher concentrations of calcium than untreated cells. Findings from this study highlight the need for

more data on the potential long-term vascular consequences of 5-FU chemotherapy. In chapter 4, we sought to test the efficacy of acute exercise as a modality to prevent 5-FU cardiotoxicity. We hypothesized that acute exercise prior to treatment with a clinically based 5-FU infusion would prevent the development of cardiovascular maladaptation in rats. We found that sedentary rats treated with 5-FU presented with an increase in aortic pulse wave velocity—an established marker of aortic stiffness—over the course of the two-hour infusion. Importantly, this finding was not apparent in control groups treated with volume matched saline, or the exercise preconditioned 5-FU group, suggesting potential utility of exercise preconditioning in the prevention of 5-FU-induced vascular changes. Reverse phase protein analysis identified differential expression of several proteins involved in focal adhesion and/or cytoskeletal regulation pathways in aortic lysate from 5-FU treated rats, offering an exciting direction for future investigation into the mechanisms of 5-FU cardiotoxicity. Taken together, the findings presented in this dissertation provide new insight into the effects of 5-FU on the vasculature as well as offer a potential modality to alleviate some of the off-target cardiovascular side effects associated with 5-FU. It is our hope that our group and others can continue to build upon these findings to help ensure patients can continue to receive this efficacious treatment without increased risk to short and/or long-term cardiovascular wellbeing.

Table of Contents

List of Figures

List of Tables

Acknowledgements

The acknowledgement section of this dissertation is a story of its own and could quite easily span 10's of pages. For the sake of anyone reading, I'll do my best to keep it short. I was first motivated to attend college for sport, not academics. Thanks to Dr. Dennis Johnson for not only giving me the opportunity to do the former, but also helping me realize my potential in the latter…and beyond. I owe my start in academic research to Dr. Stephen McGregor. It was while working with you that I first realized my passion for this field and for that, I am forever grateful. To my current mentor, Dr. Carl Ade: the passion you have for your work is contagious and I have had more fun these past 4.5 years "working" than I'd ever dreamed possible. Thank you for the opportunity to join (and to Dr. Jacob Caldwell for convincing you to let me) and contribute to your lab. You are building something special, and I am beyond excited to be a part of it. To Dr. Brad Behnke: Thank you for your expertise, time, and allowing me to work with your group on numerous projects over the years. Without your guidance and support, much of the work completed throughout my time at KSU would not have been possible. To my doctoral committee, thank you for your patience and wisdom throughout my doctoral experience.

To all of my colleagues and fellow graduate students in the KSU Kinesiology Department: thank you for making Kansas a place I can call home. So much of the joy I gain from doing science is from getting to do it alongside people like you. Specific to my Ade lab mates, please, leave some food out for the Lafene ghosts… To my family: Parents, Tom and Gigi, and siblings, Rachel and Jason: I am in continuous awe of your work ethic, love, and unwavering support. You have, and always will be, a source of constant motivation. To Olivia: Thank you for making sure I stay alive…and of course, everything else.

Lastly, thank you to the Stormont Vail Cotton O'Neil Cancer Center, the Johnson Cancer Research Center, The American College of Sports Medicine, and the Kansas Academy of Sciences for assisting with or funding this research.

Dedication

The present work is dedicated to all those battling or who have battled cancer. A special thanks goes out to those who have taken time out of their day to participate in our research.

Preface

Chapter 1 is a brief background of the work covered in this dissertation. Chapter 2 is a completed study, in preparation for submission for publication in a peer reviewed journal. Chapter 3 is a near completed study that is in the final stages of data collection. Chapter 4 is an original research study which is in the final stages of data analysis and preparation for publication in a peer reviewed journal. Chapter 5 consists of a brief conclusion of the findings presented herein.

Chapter 1 - Background

"Cancer thus exploits the fundamental logic of evolution unlike any other illness. If we, as a species, are the ultimate product of Darwinian selection, then so, too, is this incredible disease that lurks inside us."
Siddhartha Mukherjee, *The Emperor of All Maladies*

Despite several facets of modern society having contributed to cancer's rise amongst the leading causes of death worldwide [1], cancer is far from a disease for which we can be credited. The earliest known evidence of hominin cancer—dated 1.7 million years old—was unearthed in South Africa in 2013 [2]; yet evidence of malignancy dates back at least 240 million years to the prehistoric remains of stem turtles [3] suggesting that cancer has been a formidable foe far prior to modern times. The first written description of cancer is widely believed to stem from the early Egyptian medical text known as the Edwin Smith Papyrus (~3000 - 1500 BC) [4,5] where the ailment described as *bulging tumors of the breast* (Case 45) includes the unsettling statement '*there is nothing'* in the text position reserved for the prescribed treatment [6].

Thankfully, there have since been numerous advancements in our understanding of the disease, and how to effectively treat it. Specific to the present work, the rise of chemotherapy is frequently credited to the studies of German biochemist Paul Ehrlich who had begun experimenting with the use of different chemical substances to treat various diseases (e.g., syphilis) near the turn of the 20th century [7]. However, despite some early experiments citing the efficacy of chemical agents in the treatment of malignancies [8], it would take a fatal accident during the second World War for the idea of chemical modulation of cancer to truly take hold. In reviewing the medical records of victims dying of unexplained causes following the Luftwaffe air raid of Bari, Italy on December 2, 1943, Colonel Stewart Alexander—an expert in chemical

warfare—attributed the plummeting white blood cell counts of the victims to mustard gas exposure which was ultimately found to have leaked from a damaged American warship (this story is detailed in Jennet Conant's 2020 book *The Great Secret* [9]). Given the drastic effect the mustard poisoning had on white blood cells and lymph nodes, this seemingly unrelated event prompted investigations with similar mustard agents on patients with lymphoma and leukemia, which were first detailed by Goodman and colleagues in 1946 [10]. Investigation into other compounds closely followed. Notably, in 1948, Sydney Farber reported temporary remissions in children with leukemia treated with the antifolate drug aminopterin but stressed the toxic effects many of the treatments had on the patients [11]. However, it was not until 1956, with use of methotrexate, in which a chemotherapeutic agent was for the first time evidenced to cure a patient of cancer [12].

Though the use and understanding of chemotherapy has greatly improved since the pioneering works of the 1940's, a problem faced by many of these early physician-scientists is one that still persists today: *How does one effectively treat cancer while sparing healthy tissues?* This question largely encompasses the motivation of the present dissertation. Of particular focus for the remainder of this work is the pyrimidine antimetabolite chemotherapy 5-fluorouracil (5-FU) and the consequences its use in treatment may have on the cardiovascular system (i.e., cardiotoxicity). In 1957, Charles Heidelberger and colleagues first synthesized 5-FU following observations that uracil may be used preferentially for the biosynthesis of nucleic acids in tumors [13,14]. 5-FU is an analog of uracil, differing only by substitution of a fluorine for the hydrogen in the C-5 position [13,15]. As such, 5-FU enters the cell via the same facilitated transport process as uracil before ultimately being metabolized into one of three main active metabolites: fluorodeoxyuridine monophosphate (FdUMP), fluorodeoxyuridine triphosphate (FdUTP), and

fluorouridine triphosphate (FUTP) [15]. These metabolites embark down several pathways resulting in inhibition of the essential enzyme thymidylate synthase and ultimately damage to DNA and RNA [15]. Early clinical trials suggested favorable results in the use of 5-FU for several cancers including breast, head/neck, and rectal malignancies despite the occurrence of some off-target side effects [16–18]. These exciting findings were soon supported by others [19], ultimately leading to the regular use of 5-FU in the treatment of many of today's most commonly diagnosed cancers—namely, gastrointestinal, breast, and head/neck malignancies [20–23].

As documented throughout the early chemotherapeutic trials of Farber, Goodman, and Heidelberger, a major concern of all chemotherapeutic agents is potentiating the antitumor effects of the drug while minimizing harm to healthy tissue. The realization that many survivors of cancer were developing new-onset cardiovascular disease in the years following treatment resulted in the development of the field of cardio-oncology [24]—a specialty concerned with the detection, treatment, and prevention of cardiovascular maladaptation in individuals undergoing cancer therapy. Reports specific to 5-FU cardiotoxicity have been available in the literature since at least 1969 [25], and are believed to encompass the second highest incidence of cardiotoxicities induced by chemotherapeutic agents [26]. The most commonly reported symptomatic cardiotoxicity associated with 5-FU is angina with or without electrocardiographic signs of myocardial ischemia [27–32]. Other acknowledged side effects include arrythmias [30,33–35], myocarditis [36,37], bradycardia/tachycardia [31,38], blood pressure deviations [31,32,38], and in rare instances, myocardial infarction [29,35], cardiac arrest [35,38], and sudden death [31,39]. While several investigations have reported such adverse events, the documented incidence rates vary considerably—with reports ranging from 1 to 30% [27,29–31,33,35,40–44] depending on sample population, drug combination/delivery method, and the diagnostic criteria used [26,45]. A 2013

systematic review by Polk and colleagues suggests a 5-FU cardiotoxicity incidence rate of between 1.2 and 4.3% in studies including greater than 400 participants [28]. These data align with the more recent retrospective analysis by Zafar et al., which identified the occurrence of coronary vasospasm in 2.16% of a cohort of 4,019 5-FU treated patients over a 10-year period [43]. All considered, recent letters and editorials posit a likely under-diagnosis/reporting of 5-FU cardiotoxicity [45,46], emphasizing the rise in incidence when asymptomatic ECG alterations are reported. This notion is supported by the findings of others who have demonstrated asymptomatic ECG deviations indicative of "silent" myocardial ischemia in 14 - 68% of patients following 5-FU infusion [35,39]. This discordance of 5-FU cardiotoxicity reporting implies the need for more prospective work encompassing the detection of both symptomatic and asymptomatic side effects over the course of treatment.

The mechanisms responsible for 5-FU mediated cardiotoxicity remain poorly understood. Several theories have surfaced [26,47], the most prominent being the development of coronary spasm secondary to endothelial and/or smooth muscle dysfunction. However, given the invasive nature involved in investigation of the coronary circulation, the majority of support for this notion is derived from single patient case reports, experiments in the peripheral circulation, and pre-clinical animal or cell culture models. Luwaert and colleagues presented the first clinical evidence of 5-FU-induced coronary spasm in a 70-year-old male with palate squamous carcinoma in 1991 [48]. Since, few other examples of epicardial spasm have been demonstrated angiographically [49,50], leading some to postulate a role for microvascular spasm as a contributor to the 5-FU-induced side effects [26]. However, there are currently no data regarding microvascular function following 5-FU treatment. Others have demonstrated vasoconstriction—as opposed to the typical vasodilation—in response to a brachial flow mediated dilation protocol following

completion of a 5-FU infusion [51]. This finding is supported by the vasoconstrictor responses observed in rabbit and rat aortic rings following ex vivo exposure to 5-FU [52,53], suggesting a direct effect of the drug on the modulation of vascular tone. Further mechanistic insight from preclinical works is provided in analysis of tissues following in vivo treatment of 5-FU, or vascular cells following in vitro exposure of the drug, which suggest a role for the endothelium [54–59] in the onset of 5-FU cardiotoxicity. Specifically, 5-FU has been reported to alter the expression and phosphorylation of the key vasodilator protein endothelial nitric oxide synthase [54,60], induce endothelial cell apoptosis and senescence [54,55], and increase the production of reactive oxygen species [55]. Likewise, two cell culture studies in smooth muscle cells have demonstrated apoptosis [61,62], alterations in cytoskeletal structure [61] and the induction of reactive oxygen species [62] in response to 5-FU or 5-FU containing treatments. These cellular modifications at the level of the endothelium and smooth muscle not only have the potential to induce the acute side effects frequently reported to occur in patients during treatment, but also set the stage for long-term vascular maladaptation such as the development of aortic stiffness and vascular calcification in the years following treatment.

While more work is still needed to understand the mechanisms driving the onset of 5-FU cardiotoxicity, there is also a paucity of data regarding modalities to prevent and alleviate its occurrence. Attempted pharmacological alleviation of symptoms upon the appearance of cardiotoxic side effects has yielded mixed findings, with reports of varying success in the use of nitrates or calcium channel blockers in the alleviation of 5-FU induced symptoms [51,63–65]. In a recent retrospective analysis, patients receiving treatment with nitrates, calcium channel blockers, or a combination of the two therapies following the onset of 5-FU induced vasospasm had a reduced recurrence of events following 5-FU rechallenge compared to those continuing

treatment without prophylaxis [63]. However, the sample of patients continuing 5-FU treatment without prophylactic intervention was extremely small (n=3) and more data are needed before definitive conclusions can be made. Regardless, the fact that 5-FU rechallenge following symptom onset can result in recurrent cardiotoxicity in up to 90% of retreated patients (without prophylaxis) [66], coupled with recent findings that discontinuation of 5-FU treatment following the onset of cardiotoxicity is associated with a reduced overall median survival compared to those who continue treatment (18.3 months vs 47 months) [63], indicates a critical need for the establishment of modalities which can prevent or alleviate the onset of 5-FU cardiotoxicity. Preclinical studies testing the efficacy of exercise preconditioning as a method of preventing cardiotoxicity induced by other chemotherapies (e.g., anthracyclines) [67–71] have yielded promising findings, however such experiments have yet to be conducted for 5-FU. Thus, such investigations seemingly provide an exciting direction for future work.

In the present dissertation, we sought to take a 'clinic to culture' approach of better understanding how 5-FU chemotherapy impacts the cardiovascular system with special emphasis on the vasculature. Specifically, we first discuss findings from our studies in human subjects where we investigate cutaneous microvascular function in patients undergoing cancer treatment with 5-FU-based chemotherapy regimens (Chapter 2). The two chapters that follow discuss results from our work in preclinical cell culture and animal models using a clinically relevant 5-FU dosing regimen based on what patients receive in the clinical setting. In chapter 3, we aim to understand if in vivo and in vitro 5-FU treatment are associated with the calcification of aortic smooth muscle cells. Chapter 4 details our experiments in a rodent model where we test the efficacy of an acute exercise regimen in preventing cardiovascular alterations incurred over the course of a two-hour continuous infusion of 5-FU. It is our hope that the findings outlined in this

dissertation will help shed light on some of the key vascular consequences of 5-FU chemotherapy as well as a potential modality to alleviate their occurrence.

References

1. Sung, H. *et al.* Global Cancer Statistics 2020: GLOBOCAN Estimates of Incidence and Mortality Worldwide for 36 Cancers in 185 Countries. *CA Cancer J Clin* **71**, 209–249 (2021).
2. Odes, E. J. *et al.* Earliest hominin cancer: 1.7-million-year-old osteosarcoma from Swartkrans Cave, South Africa. *S Afr J Sci* **112**, 5–5 (2016).
3. Haridy, Y. *et al.* Triassic Cancer—Osteosarcoma in a 240-Million-Year-Old Stem-Turtle. *JAMA Oncol* **5**, 425–426 (2019).
4. Hajdu, S. I. A note from history: Landmarks in history of cancer, part 1. *Cancer* **117**, 1097–1102 (2011).
5. Faguet, G. B. A brief history of cancer: Age-old milestones underlying our current knowledge database. *Int J Cancer* **136**, 2022–2036 (2015).
6. *The Edwin Smith surgical papyrus: published in facsimile and hieroglyphic transliteration with translation and commentary in two volumes, by James Henry Breasted*. (The University of Chicago Press, 1930).
7. DeVita, V. T. & Chu, E. A History of Cancer Chemotherapy. *Cancer Res* **68**, 8643–8653 (2008).
8. Frank Adair, B. E., Bagg, H. J. & New York, O. Experimental and clinical studies on the treatment of cancer by dichlorethylsulphide (mustard gas). *Ann Surg* **93**, 190 (1931).
9. Conant, J. *The Great Secret: The Classified World War II Disaster that Launched the War on Cancer*. (W.W. Norton & Company, 2020).
10. Goodman, L. S. *et al.* Nitrogen Mustard Therapy: Use of Methyl-Bis(Beta-Chloroethyl)amine Hydrochloride and Tris(Beta-Chloroethyl)amine Hydrochloride for Hodgkin's Disease, Lymphosarcoma, Leukemia and Certain Allied and Miscellaneous Disorders. *J Am Med Assoc* **132**, 126–132 (1946).
11. Farber, S., Diamond, L. K., Mercer, R. D., Sylvester, R. F. Jr. & Wolff, J. A. Temporary Remissions in Acute Leukemia in Children Produced by Folic Acid Antagonist, 4-Aminopteroyl-Glutamic Acid (Aminopterin). **238**, 787–793 (1948).
12. Li, M. C., Hertz, R. & Spencer, D. B. Effect of methotrexate therapy upon choriocarcinoma and chorioadenoma. *Proc Soc Exp Biol Med* **93**, 361–366 (1956).

13. Duschinsky, R., Pleven, E. & Heidelberger, C. The synthesis of 5-Fluoropyrimidines. *J Am Chem Soc* (1957).
14. Heidelberger, C. *et al.* Fluorinated pyrimidines, a new class of tumour-inhibitory compounds. *Nature* **179**, 663–666 (1957).
15. Longley, D. B., Harkin, D. P. & Johnston, P. G. 5-Fluorouracil: Mechanisms of action and clinical strategies. *Nature Reviews Cancer* vol. 3 330–338 (2003).
16. Curreri, A., Ansfield, F., McIver, F., Waisman, H. & Heidelberger, C. Clinical studies with 5-fluorouracil. *Cancer Res.* **18**, 478–484 (1958).
17. Ansfield, F. J. & Curreri, A. R. Further Clinical Studies With 5-Fluorouracil. *JNCI: Journal of the National Cancer Institute* **22**, 497–507 (1959).
18. Ansfield, F. J., Schroeder, J. M. & Curreri, A. R. Five Years Clinical Experience with 5-Fluorouracil. *JAMA* **181**, 295–299 (1962).
19. Schneiderman, M. A. The clinical excursion into 5-fluorouracil. *J Chronic Dis* **15**, 283–295 (1962).
20. Sargent, D. *et al.* Evidence for Cure by Adjuvant Therapy in Colon Cancer: Observations Based on Individual Patient Data From 20,898 Patients on 18 Randomized Trials. *Journal of Clinical Oncology* **27**, 872 (2009).
21. Hortobagyi, G. N. Developments in chemotherapy of breast cancer. *Cancer* **88**, 3073–3079 (2000).
22. Forastiere, A. A. Chemotherapy in the treatment of locally advanced head and neck cancer. *J Surg Oncol* **97**, 701–707 (2008).
23. Gustavsson, B. *et al.* A review of the evolution of systemic chemotherapy in the management of colorectal cancer. *Clin Colorectal Cancer* **14**, 1–10 (2015).
24. Cardinale, D., Biasillo, G. & Cipolla, C. M. Curing Cancer, Saving the Heart: A Challenge That Cardioncology Should Not Miss. *Curr Cardiol Rep* **18**, 1–10 (2016).
25. Gaveau, T., Banzet, P., Marneffe, H. & Viars, P. Cardiovascular disorders in the course of antimitotic infusions at high doses. 30 clinical cases. *Anesth Analg* **26**, 311–27 (1969).
26. Sara, J. D. *et al.* 5-fluorouracil and cardiotoxicity: a review. *Ther Adv Med Oncol* **10**, 1–18 (2018).
27. Dyhl-Polk, A. *et al.* Incidence and risk markers of 5-fluorouracil and capecitabine cardiotoxicity in patients with colorectal cancer. *Acta Oncol (Madr)* **59**, 475–483 (2020).

28. Polk, A., Vaage-Nilsen, M., Vistisen, K. & Nielsen, D. L. Cardiotoxicity in cancer patients treated with 5-fluorouracil or capecitabine: A systematic review of incidence, manifestations and predisposing factors. *Cancer Treat Rev* **39**, 974–984 (2013).
29. Labianca, R., Beretta, G., Clerici, M., Fraschini, P. & Luporini, G. Cardiac toxicity of 5-fluorouracil: A study on 1083 patients. *Tumori* **68**, 505–510 (1982).
30. Eskilsson, J., Albertsson, M. & Mercke, C. Adverse cardiac effects during induction chemotherapy treatment with cis-platin and 5-fluorouracil. *Radiotherapy and Oncology* **13**, 41–46 (1988).
31. Meyer, C. C., Calis, K. A., Burke, L. B., Walawander, C. A. & Grasela, T. H. Symptomatic cardiotoxicity associated with 5-fluorouracil. *Pharmacotherapy* **17**, 729–736 (1997).
32. de Forni, M. de *et al.* Cardiotoxicity of high-dose continuous infusion fluorouracil: a prospective clinical study. **10**, 1795–1801 (2016).
33. Jin, X., Bai, Y., Gao, · Lan & Wu, · Shikai. Incidence of and risk factors for cardiotoxicity after fluorouracil-based chemotherapy in locally advanced or metastatic gastric cancer patients. *Cancer Chemother Pharmacol* **84**, 599–607 (2019).
34. Chen, G. *et al.* Cardiotoxicity in Chinese cancer patients treated with 5-fluorouracil or capecitabine: A multicenter prospective observational study. **35**, 553–553 (2017).
35. Dyhl-Polk, A. *et al.* Myocardial Ischemia Induced by 5-Fluorouracil: A Prospective Electrocardiographic and Cardiac Biomarker Study. *Oncologist* **9999**, (2020).
36. Sasson, Z. *et al.* 5-Fluorouracil related toxic myocarditis: case reports and pathological confirmation. *Can J Cardiol* **10**, 861–864 (1994).
37. Çalik, A. N., Çeliker, E., Velibey, Y., Çağdaş, M. & Güzelburç, Ö. Initial dose effect of 5-fluorouracil: Rapidly improving severe, acute toxic myopericarditis. *American Journal of Emergency Medicine* **30**, 257.e1-257.e3 (2012).
38. Khan, M. A. *et al.* A retrospective study of cardiotoxicities induced by 5-Fluouracil (5-FU) and 5-FU based chemotherapy regimens in Pakistani adult cancer patients at Shaukat Khanum Memorial Cancer Hospital & Research Center. *J Pak Med Assoc* **62**, (2012).
39. Rezkalla, S. *et al.* Continuous ambulatory ECG monitoring during fluorouracil therapy: A prospective study. *Journal of Clinical Oncology* **7**, 509–514 (1989).

40. Wacker, A., Lersch, C., Scherpinski, U., Reindl, L. & Seyfarth, M. High incidence of angina pectoris in patients treated with 5-fluorouracil: A planned surveillance study with 102 patients. *Oncology* **65**, 108–112 (2003).
41. Tsibiribi, P. *et al.* Cardiotoxicity of 5-fluorouracil in 1350 patients with no prior history of heart disease. *Bull Cancer* **93**, E27-30 (2006).
42. Lestuzzi, C. *et al.* Effort myocardial ischemia during chemotherapy with 5-fluorouracil: an underestimated risk. *Annals of Oncology* **25**, 1059–1064 (2014).
43. Zafar, A. *et al.* The Incidence, Risk Factors, and Outcomes With 5-Fluorouracil–Associated Coronary Vasospasm. *JACC CardioOncol* **3**, 101–109 (2021).
44. Peng, J. *et al.* Cardiotoxicity of 5-fluorouracil and capecitabine in Chinese patients: a prospective study. *Cancer Commun (Lond)* **38**, 22–22 (2018).
45. Lestuzzi, C. *et al.* Fluoropyrimidine-Associated Cardiotoxicity: Probably Not So Rare As It Seems. *Oncologist* **25**, e1254–e1254 (2020).
46. Brell, J. M. 5-Fluorouracil cardiotoxicity. *JACC CardioOncol* **3**, 110–112 (2021).
47. Polk, A., Vistisen, K., Vaage-Nilsen, M. & Nielsen, D. L. A systematic review of the pathophysiology of 5-fluorouracil-induced cardiotoxicity. *BMC Pharmacol Toxicol* **15**, 1–11 (2014).
48. Luwaert, R., Descamps, O., Majois, F., Chaudron, JM. & Beauduin, M. Coronary artery spasm induced by 5-fluorouracil. *Eur Heart J* **12**, 468–470 (1991).
49. Shoemaker, L. K., Arora, U. & Rocha Lima, C. M. S. 5-Fluorouracil–Induced Coronary Vasospasm. **11**, 46–49 (2017).
50. Dechant, C. *et al.* Acute Reversible Heart Failure Caused by Coronary Vasoconstriction due to Continuous 5-Fluorouracil Combination Chemotherapy. *Case Rep Oncol* **5**, 296–301 (2012).
51. Südhoff, T. *et al.* 5-Fluorouracil induces arterial vasocontractions. *Annals of Oncology* **15**, 661–664 (2004).
52. Mosseri, M., Fingert, H. J., Varticovski, L., Chokshi, S. & Isner, J. M. In Vitro Evidence That Myocardial Ischemia Resulting from 5-Fluorouracil Chemotherapy Is Due to Protein Kinase C-mediated Vasoconstriction of Vascular Smooth Muscle. *Cancer Res* **53**, (1993).
53. Hayward, R. *et al.* Training Enhances Vascular Relaxation after Chemotherapy-Induced Vasoconstriction. *Med Sci Sports Exerc* **36**, 428–434 (2004).

54. Altieri, P. *et al.* 5-fluorouracil causes endothelial cell senescence: potential protective role of glucagon-like peptide 1. *Br J Pharmacol* **174**, 3713–3726 (2017).
55. Focaccetti, C. *et al.* Effects of 5-fluorouracil on morphology, cell cycle, proliferation, apoptosis, autophagy and ros production in endothelial cells and cardiomyocytes. *PLoS One* **10**, (2015).
56. Kinhult, S., Albertsson, M., Eskilsson, J. & Cwikiel, M. Antithrombotic treatment in protection against thrombogenic effects of 5-fluorouracil on vascular endothelium: A scanning microscopy evaluation. *Scanning* **23**, 1–8 (2001).
57. Kinhult, S., Albertsson, M., Eskilsson, J. & Cwikiel, M. Effects of probucol on endothelial damage by 5-fluorouracil. *Acta Oncol (Madr)* **42**, 304–308 (2003).
58. Cwikiel, M., Eskilsson, J., Albertsson, M. & Stavenow, L. The influence of 5-fluorouracil and methotrexate on vascular endothelium. An experimental study using endothelial cells in the culture. *Annals of Oncology* **7**, 731–737 (1996).
59. Cwikiel, M., Eskilsson, J., Wieslander, J., Stjernquist, M. & Albertsson, M. The appearance of endothelium in small arteries after treatment with 5-fluorouracil. An electron microscopic study of late effects in rabbits. *Scanning Microsc.* **10**, 805–819 (1996).
60. Muhammad, R. N., Sallam, N. & El-Abhar, H. S. Activated ROCK/Akt/eNOS and ET-1/ERK pathways in 5-fluorouracil-induced cardiotoxicity: modulation by simvastatin. *Sci Rep* **10**, 14693 (2020).
61. Filgueiras, M. de C., Morrot, A., Soares, P. M. G., Costa, M. L. & Mermelstein, C. Effects of 5-Fluorouracil in Nuclear and Cellular Morphology, Proliferation, Cell Cycle, Apoptosis, Cytoskeletal and Caveolar Distribution in Primary Cultures of Smooth Muscle Cells. *PLoS One* **8**, e63177 (2013).
62. Güçlü, O., Doğanlar, O., Yüksel, V. & Doğanlar, Z. B. FOLFIRI-Mediated Toxicity in Human Aortic Smooth Muscle Cells and Possible Amelioration with Curcumin and Quercetin. *Cardiovasc Toxicol* **20**, 139–154 (2020).
63. Zafar, A. *et al.* The efficacy and safety of cardio-protective therapy in patients with 5-FU (Fluorouracil)-associated coronary vasospasm. *PLoS One* **17**, e0265767 (2022).
64. Patel, B. *et al.* 5-Fluorouracil Cardiotoxicity: Left Ventricular Dysfunction and Effect of Coronary Vasodilators. *Am J Med Sci* **294**, 238–243 (1987).

65. Eskilsson, J. & Albertsson, M. Failure of Preventing 5-Fluorouracil Cardiotoxicity by Prophylactic Treatment with Verapamil. **29**, 1001–1003 (2009).
66. Shiga, T. & Hiraide, M. Cardiotoxicities of 5-Fluorouracil and Other Fluoropyrimidines. *Curr Treat Options Oncol* **21**, 1–21 (2020).
67. Kavazis, A. N., Smuder, A. J. & Powers, S. K. Effects of short-term endurance exercise training on acute doxorubicin-induced FoxO transcription in cardiac and skeletal muscle. *J Appl Physiol* **117**, 223–230 (2014).
68. Kavazis, A. N., Smuder, A. J., Min, K., Tümer, N. & Powers, S. K. Short-term exercise training protects against doxorubicin-induced cardiac mitochondrial damage independent of HSP72. *American Journal of Physiology-Heart and Circulatory Physiology* **299**, H1515–H1524 (2010).
69. Ascensão, A. *et al.* Acute exercise protects against calcium-induced cardiac mitochondrial permeability transition pore opening in doxorubicin-treated rats. *Clin Sci* **120**, 37–49 (2011).
70. Marques-Aleixo, I. *et al.* Physical exercise prior and during treatment reduces sub-chronic doxorubicin-induced mitochondrial toxicity and oxidative stress. *Mitochondrion* **20**, 22–33 (2015).
71. Wonders, K. Y., Hydock, D. S., Schneider, C. M. & Hayward, R. Acute exercise protects against doxorubicin cardiotoxicity. *Integr Cancer Ther* **7**, 147–154 (2008).

Chapter 2 - Impaired cutaneous microvascular reactivity in cancer patients treated with 5-fluorouracil chemotherapy

Abstract

Background: 5-fluorouracil (5-FU) is the second most common cancer chemotherapy associated with short- and long-term cardiotoxicity. Though the mechanisms mediating these toxicities are not well understood, preclinical models have proposed a role for microvascular dysfunction. We tested the hypotheses that 5-FU-treated cancer patients would present with impaired microvascular reactivity and that these findings would be substantiated by decrements in endothelial nitric oxide synthase (eNOS) gene expression in 5-FU treated human coronary endothelial cells (HCAEC). **Methods:** We first performed a cross-sectional analysis of 30 5-FU treated cancer patients (5-FU) and 32 matched healthy controls (CON). Cutaneous microvascular reactivity was evaluated by laser Doppler flowmetry in response to 1) local skin heating, with and without Nω-Nitro-L-arginine methyl ester (L-NAME, eNOS inhibitor), 2) iontophoresis of acetylcholine (ACh), and 3) iontophoresis of sodium nitroprusside (SNP). In vitro experiments in HCAEC were completed to assess the effects of 5-FU on eNOS gene expression. **Results:** In support of our hypotheses, 5-FU presented with diminished vasodilation following NO-dependent local heating compared to CON ($P = 0.001$, ES = 0.93). Further, L-NAME failed to reduce the heating response in 5-FU ($P = 0.95$, ES = 0.03), with significant changes in CON ($P = 0.04$, ES = 1.21). These findings were corroborated by lower eNOS gene expression in HCAEC treated with 5-FU ($P < 0.01$) compared to control. Interestingly, peak vasodilation to neither Ach ($P = 0.58$) nor SNP ($P = 0.39$) were different between groups. **Conclusion:** The present findings suggest diminished cutaneous microvascular function along the eNOS-NO vasodilatory pathway

in patients with cancer undergoing treatment with 5-FU-based chemotherapy regimens and thus, may provide insight into the underlying mechanisms of 5-FU cardiotoxicity.

Introduction

5-fluorouracil (5-FU) is one of the most frequently administered chemotherapeutic agents used in the treatment of cancer and is a central component of the preferred treatment regimens for gastrointestinal and head/neck malignancies (e.g., FOLFOX, FOLFIRI, FOLFIRINOX). Yet, despite established effectiveness as an anticancer agent, the efficacy of 5-FU-containing regimens can be limited by its off-target cardiovascular side effects (i.e., cardiotoxicity), which most commonly arise as angina with or without ST-segment alterations indicative of myocardial ischemia [1–5]. The onset of symptomatic cardiotoxicity has been documented to occur in 1-20% of patients treated with 5-FU [1,4,6–9]. However, these incidence rates may be underestimated [10,11] with at least one report demonstrating asymptomatic ST segment alterations suggestive of decreased myocardial perfusion in greater than 50% of 5-FU treated patients [12]. Notably, the development of adverse cardiovascular side effects during cancer treatment can prompt deviation from optimal chemotherapy dosing regimens [13] resulting in an increased likelihood of cancer reoccurrence and significant reductions in overall survival [14–16]. As such, there is a critical need to investigate the mechanistic underpinnings by which 5-FU alters vital aspects of cardiovascular health.

To date, the pathophysiological mechanisms driving 5-FU cardiotoxicity remain poorly understood. Among the most prominent theories is the development of coronary epicardial or microvascular spasm provoked by a direct effect of 5-FU on the coronary endothelium and/or smooth muscle [4,5,17]. However, evidence of the effect of 5-FU on coronary circulation is limited to single-patient case reports [18,19]. This lack of evidence is seemingly due, at least in part, to the high invasiveness required in investigating the coronary circulation. As such, others have turned to the peripheral vasculature to better understand how 5-FU may impact vascular function. Reductions in flow-mediated dilation in large vessels such as the brachial artery following 5-FU

treatment have been demonstrated [20], yet it remains unknown whether 5-FU or 5-FU-containing regimens negatively impact the microcirculation. Our group has previously used laser Doppler flowmetry coupled with iontophoresis of acetylcholine (ACh) and sodium nitroprusside (SNP) to demonstrate alterations in cutaneous microvascular reactivity in chemotherapy [21] and radiation [22] treated patients with cancer. However, to our knowledge, there are currently no data specific to 5-FU-based regimens. Therefore, the present investigation aimed to assess potential impairments in cutaneous microvascular reactivity in patients treated for cancer with 5-FU-based chemotherapy regimens. Additionally, to further explore the mechanisms driving these impairments, we utilized a human coronary endothelial cell (HCAEC) culture model treated with multiple concentrations of 5-FU. We hypothesized that 5-FU treatment would diminish microvascular reactivity, as determined by responses to local skin heating and iontophoresis of ACh, and that these impairments would be corroborated by decreased eNOS gene expression.

To test these hypotheses, we conducted a series of both in vivo and in vitro experiments designed to assess how 5-FU-based chemotherapy regimens impact vascular function. First, cutaneous microvascular responses to endothelium-dependent (local skin heating, ACh iontophoresis) and -independent (SNP iontophoresis) stimuli were assessed in groups of patients undergoing cancer treatment with 5-FU based chemotherapy and matched controls. Follow-up experiments were conducted in HCAEC cells to determine how 5-FU influences eNOS gene expression within a model of the coronary endothelium.

Methods

Participants

We used a case-control study design in which 30 patients undergoing cancer treatment with 5-FU-based chemotherapy regimens (5-FU) participated in this study. Cancer diagnoses for enrolled participants included colon/rectal, pancreatic, appendiceal, duodenal, stomach/esophageal, and common bile duct cancers which were confirmed by the patient's oncologist. Patients treated with the following 5-FU-based chemotherapy regimens: FOLFOX (folinic acid, 5-FU, oxaliplatin), FOLFIRINOX (folinic acid, 5-FU, irinotecan, oxaliplatin), FOLFIRI (folinic acid, 5-FU, irinotecan), or FOLFOX→FOLFIRI, were eligible to enroll in the study (**Table 2.1**)**.** Despite components of some of these regimens differing slightly, current chemotherapy practice generally includes the use of multiple agents depending on cancer type, tumor stage, and the patient's response to treatment. Therefore, we included patients treated with a variety of standard 5-FU-based regimens. Patients were matched with 32 control subjects for age, sex, body mass index, and smoking status, as well as prior non-cancer related health history, including the presence of cardiovascular disease and documented history of cardiovascular disease risk factors (hyperlipidemia, high blood pressure, and metabolic disease) (**Table 2.2**). Further, we recorded any medications used to treat the aforementioned cardiovascular disease risk factors (diabetic, hypertensive, and cholesterol medications). All participants provided written informed consent approved by the institutional review boards at Kansas State University, with all procedures conforming to the Declaration of Helsinki.

Table 2.1. Cancer diagnosis and chemotherapy information for the complete cohort

Combined Cohorts		
Cancer Diagnoses, n	Stages I-III	Stage IV
Colon/rectum	7	8
Pancreatic	6	1
Appendiceal	0	3
Stomach/Esophageal	1	1
Duodenal	2	0
Common Bile	1	0
Chemotherapy regimen, n	-	
FOLFOX	15	
FOLFIRINOX	10	
FOLFIRI	1	
FOLFOX + FOLFIRI	4	
Cumulative 5-FU dose mg/m^2, median (25^{th}-75^{th} percentile)	21,510 (9,600 – 33,120)	

Patient cancer and chemotherapy treatment demographics. The components of the common 5-FU based chemotherapy regimens used in treatment of patients included in this study are as follows: FOLFOX (Leucovorin, 5-fluorouracil, Oxaliplatin), FOLFIRINOX (Leucovorin, 5-fluorouracil, Irinotecan, Oxaliplatin); FOLFIRI (Leucovorin, 5-fluorouracil, Irinotecan).

Table 2.2. Demographic variables for the complete participant cohort

Combined Cohorts		
	CON	5-FU
N	32	30
Age, years	58.9±12.8	62.0±11.7
BMI, kg/m^2	28.9±4.9	29.6±4.5
MAP, mmHg	90±9	85±10
No. of women, n (%)	15 (47)	10 (33)
No. with ≥1	14 (44)	23 (77)
CVD risk factor, n (%)		
Diagnosed CVD, n (%)	6 (19)	5 (17)
CVD risk meds., n (%)	14 (44)	23 (77)
Current smoker, n (%)	0 (0)	5 (17)

Subject demographics for the combined cohort of participants. BMI = body mass index. CVD = cardiovascular disease. MAP = mean arterial pressure. Data presented as mean ± SD or n (%).

All testing was conducted during a single 90–120-minute visit, with the subject in a seated recliner at the cancer treatment facility (Stormont Vail Cotton O'Neil Cancer Center, Topeka, KS) or the investigators' dedicated laboratory space (Lafene Health Center, Kansas State University, Manhattan, KS). Data collection for all patients with cancer was arranged to begin immediately following the completion of their regularly scheduled 5-FU chemotherapy treatment, while control experiments were subject to participant availability. Generally, patients received a single bolus injection of 5-FU immediately followed by a 46-hour continuous infusion of 5-FU with doses, durations, and use of additional chemotherapies varying slightly between patients depending on the individually prescribed regimen. Upon completion of therapy and removal of the 5-FU pump, patients were seated in a reclined chair and instrumented with an automated blood pressure cuff (HEM-907XL, OMRON Healthcare, Kyoto, Japan) for measurement of systolic and diastolic blood pressures. All blood pressure measurements were made at heart level.

Laser Doppler flowmetry

To assess cutaneous microvascular reactivity, we conducted experiments using laser Doppler flowmetry in combination with both endothelium-dependent and -independent stimuli. Due to the availability of patient time and measurement sites, we completed one or two of the following experimental studies in each participant: 1) local skin heating at 42°C, 2) local skin heating with iontophoresis of L-NAME (see *Microvascular Reactivity to Localized heating and L-NAME iontophoresis*), 3) iontophoresis of ACh (see *Microvascular Reactivity to ACh*), and 4) iontophoresis of sodium nitroprusside (SNP) (see *Microvascular Reactivity to SNP*). Iontophoresis was selected as the mode of drug delivery to avoid the vascular consequences of needle trauma associated with inserting intradermal microdialysis fibers [23] and to minimize the

patient time requirement, invasiveness, and pain. It is well established that chemotherapy-induced neuropathic pain is one of the most common and severe off-target effects of anticancer agents, with symptoms often affecting the extremities of the upper and lower limbs [24,25]. Therefore, the use of intradermal microdialysis was contraindicated in this population. For all experiments, two drug delivery electrodes (PF 383, Perimed, Järfälla, Sweden) instrumented with laser Doppler flowmeters and temperature regulators were randomly assigned and placed immediately proximal to the wrist or distal to the elbow on the ventral right forearm. The skin was pre-cleaned with commercially available alcohol wipes before probe placement, and the probes were held in place with two strips of surgical tape. A single hydrogel drug dispersive electrode (PF 384; Perimed) was fixed to the skin of the same forearm at least 10 cm away from the drug delivery electrodes. The drug delivery and dispersive electrodes formed a complete circuit via connection to a USB power supply (PF 751; Perimed) that controlled current delivery intensity, duration, and interval using available software (PerIont Software; Perimed). An integrated laser Doppler flowmeter (PeriFlux 5010; Perimed) measured cutaneous red blood cell flux (RBC flux), which was used as an index of cutaneous blood flow and recorded using data acquisition software (DI-720; DATAAQ Instruments, Akron, OH) for future offline analyses. The laser Doppler flowmeter was calibrated according to factory standards using Brownian motility standard solution (PF 1001; Perimed). Upon completion of setup and prior to any local heating or iontophoresis experiments, steady resting RBC flux values were assured and at least two minutes of baseline RBC flux was collected from each probe with the localized probe temperature set to 33°C.

To account for potential differences and fluctuations in mean arterial pressure (MAP) between participants, all RBC flux data are presented as percent changes in cutaneous vascular

conductance (CVC) from baseline. MAP was calculated as MAP = 1/3 (pulse pressure) + diastolic blood pressure. CVC was calculated as CVC = (RBC flux / MAP) x 100. Relative changes in CVC from baseline to peak (%ΔCVC) were calculated as: [(peak - baseline CVC) / baseline CVC] x 100, as demonstrated previously [21,22].

Microvascular reactivity to local heating and L-NAME iontophoresis

Local heating of the forearm skin elicits a biphasic vasodilatory response which culminates in a plateau in cutaneous blood flow that is highly reliant on nitric oxide (NO) [26–32]. Briefly, local heating stimulates an initial axon-mediated increase in blood flow that occurs within the first few minutes of heat onset [27,33], followed by a brief nadir and successive gradual rise to a sustained endothelium-derived NO-dependent plateau [26–29]. To assess this NO-dependent response, one of the two laser Doppler probes was randomly selected for a standardized local heating protocol (n=20 CON, n=17 5-FU). Following a short baseline period, the local probe temperature was increased from 33°C by 1°C every 10 seconds until a temperature of 42°C was achieved. The local temperature remained clamped at 42°C for ~35 minutes until a plateau in RBC flux was reached. The highest 5-minute average of RBC flux during the plateau period was used for subsequent calculations of CVC, as described above. This protocol has previously been used as a non-invasive/pain-free method of assessing the endothelial-derived NO vasodilator pathway in participants afflicted by external stressors [34] or various disease states [26,31,35–38].

In a subset of these participants (n= 7 CON, n=7 5-FU), an additional local heating site was included at a second laser Doppler probe in which otherwise identical procedures to those presented above were preceded by iontophoresis of a 2% L-NAME solution (Product #: N5751, Sigma-Aldrich, St. Louis, MO, USA). For these experiments, 200 µL of 2% L-NAME dissolved

in deionized water was added to the drug delivery electrode and placed at the predetermined forearm site as mentioned above. Following the collection of baseline measures, 20 minutes of L-NAME iontophoresis commenced using a 50 μA anodal current, as demonstrated by others [39,40]. Before probe placement, measurement sites were pretreated for ~10 minutes with a topical anesthetic (removed via alcohol swab prior to probe placement) that included 4% lidocaine (Aspercreme, Chattem, Chattanooga, TN) to minimize any potential discomfort caused by the current and simultaneously inhibit a current induced increase in basal RBC flux. Notably, the use of like anesthetic procedures has been shown to blunt the initial sensory neuron-related spike in RBC flux without affecting the sustained heated plateau [27]. As such, data comparing potential differences in the initial peak in RBC flux are not presented herein.

Microvascular reactivity to ACh

The cutaneous vasodilatory response to exogenous ACh is mediated by a combination of factors including endothelial-derived NO, prostanoids, and endothelial-derived hyperpolarizing factors and therefore is often used as a standard method to assess broad endothelium-dependent microvascular reactivity [41–45]. As such, to test potential endothelium-dependent differences beyond the primarily NO-mediated effects of local heating, 5-FU patients (n=17) and controls (n=15) completed an ACh iontophoresis protocol. As demonstrated previously by our group [21,22], a 100 μA anodal current was used to deliver 200 μL of 2% ACh solution (Product #A6625, Sigma-Aldrich) dissolved in deionized water in 7 sequential iontophoresis pulses (i.e., doses) separated by a 60-second rest interval. Data recording persisted for at least 5 minutes into the recovery period following administration of the final iontophoresis pulses. The local probe temperature for ACh iontophoresis remained clamped at 33°C throughout the experiment. The

ACh-induced peak was considered the highest 10-second mean CVC recorded at any point during the 7 successive ACh iontophoresis pulses [21,22].

Microvascular reactivity to SNP

Endothelium-independent microvascular reactivity was evaluated in a separate cohort of CON (n=9) and 5-FU (n=6) participants via iontophoresis of SNP. Briefly, a 20 µA cathodal current was used to deliver 200 µL of a 1% SNP solution **(**Product #: 71780, Honeywell, Charlotte, NC, USA) dissolved in 0.9% saline over the course of 400 seconds [46]. Following completion of SNP delivery, data recording continued for at least 5 minutes to ensure a peak vasodilatory response had been achieved. The SNP peak was considered the highest 1-min CVC average recorded during the 400 second delivery period or in the 5-minutes following the iontophoresis protocol.

Human coronary artery endothelial cells (HCAEC)

Previously frozen primary HCAEC (PCS-100-020; ATCC, Manassas, VA, USA) were plated at 35,000 cells per well in tissue culture treated 6-well plates (3516; Corning, Glendale, AZ, USA) and maintained in 2 mL vascular cell growth medium (PCS-100-030 supplemented with PCS-100-041; ATCC) and placed in an incubator at 37°C/5% CO_2 as per manufacturer instructions. Following a 24-hour attachment period, growth medium was aspirated, and wells were randomly assigned to receive fresh growth medium, growth medium treated with 0.7 mM of 5-FU, or growth medium treated with 7 mM of 5-FU, for 24 hours (n=3 cultures per group). These concentrations were selected for their use in studies demonstrating ex vivo vascular reactivity in response to 5-FU [47,48]. Following the 24-hour treatment period, the growth medium was aspirated, and all wells were washed twice with sterile 1x D-PBS before cell collection via incubation with Trypsin EDTA for Primary Cells (PCS-999-003; ATCC). Before proceeding, all

wells were inspected to ensure similar cell removal from each well. Cells were then centrifuged according to manufacturer standards and subsequently lysed using a 1% DNase I lysis solution (Ref#: AM8728, Thermo Fisher Scientific) prior to storage at -80°C for future analyses.

Quantitative reverse transcription-polymerase chain reaction (RT-PCR)

Complimentary DNA (cDNA) was prepared from cell lysates using the TaqMan Fast Cells-to-Ct kit (Product #: 4399003; Life Technologies, Carlsbad, CA) according to manufacturer instructions. cDNA samples were subsequently used in two-step RT-PCR experiments using TaqMan gene expression assays (Applied Biosystems; Bedord, MA, USA) for eNOS (assay ID: Hs01574659_m1) and GAPDH (assay ID: Hs99999905_m1) on 96-well TaqMan Plates in a QuantStudio 3 RT-PCR System (Applied Biosystems). All samples were run in duplicate for genes of interest and endogenous control (GAPDH) and analyzed using the comparative threshold (ΔΔCt) method.

Statistical analysis

All data were analyzed using a commercially available software package (GraphPad Prism 9; San Diego, Ca, USA). Demographic variables (proportion of male/female, cardiovascular disease risk, etc.) were compared using Fisher's exact test. Independent-samples t-tests and Welch’s t-test were used to determine pair differences between 5-FU and CON groups and within-group differences between L-NAME (L+SH) and standard local heating (SH) sites for normally distributed data with and without equal variance, respectively. Differences in baseline measurements for standard heating and L-NAME treated sites, as well as gene expression in HCAEC were compared using One-way ANOVA, while multiple comparisons were assessed using Tukey's HSD when appropriate. A two-way repeated measures ANOVA was used to compare CVC differences following each Ach-iontophoresis delivery period

between groups (group x dose) with the Holm-Šidák method used to analyze multiple comparisons. To provide additional insight on the magnitude of differences between groups, effect sizes (ES) were calculated using Hedges' g unless standard deviations were significantly different between the groups (i.e., F-test <0.05); in which case, Glass's delta was calculated instead. The threshold values for ES were classified as: small = 0.2, moderate = 0.5, and large = > 0.8 [49]. All data are presented as mean ± standard deviation unless otherwise stated. Cumulative 5-FU doses received by each cohort are presented as median (25^{th}-75^{th} percentile). Alpha was set to .05 for all tests.

Results

Cancer cohort diagnosis, staging, and 5-FU chemotherapy regimen data are located in **Table 2.1,** whereas participant demographics are presented in **Table 2.2** This information is provided separately for each experimental cohort in **Tables 2.3 and 2.4, respectively**. There were no statistical differences between individual cohorts for participant age, BMI, percentages of men and women, participants diagnosed with cardiovascular disease, use of cardiovascular-related medications, or current smokers (all $P>0.05$) (**Table 2.4**). In addition, no differences were present concerning the number of participants with cardiovascular disease-related risk factors aside from the SNP cohort in which the 5-FU treated patients presented with a significantly higher percentage of participants with risk factors for CVD compared to the control group (22% of CON vs 100% of 5-FU; $P=0.01$) (**Table 2.4**).

Table 2.3. Cancer diagnosis and treatment information by individual cohort

	Local Heating (n=17)		Local Heat + L-NAME (n=7)		Ach (n=17)		SNP (n=6)	
Cancer Type, n	Stages I-III	Stage IV	Stages I-III	Stage IV	Stages I-III	Stage IV	Stages I-III	Stage IV
Colon/Rectum	3	3	2	2	3	5	2	1
Pancreatic	3	1	1	0	3	1	1	1
Appendiceal	0	3	0	1	0	2	0	0
Stomach/Esophageal	1	0	0	0	1	0	0	1
Duodenal	2	0	0	0	2	0	0	0
Common Bile	1	0	1	0	0	0	0	0
Chemotherapy Regimen, n	Alone	+ CAPE	Alone	+ CAPE	Alone	+ CAPE	Alone	+ CAPE
FOLFOX	6	3	2	2	7	1	3	0
FOLFIRINOX	6	0	2	0	4	1	3	0
FOLFIRI	0	0	0	0	0	1	0	0
FOLFOX + FOLFIRI	1	1	1	0	2	1	0	0
Cumulative 5-FU dose mg/m^2, median (25^{th}-75^{th} percentile)	12,000 (7,000 – 31,720)		9,000 (2,800 - 27,600)		25,045 (12,500 – 42,200)		21,000 (15,100 - 27,100)	
Additional Chemotherapies, name (n)	bevacizumab (n=2), gemcitabine (n=4), trastuzumab (n=2), panitumumab (n=1)		gemcitabine (n=2), panitumumab (n=1)		bevacizumab (n=3), gemcitabine (n=3), trastuzumab (n=2), panitumumab (n=3), mitomycin (n=1), paclitaxel (n=1), cetuximab (n=1)		paclitaxel (n=1), carboplatin (n=1), nivolumab (n=1)	

Patient cancer and chemotherapy treatment demographics. The components of the common 5-FU based chemotherapy regimens used in treatment of patients included in this study are as follows: FOLFOX (Leucovorin, 5-fluorouracil, Oxaliplatin), FOLFIRINOX (Leucovorin, 5-fluorouracil, Irinotecan, Oxaliplatin); FOLFIRI (Leucovorin, 5-fluorouracil, Irinotecan). Some patients may have also received capecitabine (CAPE) which is an oral prodrug that is converted to 5-FU upon consumption.

Table 2.4. Individual cohort demographics

	Local Heating			Local Heating + L-NAME			ACh			SNP		
	CON	5-FU	P-value	CON	5-FU	P-value	CON	5-FU	P-value	CON	5-FU	P-value
n	20	17	n/a	7	7	n/a	15	17	n/a	9	6	n/a
Age, years	62.0±12.9	62.9±10.6	0.81	62.4±8.5	61.1±11.2	0.81	58.7±16.5	63.5±12.1	0.35	57.3±9.3	58.5±12.8	0.86
BMI, kg/m^2	30.0±5.0	29.9±4.7	0.94	27.5±5.5	31.6±4.7	0.16	30.6±4.5	28.3±4.2	0.16	26.6±3.8	30.8±5.4	0.10
MAP, mmHg	93±9	86±11	0.04*	98±11	86±11	0.07	90±7	84±10	0.08	86±10	84±10	0.79
No. of women, n (%)	9 (45)	7 (41)	>0.99	3 (43)	3 (43)	>0.99	7 (47)	4 (24)	0.27	4 (44)	3 (50)	>0.99
No. with ≥1 CVD risk factor, n (%)	12 (60)	15 (88)	0.07	5 (71)	7 (100)	0.46	8 (53)	10 (59)	>0.99	2 (22)	6 (100)	0.01*
CVD risk meds., n (%)	9 (55)	13 (76)	0.30	5 (71)	7 (100)	0.46	8 (53)	8 (47)	>0.99	2 (22)	3 (50)	0.33
Diagnosed CVD, n (%)	5 (25)	3 (18)	0.70	1 (14)	1 (14)	>0.99	4 (27)	3 (18)	0.68	1 (11)	1 (17)	>0.99
Current smoker, n (%)	0 (0)	2 (12)	0.20	0 (0)	2 (29)	0.46	0 (0)	2 (12)	0.49	0 (0)	1 (17)	0.40

Subject demographics for each individual cohort. Group means for age, BMI, and MAP were compared using independent samples T-tests. Proportion of patients in each group who were women, have been diagnosed with CVD, who have been diagnosed with common CVD risk factors, who take medications associated with CVD and/or CVD associated risk factors, and who are current smokers were compared between groups using Fisher's exact test. BMI = body mass index. CVD = cardiovascular disease. MAP = mean arterial pressure. Data presented as mean ± SD or n (%).

Local heating and L-NAME iontophoresis

The median 5-FU dose received by patients with cancer in the local heating cohort was 12,000 mg/m^2 (range 7,000 – 31,720) (**Table 2.3**). **Figure 2.1a** illustrates a representative tracing of the %ΔCVC response to local heating in a patient treated with a 5-FU-based chemotherapy regimen and an age- and sex-matched control subject. The response to local heating expressed as %ΔCVC was significantly lower in the 5-FU-based chemotherapy group (n=17) compared to controls (n=20) (CON: 566 ± 305%; 5-FU: 282 ± 172%; P = 0.001, ES = 0.93). (**Figure 2.1b**). Importantly, the CVC at baseline was not different between groups (CON: 6.9 ± 3.1 PU mmHg^{-1}; 5-FU: 8.8 ± 5.8 PU mmHg^{-1}; P = 0.42); however, 5-FU patients did present with significantly lower resting MAP (CON: 93 ± 9 mmHg; 5-FU: 86 ± 11 mmHg; P = 0.04) **(Table 2.4).**

Figure 2.1. Cutaneous microvascular responses to local heating

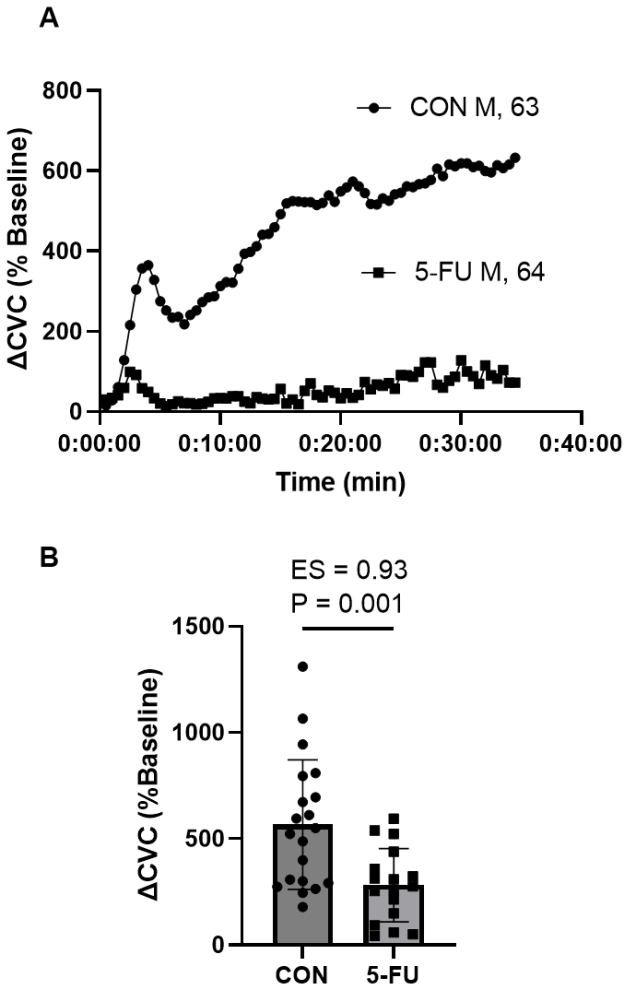

Impaired cutaneous microvascular reactivity following local heating in cancer patients treated with 5-FU**. A)** A representative tracing of the rise in CVC from baseline during a 35 min local heating protocol for a 5-FU treated patient (5-FU, Male 64 years old) and matched control (CON, Male, 63 years old). **B)** 5-FU patients (n=17, 7 women) presented with a significantly lower %ΔCVC than control subjects (n=20, 9 women) (CON: 566 ± 305%; 5-FU: 282 ± 172%; P=0.001, ES=0.93) following 35 min of local heating suggesting the presence of impairment along the eNOS-NO vasodilator pathway following 5-FU chemotherapy. Data were compared using the Welch's t-test and presented as mean ± SD.

Given that the work of others has demonstrated the role of NO in the vasodilator response to local skin heating [26–31], we further evaluated the local heating response in a subset of these participants following iontophoresis of the constitutive NOS inhibitor L-NAME (CON: n=7, 5-FU: n=7). The median 5-FU dose received by patients with cancer in the L-NAME subgroup was 9,000 mg/m^2 (range: 2,800 - 27,600). No resting CVC differences were detected between standard local heating and L-NAME testing sites within each group or between groups (CON+SH = 6.3 ± 2.3 PU mmHg^{-1}, CON+L = 6.3 ± 2.9 PU mmHg^{-1}, 5-FU+SH = 8.80 ± 5.8 PU mmHg^{-1}, 5-FU+L = 5.6 ± 2.3 PU mmHg^{-1}; main effect: P = 0.378). Further, there were no differences in resting MAP between the groups (CON: 98 ± 11 mmHg; 5-FU: 86 ± 11 mmHg; P = 0.07) (**Table 2.4**). In control subjects, the L-NAME treated site (L+SH) had a significantly lower %ΔCVC when compared to the standard local heating (SH) site (SH: 564 ± 371%; L+SH: 175 ± 122%; P = 0.03; ES = 1.05) (**Figure 2.2a**). Interestingly, this difference was not reciprocated in the 5-FU group as the SH site was not significantly different from the L+SH site (SH: 327 ± 118%; L+SH: 333 ± 227%; P = 0.95; ES = 0.03) (**Figure 2.2b**), suggesting that patients treated with 5-FU based chemotherapy regimens may have a blunted cutaneous vasodilatory response to endothelial NO. The difference between the %ΔCVC at the SH and L+SH sites was calculated and subsequently compared between the groups. The matched controls had a significantly greater difference between the SH and L+SH sites compared to the patients receiving 5-FU-based chemotherapy (CON: 389 ± 388%; 5-FU: -6 ± 247%; P = 0.04; ES = 1.21) (**Figure 2.2c**).

Figure 2.2. Cutaneous microvascular responses to local heating with L-NAME

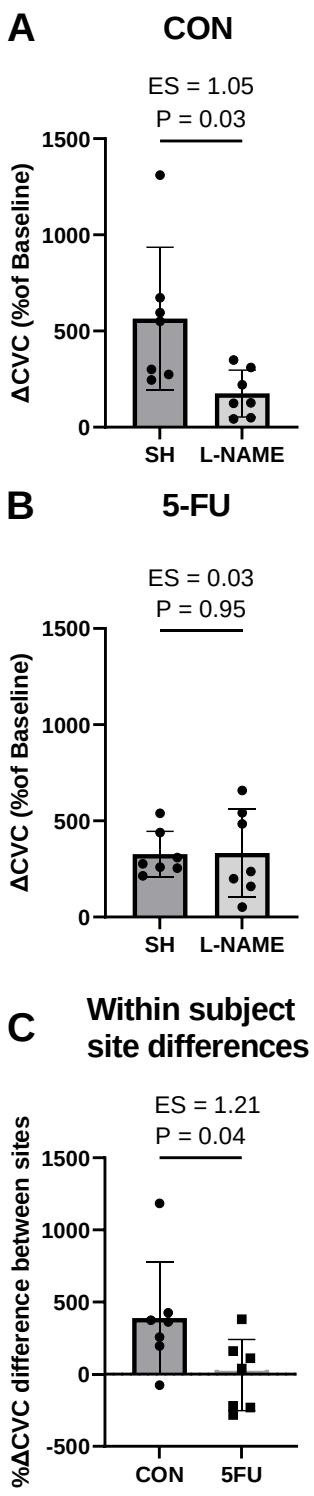

L-NAME fails to reduce the local heating response in 5-FU-treated cancer patients. **A)** L-NAME iontophoresis significantly reduced the %ΔCVC response to local heating in control patients (n=7, 3 women) (SH: 564 ± 371%; L: 175 ± 122%; P = 0.03, ES = 1.05) but not in **B)** cancer patients (n=7, 3 women) treated with 5-FU (SH: 327 ± 118%; L: 333 ± 227%; P = 0.95, ES = 0.03) suggesting a lesser contribution of NO to the heated plateau following treatment with 5-FU chemotherapy. **C)** The absolute difference in the percent change between the SH and L treated sites was significantly greater in control patients compared to 5-FU treated cancer patients (CON: 389 ± 388%; 5-FU: -6 ± 247%; P = 0.04). SH = standard heating; L = L-NAME + standard heating. Data were compared using Welch's t-test (A) and independent-samples t-test (B and C) and presented as mean ± SD.

ACh iontophoresis

The median 5-FU dose for 5-FU treated patients in the ACh cohort was 25,045 mg/m^2 (range: 12,500 – 42,200) (**Table 2.3**). There was no difference detected in baseline CVC (CON: 6.5 ± 2.9 PU mmHg^{-1}; 5-FU: 11.3 ± 9.2 PU mmHg^{-1}; P = 0.22) or MAP (CON: 90 ± 7 mmHg; 5-FU: 84 ± 10 mmHg; P = 0.08) (**Table 2.4**) between the groups. Both 5-FU (n=17) and CON (n=15) groups experienced significant increases in CVC with successive ACh doses (P = <0.001) (**Figure 2.3a**). However, contrary to our hypothesis, there were no differences between groups at any of the ACh iontophoresis impulse time points (P = 0.44) **(Figure 2.3a**) nor in the peak ACh induced response from baseline (CON: 920 ± 416%; 5-FU: 835 ± 448%; P = 0.58) (**Figure 2.3b**) suggesting that 5-FU treatment may not hinder all endothelium-dependent vasodilatory pathways.

Figure 2.3. Cutaneous microvascular responses to iontophoresis of ACh

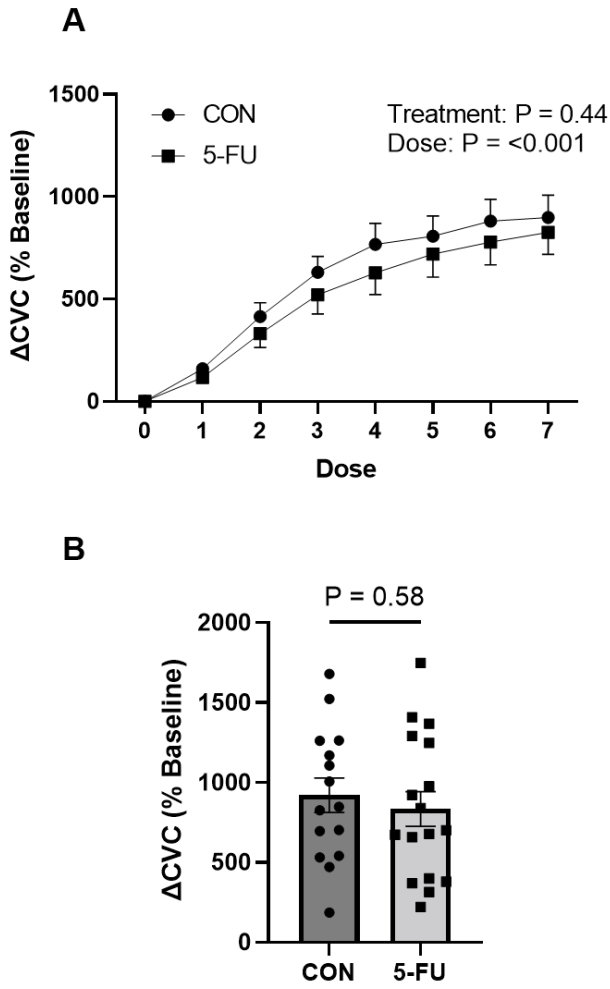

Cutaneous microvascular reactivity in response to ACh iontophoresis is maintained in 5-FU-treated cancer patients. **A)** ACh iontophoresis resulted in a significant rise in %ΔCVC with successive doses (P = <0.001); however, this rise was not different between 5-FU patients (n=17, 4 women) and control subjects (n=15, 7 women) (P = 0.44). **B)** This finding was corroborated by the similarity in the peak response to ACh between groups (CON: 920 ± 416%; 5-FU: 835 ± 448%; P = 0.58), suggesting some endothelium-dependent vasodilatory pathways may remain intact following 5-FU-based chemotherapy. Data were compared using two-way repeated measures ANOVA (A) and independent- samples t-test (B). All data are presented as mean ± SD.

SNP iontophoresis

The cumulative dose of 5-FU received by patients in the SNP cohort was 21,000 (15,100 – 27,100) mg/m^2 (**Table 2.3**). There were no differences in resting MAP between the groups (CON: 86 ± 10 mmHg; 5-FU: 84 ± 10 mmHg; P = 0.79) (**Table 2.4**). Baseline CVC before SNP delivery was not different between CON (n=9) and 5-FU (n=6) groups (CON: 7.0 ± 1.6 PU mmHg^{-1};5-FU: 6.0 ± 2.6 PU mmHg^{-1}; P = 0.38) nor was the response to SNP iontophoresis (CON: 188 ± 270%; 5-FU: 245 ± 234%; P = 0.39) suggesting no difference between groups in the ability of the vascular smooth muscle to respond to an exogenous NO donor.

In vitro experiments

In support of our in vivo findings, HCAEC incubated with both 0.7 mM (0.711 ± 0.12 a.u.; P = 0.008, ES = 0.52) and 7.0 mM (0.578 ± 0.13 a.u; P = 0.002, ES = 0.69) of 5-FU for 24 hours presented with significant decrements in eNOS gene expression when compared to HCAEC incubated in standard growth medium (1.11 ± 0.06 a.u.) alone. However, there were no differences between the high and low 5-FU concentrations (P = 0.34) (**Figure 2.4**.).

Figure 2.4. Effect of in vitro 5-FU on eNOS gene expression in HCAEC

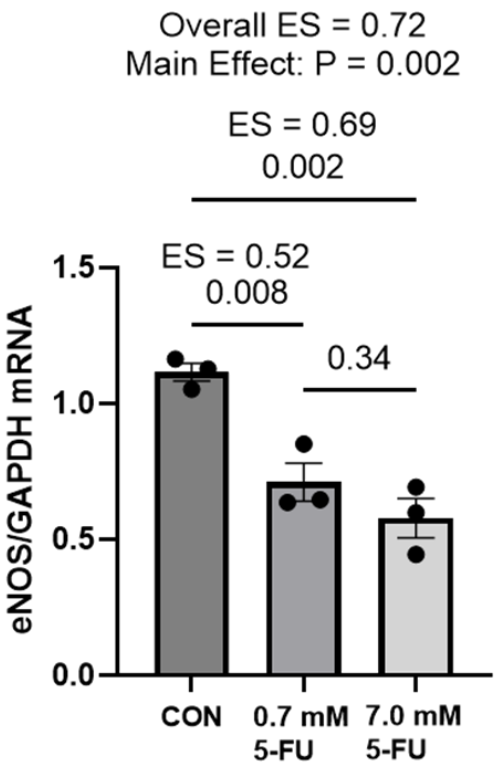

eNOS gene expression is reduced in 5-FU treated HCAEC**.** There was a significant main effect for differences in eNOS gene expression between the groups following the 24-hr. incubation period (P = 0.002, ES = 0.72). CON cells (1.114 ± 0.06 a.u) had significantly higher levels of eNOS gene expression compared to cells treated with both 0.7 mM (0.711 ± 0.12 a.u; P = 0.008, ES = 0.52) and 7.0 mM (0.578 ± 0.13 a.u; P = 0.002, ES = 0.69) of 5-FU, while no differences were detected between the two 5-FU concentrations (P = 0.34). n=3 cultures per group. All samples were run in duplicate. Data were analyzed using One-way ANOVA and are presented as mean ± SD. a.u. = arbitrary units. eNOS = endothelial nitric oxide synthase.

Discussion

Our primary finding was that patients undergoing treatment for cancer with 5-FU-based chemotherapy regimens had significant impairments in cutaneous microvascular reactivity in response to local skin heating—a process believed to be primarily facilitated by eNOS-derived NO production [26,32].

The inability of L-NAME to reduce the local heating-induced rise in CVC in 5-FU treated patients, along with the lack of CVC differences between groups following iontophoresis of SNP, support these findings and suggest potential perturbations occur along the eNOS-NO vasodilator pathway in patients treated with 5-FU based regimens. Our follow-up experiments in HCAEC culture substantiate this notion, as decrements in eNOS gene expression were evident in HCAEC treated with high and low concentrations of 5-FU compared to control. Interestingly, the response to iontophoresis of ACh was unaltered following 5-FU treatment, implying that endothelium-dependent vasodilatory pathways, which rely on contributions from vasodilatory substances other than NO alone [41–43] may remain intact. Taken together, these findings offer evidence for 5-FU-induced microvascular impairment, presumably through pathways involving eNOS-derived NO, and thus may provide valuable insight into the mechanistic pathophysiology of 5-FU-related cardiotoxicity.

Dysfunction of the vascular endothelium is a well-established precursor to a vast array of cardiovascular diseases and events and is generally attributed, at least in part, to decrements in the bioavailability of NO (for review, see [50]). Specifically, impairments in endothelium-dependent vasodilatory function within the coronary circulation are associated with angina [51], coronary vasospasm [52], and myocardial ischemia [53]—the main cardiotoxicities often affiliated with 5-FU treatment. Alterations to both epicardial and microcirculatory vessels are believed to

contribute to these maladies, with microcirculatory dysfunction considered one of the earliest signs of impending cardiovascular disarray [54]. Importantly, endothelial inadequacies in these populations are not exclusive to the coronary vasculature and are also apparent throughout the systemic circulation [55]. Pertinent to the present investigation, the cutaneous circulation has regularly been used to assess potential mechanistic vascular alterations in disease states such as hypertension [38], type II diabetes [56], hypercholesteremia [35], kidney disease [37], psoriasis [57], postural tachycardia syndrome [31], coronary artery disease [58], heart failure [59], and cancer [21,22,60]. Given the invasiveness in investigating the coronary circulation, this latter point is critical as evaluation of the cutaneous vascular beds may deliver a first glimpse into global endothelial microcirculatory health of at-risk populations and in vivo justification for the more invasive and conclusive study of the coronary vasculature. It is important to note, however, that while some have demonstrated statistically significant correlations between vasodilatory responses in the cutaneous and coronary circulations [61], these correlations appear relatively modest and, to our knowledge, have only been studied in a small group of healthy participants. Thus, future work that aims to characterize this relationship further would be beneficial in understanding how alterations in cutaneous microvascular function reflect those occurring within the coronary vasculature.

To the best of our knowledge, the present investigation is the first attempt at deciphering how 5-FU-based chemotherapy regimens may impact microcirculatory function in patients undergoing cancer treatment. Südhoff and colleagues [20] report the occurrence of brachial artery vasoconstriction—rather than the typical vasodilation—in 50% of patients receiving 5-FU in response to a standard flow-mediated dilation (FMD) protocol [20]. Given that endothelium-derived NO mediates up to 67% of the vasodilatory response to FMD [62], these data imply the presence of NO-dependent alterations in conduit vessel function immediately following 5-FU

treatment. The findings herein support this notion, albeit in the microcirculation, with the vasodilatory response to local heating in 5-FU patients significantly reduced to that in matched controls. Further, given that the change in %ΔCVC following NOS inhibition with L-NAME was insignificant in 5-FU treated patients, coupled with the lack of differences demonstrated between groups in response to iontophoresis of SNP, we can postulate that NO-mediated dilation may indeed be diminished. As such, our findings suggest that 5-FU-based regimens may result in either lesser production of eNOS-derived NO or increased scavenging of NO by reactive oxygen species (ROS) [63]. Additional insight is provided by our observed decrements in eNOS gene expression in HCAEC treated with 5-FU. This finding is consistent with other preclinical models that have found either decreased eNOS protein content in human umbilical vein endothelial cells cells [64] or reduced phosphorylation of eNOS activation sites (Ser1177) in rat myocardium [65] following 5-FU administration.

Though microcirculatory responses to local heating were altered following 5-FU treatment, to our surprise, ACh-induced vasodilatory pathways were seemingly unaffected. Prior work by our group has shown apparent attenuation in ACh-induced cutaneous microvascular reactivity in cancer populations treated with heterogeneous chemotherapy regimens compared to controls [21] and between radiated and contralateral non-radiated sites in patients with breast cancer [22]. Similarly, Mourad and colleagues note a reduced cutaneous red blood cell flux, not corrected for arterial pressure, in response to iontophoresis of the ACh analog pilocarpine in metastatic colon cancer patients following 6-months of bevacizumab treatment [60]. Interestingly, these patients were also treated with the 5-FU containing regimens FOLFIRI and XELOX (5-FU prodrug capecitabine and oxaliplatin). However, the authors do not mention how the 6-months of bevacizumab treatment overlapped with the 5-FU regimens, the dose of 5-FU administered, or

the time between 5-FU administration and experimental testing. Therefore, differences in cutaneous microvascular reactivity between the present work and those stated above may result from methodological differences, specifically the cancer type and severity, the cancer-treatment regimen, and the presence of underlying comorbidities.

This now begs the question: With the local heating and ACh iontophoresis protocols both acting through endothelium-dependent vasodilatory pathways, how could one present with differences while the other remains unaltered between groups? There are several possible explanations. First, local heating and ACh-induced cutaneous vasodilation are mediated by different endothelium-dependent pathways. The plateau phase of the local heating protocol is mediated primarily (~70%) via endothelium-derived NO [26]. In contrast, responses to exogenous ACh occur due to the combined actions of NO, prostanoid, and non-prostanoid/non-NO dependent pathways [41,43,45]. Moreover, multiple reports demonstrate minimal contributions from NO in response to exogenous ACh in the cutaneous microcirculation [42,44]. Thus, whereas reductions in NO may drastically impact the vasodilatory response to local heating, this reduction may not be equally reciprocated in response to ACh iontophoresis. Second, other chemotherapy drugs regularly included in 5-FU-based regimens have been demonstrated to alter the function of sensory neurons—which are key contributors to the initial peak in cutaneous RBC flux seen during local heating. Specifically, oxaliplatin is used alongside 5-FU in both FOLFOX and FOLFIRINOX regimens and is one of the most frequently reported causes of peripheral neuropathy in treated patients. While an alteration to the sensation of heat secondary to oxaliplatin is possible, it appears unlikely as oxaliplatin appears to primarily influence cold, but seemingly not heat sensitivity [66,67]. Further, inhibition of sensory neurons with EMLA cream has been demonstrated to diminish the initial axon reflex to local heat without altering the NO

mediated plateau [27,68] suggesting mechanisms beyond those mediated by sensory neurons are responsible for the group differences observed herein.

The present data support the involvement of the eNOS-NO signaling in the pathophysiology of 5-FU-induced vascular dysfunction. Given the in vitro and in vivo evidence of alterations along the eNOS-NO vasodilatory pathway presented herein, coupled with preclinical works suggesting eNOS attenuation demonstrated elsewhere [64,65], it seems worthy of consideration that reductions in NO bioavailability could facilitate a pathological phenotype within the vasculature of patients treated with 5-FU based regimens. Furthermore, reductions in NO bioavailability give rise to superoxide and endothelium-derived ET-1 [69], the latter of which has been measured at high levels within the blood of 5-FU treated patients [70,71] as well as within the aorta of 5-FU treated rats [65]. Thus, despite the in vitro data of Mosserri et al. [47] suggesting no difference in the vasoconstrictor response between endothelium-denuded and intact aortas, these in vivo findings are provocative in that decrements in eNOS gene expression as well as NO-mediated vasodilation are known precursors to many of the symptoms experienced by 5-FU treated patients. It is worth noting, however, that although our in vitro findings suggest the in vivo alterations in NO dependent cutaneous microvascular reactivity may occur at the level of the endothelium, we cannot entirely discount the possibility of perturbations in the eNOS-NO vasodilator pathway happening downstream of the NO produced by eNOS, as assessment of the production of ROS were beyond the scope of the present investigation. Regardless, future research aimed at elucidating how these factors intertwine to influence coronary vascular health in these patients could ultimately shed light on the mechanisms driving both acute and long-term cardiovascular complications associated with this drug.

Limitations

This study provides important insight into the potential mechanisms contributing to the development of 5-FU cardiotoxicity. However, it does not come without experimental considerations. Importantly, these findings should be kept in context of the model in which they were collected, as impairments in the cutaneous microcirculation, as demonstrated herein, may not be wholly recapitulated within the coronary microcirculation or other vascular beds. Khan and colleagues [61] show a modest, albeit statistically significant, correlation between coronary velocity reserve and iontophoresis of both ACh and SNP in healthy subjects. Nevertheless, more research is needed to elucidate the relationship between the two vascular beds fully. Further, iontophoretic currents can induce non-specific vasodilatory responses that may occur in parallel with those elicited by the administered drug. While we cannot wholly negate the potential contributions of the current, we took numerous precautions to ensure the minimal effect, as detailed in our methodology and confirmed via statistical analyses. Our decision to employ iontophoresis rather than other more invasive protocols (e.g., microdialysis) was made to minimize the risk of potential discomfort experienced by patients. However, this decision requires an increased reliance on consistent resting CVC values across groups and measurement sites. Importantly, we found no statistical differences in our resting CVC values. Lastly, our sample population was treated with a variety of chemotherapeutic regimens containing 5-FU, along with several other medications (e.g., angiotensin-converting enzyme inhibitors, calcium channel blockers, diabetic medications, etc.) as is common in clinical practice, that we were unable to control for in the present investigation. However, all of these medications were documented by the investigators and their use (minus chemotherapeutics) was of similar proportion between groups (all $P > .05$).

Conclusion

The present study demonstrates significantly lower cutaneous microvascular reactivity in cancer patients treated with 5-FU chemotherapy compared to matched healthy controls. Of note, these findings suggest alterations along vasodilatory pathways reliant on endothelium-dependent eNOS-derived NO production. This conclusion is supported by our in vitro findings of decreased eNOS gene expression in 5-FU-treated HCAEC. This study provides mechanistic insight into the vascular toxicities associated with 5-FU chemotherapy and provides the experimental basis for future investigation into potential alterations along the eNOS-NO vasodilatory pathway within the coronary circulation and its relationship with acute and long-term clinical outcomes following 5-FU chemotherapy.

References

1. Dyhl-Polk, A. *et al.* Incidence and risk markers of 5-fluorouracil and capecitabine cardiotoxicity in patients with colorectal cancer. *Acta Oncol (Madr)* **59**, 475–483 (2020).
2. Polk, A., Vaage-Nilsen, M., Vistisen, K. & Nielsen, D. L. Cardiotoxicity in cancer patients treated with 5-fluorouracil or capecitabine: A systematic review of incidence, manifestations and predisposing factors. *Cancer Treat Rev* **39**, 974–984 (2013).
3. Wacker, A., Lersch, C., Scherpinski, U., Reindl, L. & Seyfarth, M. High incidence of angina pectoris in patients treated with 5-fluorouracil: A planned surveillance study with 102 patients. *Oncology* **65**, 108–112 (2003).
4. Sara, J. D. *et al.* 5-fluorouracil and cardiotoxicity: a review. *Ther Adv Med Oncol* **10**, 1–18 (2018).
5. Fabin, N., Bergami, M., Cenko, E., Bugiardini, R. & Manfrini, O. The Role of Vasospasm and Microcirculatory Dysfunction in Fluoropyrimidine-Induced Ischemic Heart Disease. *Journal of Clinical Medicine 2022, Vol. 11, Page 1244* **11**, 1244 (2022).
6. Wacker, A., Lersch, C., Scherpinski, U., Reindl, L. & Seyfarth, M. High Incidence of Angina pectoris in Patients Treated with 5-Fluorouracil. *Oncology* **65**, 108–112 (2003).
7. Eskilsson, J., Albertsson, M. & Mercke, C. Adverse cardiac effects during induction chemotherapy treatment with cis-platin and 5-fluorouracil. *Radiotherapy and Oncology* **13**, 41–46 (1988).
8. Khan, M. A. *et al.* A retrospective study of cardiotoxicities induced by 5-Fluouracil (5-FU) and 5-FU based chemotherapy regimens in Pakistani adult cancer patients at Shaukat Khanum Memorial Cancer Hospital & Research Center. *J Pak Med Assoc* **62**, (2012).
9. Lestuzzi, C. *et al.* Effort myocardial ischemia during chemotherapy with 5-fluorouracil: an underestimated risk. *Annals of Oncology* **25**, 1059–1064 (2014).
10. Lestuzzi, C. *et al.* Fluoropyrimidine-Associated Cardiotoxicity: Probably Not So Rare As It Seems. *Oncologist* **25**, e1254–e1254 (2020).
11. Lestuzzi, C. *et al.* Effort myocardial ischemia during chemotherapy with 5-fluorouracil: an underestimated risk. *Annals of Oncology* **25**, 1059–1064 (2014).
12. Rezkalla, S. *et al.* Continuous ambulatory ECG monitoring during fluorouracil therapy: A prospective study. *Journal of Clinical Oncology* **7**, 509–514 (1989).

13. Jin, X., Bai, Y., Gao, · Lan & Wu, · Shikai. Incidence of and risk factors for cardiotoxicity after fluorouracil-based chemotherapy in locally advanced or metastatic gastric cancer patients. *Cancer Chemother Pharmacol* **84**, 599–607 (2019).
14. Bonadonna, G., Valagussa, P., Moliterni, A., Zambetti, M. & Brambilla, C. Adjuvant Cyclophosphamide, Methotrexate, and Fluorouracil in Node-Positive Breast Cancer — The Results of 20 Years of Follow-up. *N Engl J Med* **332**, 901–906 (1995).
15. Colleoni, M. *et al.* Dose-response effect of adjuvant cyclophosphamide, methotrexate, 5-fluorouracil (CMF) in node-positive breast cancer. International Breast Cancer Study Group. *Eur J Cancer* **34**, 1693–1700 (1998).
16. Aspinall, S. L. *et al.* Adjuvant chemotherapy for stage III colon cancer: Relative dose intensity and survival among veterans. *BMC Cancer* **15**, 1–13 (2015).
17. Polk, A., Vistisen, K., Vaage-Nilsen, M. & Nielsen, D. L. A systematic review of the pathophysiology of 5-fluorouracil-induced cardiotoxicity. *BMC Pharmacol Toxicol* **15**, 1–11 (2014).
18. Luwaert, R., Descamps, O., Majois, F., Chaudron, JM. & Beauduin, M. Coronary artery spasm induced by 5-fluorouracil. *Eur Heart J* **12**, 468–470 (1991).
19. Shoemaker, L. K., Arora, U. & Rocha Lima, C. M. S. 5-Fluorouracil–Induced Coronary Vasospasm. **11**, 46–49 (2017).
20. Südhoff, T. *et al.* 5-Fluorouracil induces arterial vasocontractions. *Annals of Oncology* **15**, 661–664 (2004).
21. Sutterfield, S. L. *et al.* Lower cutaneous microvascular reactivity in adult cancer patients receiving chemotherapy. *J Appl Physiol* **125**, 1141–1149 (2018).
22. Banister, H. R. *et al.* Lower endothelium-dependent microvascular function in adult breast cancer patients receiving radiation therapy. *Cardio-Oncology* **7**, 1–8 (2021).
23. Hodges, G. J., Chiu, C., Kosiba, W. A., Zhao, K. & Johnson, J. M. The effect of microdialysis needle trauma on cutaneous vascular responses in humans. *J Appl Physiol* **106**, 1112–1118 (2009).
24. Was, H. *et al.* Mechanisms of Chemotherapy-Induced Neurotoxicity. *Front Pharmacol* **13**, (2022).
25. Quintão, N. L. M. *et al.* Pharmacological Treatment of Chemotherapy-Induced Neuropathic Pain: PPARγ Agonists as a Promising Tool. *Front Neurosci* **13**, (2019).

26. Bruning, R. S. *et al.* Endothelial nitric oxide synthase mediates cutaneous vasodilation during local heating and is attenuated in middle-aged human skin. *J Appl Physiol* **112**, 2019–2026 (2012).
27. Minson, C. T., Berry, L. T. & Joyner, M. J. Nitric oxide and neurally mediated regulation of skin blood flow during local heating. *J Appl Physiol* **91**, 1619–1626 (2001).
28. Kellogg, D., Zhao, JL. & Wu, Y. Roles of nitric oxide synthase isoforms in cutaneous vasodilation induced by local warming of the skin and whole body heat stress in humans. *J. Appl. Physiol.* **107**, 1438–1444 (2009).
29. Kellogg, DL., Liu, Y., Kosiba, I. F. & O'Donnell, D. Role of nitric oxide in the vascular effects of local warming of the skin in humans. *J. Appl. Physiol.* **86**, 1185–1190 (1999).
30. Medow, M. S., Taneja, I. & Stewart, J. M. Cyclooxygenase and nitric oxide synthase dependence of cutaneous reactive hyperemia in humans. *American Journal of Physiology-Heart and Circulatory Physiology* **293**, H425–H432 (2007).
31. Medow, M. S., Minson, C. T. & Stewart, J. M. Decreased microvascular nitric oxide-dependent vasodilation in postural tachycardia syndrome. *Circulation* **112**, 2611–2618 (2005).
32. Kellogg, D. L., Zhao, J. L. & Wu, Y. Endothelial nitric oxide synthase control mechanisms in the cutaneous vasculature of humans in vivo. *Am J Physiol Heart Circ Physiol* **295**, 123–129 (2008).
33. Magerl, W. & Treede, R. D. Heat-evoked vasodilatation in human hairy skin: axon reflexes due to low-level activity of nociceptive afferents. *J Physiol* **497**, 837–848 (1996).
34. Wauters, A. *et al.* Acute exposure to diesel exhaust impairs nitric oxide-mediated endothelial vasomotor function by increasing endothelial oxidative stress. *Hypertension* **62**, 352–358 (2013).
35. Alexander, L. M., Kutz, J. L. & Larry Kenney, W. Tetrahydrobiopterin increases NO-dependent vasodilation in hypercholesterolemic human skin through eNOS-coupling mechanisms. *Am J Physiol Regul Integr Comp Physiol* **304**, 164–169 (2013).
36. Stanhewicz, A. E., Jandu, S., Santhanam, L. & Alexander, L. M. Increased Angiotensin II Sensitivity Contributes to Microvascular Dysfunction in Women Who Have Had Preeclampsia. *Hypertension* **70**, 382–389 (2017).

37. Kirkman, D. L., Muth, B. J., Ramick, M. G., Townsend, R. R. & Edwards, D. G. Role of mitochondria-derived reactive oxygen species in microvascular dysfunction in chronic kidney disease. *Am J Physiol Renal Physiol* **314**, F423–F429 (2018).
38. Smith, C. J. *et al.* Upregulation of inducible nitric oxide synthase contributes to attenuated cutaneous vasodilation in essential hypertensive humans. *Hypertension* **58**, 935–942 (2011).
39. Dreyfuss, C. *et al.* L-NAME iontophoresis: A tool to assess NO-mediated vasoreactivity during thermal hyperemic vasodilation in humans. *J Cardiovasc Pharmacol* **61**, 361–368 (2013).
40. Wauters, A. *et al.* Acute exposure to diesel exhaust impairs nitric oxide-mediated endothelial vasomotor function by increasing endothelial oxidative stress. *Hypertension* **62**, 352–358 (2013).
41. Noon, J. P., Walker, B. R., Hand, M. F. & Webb, D. J. Studies with iontophoretic administration of drugs to human dermal vessels in vivo: cholinergic vasodilatation is mediated by dilator prostanoids rather than nitric oxide. *Br J Clin Pharmacol* **45**, 545–550 (1998).
42. Holowatz, L. A., Thompson, C. S., Minson, C. T. & Kenney, W. L. Mechanisms of acetylcholine-mediated vasodilation in young and aged human skin. *Journal of Physiology* **563**, 965–973 (2005).
43. Kellogg, D. L., Zhao, J. L., Coey, U. & Green, J. V. Acetylcholine-induced vasodilation is mediated by nitric oxide and prostaglandins in human skin. *J Appl Physiol* **98**, 629–632 (2005).
44. Khan, F. *et al.* Cutaneous Vascular Responses to Acetylcholine are Mediated by a Prostanoid-Dependent Mechanism in Man. *Vascular Medicine* **2**, 82–86 (1997).
45. Newton, DJ., Davies, J., Belch, JJF., Khan, F. Role of endothelium-derived hyperpolarising factor in acetylcholine-mediated vasodilatation in skin. *International Angiology* **32**, 312–8 (2013).
46. Loader, J. *et al.* Assessing cutaneous microvascular function with iontophoresis: Avoiding non-specific vasodilation. *Microvasc Res* **113**, 29–39 (2017).

47. Mosseri, M., Fingert, H. J., Varticovski, L., Chokshi, S. & Isner, J. M. In Vitro Evidence That Myocardial Ischemia Resulting from 5-Fluorouracil Chemotherapy Is Due to Protein Kinase C-mediated Vasoconstriction of Vascular Smooth Muscle. *Cancer Res* **53**, (1993).
48. Hayward, R. *et al.* Training Enhances Vascular Relaxation after Chemotherapy-Induced Vasoconstriction. *Med Sci Sports Exerc* **36**, 428–434 (2004).
49. Weir, J. P. & Vincent, W. J. *Statistics in kinesiology*. (Human Kinetics, 2021).
50. Widlansky, M. E., Gokce, N., Keaney, J. F. & Vita, J. A. The clinical implications of endothelial dysfunction. *J Am Coll Cardiol* **42**, 1149–1160 (2003).
51. Quyyumi, A. A., Cannon, R. O., Panza, J. A., Diodati, J. G. & Epstein, S. E. Endothelial dysfunction in patients with chest pain and normal coronary arteries. *Circulation* **86**, 1864–1871 (1992).
52. Kugiyama, K. *et al.* Nitric Oxide Activity Is Deficient in Spasm Arteries of Patients With Coronary Spastic Angina. *Circulation* **94**, 266–272 (1996).
53. Quyyumi, A. A. *et al.* Contribution of nitric oxide to metabolic coronary vasodilation in the human heart. *Circulation* **92**, 320–326 (1995).
54. van den Heuvel, M. *et al.* Coronary microvascular dysfunction in a porcine model of early atherosclerosis and diabetes. *Am J Physiol Heart Circ Physiol* **302**, 85–94 (2012).
55. Anderson, T. J. *et al.* Close relation of endothelial function in the human coronary and peripheral circulations. *J Am Coll Cardiol* **26**, 1235–1241 (1995).
56. Sokolnicki, L. A., Roberts, S. K., Wilkins, B. W., Basu, A. & Charkoudian, N. Contribution of nitric oxide to cutaneous microvascular dilation in individuals with type 2 diabetes mellitus. *Am J Physiol Endocrinol Metab* **292**, 314–318 (2007).
57. Alba, B. K., Greaney, J. L., Ferguson, S. B. & Alexander, L. M. Endothelial function is impaired in the cutaneous microcirculation of adults with psoriasis through reductions in nitric oxide-dependent vasodilation. *Am J Physiol Heart Circ Physiol* **314**, H343–H349 (2018).
58. Agarwal, S. C., Allen, J., Murray, A. & Purcell, I. F. Laser Doppler assessment of dermal circulatory changes in people with coronary artery disease. *Microvasc Res* **84**, 55–59 (2012).
59. Green, D. J. *et al.* Impaired skin blood flow response to environmental heating in chronic heart failure. *Eur Heart J* **27**, 338–343 (2006).

60. Mourad, J. J., des Guetz, G., Debbabi, H. & Levy, B. I. Blood pressure rise following angiogenesis inhibition by bevacizumab. A crucial role for microcirculation. *Annals of Oncology* **19**, 927–934 (2008).
61. Khan, F., Patterson, D., Belch, J., Hirata, K. & Lang, C. Relationship between peripheral and coronary function using laser Doppler imaging and transthoracic echocardiography. *Clin Sci* **15**, 295–300 (2008).
62. Green, D. J., Dawson, E. A., Groenewoud, H. M. M., Jones, H. & Thijssen, D. H. J. Is flow-mediated dilation nitric oxide mediated?: A meta-analysis. *Hypertension* **63**, 376–382 (2014).
63. Kirkman, D. L., Robinson, A. T., Rossman, M. J., Seals, D. R. & Edwards, D. G. Mitochondrial contributions to vascular endothelial dysfunction, arterial stiffness, and cardiovascular diseases. *Am J Physiol Heart Circ Physiol* **320**, H2080–H2100 (2021).
64. Altieri, P. *et al.* 5-fluorouracil causes endothelial cell senescence: potential protective role of glucagon-like peptide 1. *Br J Pharmacol* **174**, 3713–3726 (2017).
65. Muhammad, R. N., Sallam, N. & El-Abhar, H. S. Activated ROCK/Akt/eNOS and ET-1/ERK pathways in 5-fluorouracil-induced cardiotoxicity: modulation by simvastatin. *Sci Rep* **10**, 14693 (2020).
66. Xiao, W. H., Zheng, H. & Bennett, G. J. Characterization of oxaliplatin-induced chronic painful peripheral neuropathy in the rat and comparison with the neuropathy induced by paclitaxel. *Neuroscience* **203**, 194–206 (2012).
67. Descoeur, J. *et al.* Oxaliplatin-induced cold hypersensitivity is due to remodelling of ion channel expression in nociceptors. *EMBO Mol Med* **3**, 266 (2011).
68. Carter, S. J. & Hodges, G. J. Sensory and sympathetic nerve contributions to the cutaneous vasodilator response from a noxious heat stimulus. *Exp Physiol* **96**, 1208–1217 (2011).
69. Hink, U. & Münzel, T. COX-2, another important player in the nitric oxide-endothelin cross-talk: Good news for COX-2 inhibitors? *Circ Res* **98**, 1344–1346 (2006).
70. Thyss, A. *et al.* Very high endothelin plasma levels in patients with 5-FU cardiotoxicity. *Annals of Oncology* **3**, 88 (1992).
71. Porta, C., Moroni, M., Ferrari, S. & Nastasi, G. Endothelin-1 and 5-fluorouracil-induced cardiotoxicity. *Neoplasma* **45**, 81–82 (1998).

Chapter 3 - 5-fluorouracil promotes calcification of vascular smooth muscle cells

Abstract

Background: 5-flurouracil (5-FU) chemotherapy is a critical component of many gastrointestinal, head/neck, and breast cancer treatment regimens. Its use is regularly associated with cardiotoxicity, which may result from a direct effect of the drug on vascular endothelium and/or smooth muscle. While reports of vascular alterations are commonplace during or shortly following cessation of treatment, the latent effect 5-FU may have on the vasculature years into cancer survivorship remains unknown. Thus, the present work aimed to test the effect of 5-FU on the development of calcification—a key to long-term cardiovascular outcomes—in rat aortic smooth muscle cells (SMC). We hypothesized that exposure to 5-FU would result in calcium deposition when exposed to a calcification-inducing media and that in vitro treatment with 5-FU would increase calcium concentrations in previously untreated cells. **Methods:** We conducted experiments on primary SMC derived from the thoracic aortas of male Sprague-Dawley rats following a 2h infusion of either a clinically relevant dose of 5-FU (n=3) or volume-matched saline (n=4). SMC from 5-FU and saline (CON) treated animals were cultured in normal growth medium (Grow. M.) or a high-phosphate (3.2 mmol/L Pi) calcification medium (Calc. M.) for 5- and 8-day periods to assess the effect of in vivo 5-FU exposure on the development of calcium deposition in culture. Subsequent experiments assessed whether the inclusion of 5-FU (7mM for 60h) in the culture medium of cells derived from CON resulted in increased calcium levels. We assessed calcification using an Alizarin Red S stain with quantification assay (ARS) and a calcium concentration assay. **Results:** In SMC derived from CON animals, there were no significant differences in ARS concentration when treated with Grow M. or Calc. M. for 5 or 8

days. However, 5-FU-derived cells treated with Calc. M. had a significantly higher ARS concentration at 5 and 8 days than 5-FU cells treated with Grow. M. Calcium concentration assay at the 8-day time point supported these findings. When CON-derived cells were exposed to 5-FU in vitro, a significant calcium concentration increase was present compared to the culture in Grow. M. alone. **Conclusion:** Findings from the present work suggest that SMC exposed to 5-FU—whether under in vivo or in vitro conditions—are prone to the development of calcium deposition in cell culture. These findings provide preclinical support for further investigation into the potential long-term consequences of 5-FU chemotherapy which may arise years into survivorship.

Introduction

A continuous decline in cancer mortality has been evident since 1991, resulting in the avoidance of nearly 3.8 million cancer deaths [1]. These improvements are due to various factors, including the strategic use of various anti-cancer chemotherapies [1]. Among these efficacious treatments is 5-fluorouracil—a pyrimidine antimetabolite chemotherapy primarily used to treat gastrointestinal, head/neck, and breast cancers [2]. 5-FU mediates its anti-tumor effects on cancer cells via intracellular conversion to one of several active metabolites, ultimately damaging RNA and DNA synthesis and repair mechanisms [3]. While this outcome is desirable concerning cancer treatment, 5-FU has also gained notoriety for its unfortunate association with off-target clinical side effects, including myelosuppression, cardiotoxicity, nephrotoxicity, and mucositis. The vast majority of the literature on this topic has emphasized the short-term cardiovascular consequences of 5-FU which arise during or shortly following cessation of therapy. These side effects most frequently include angina or acute coronary syndromes at rest or with exertion, ECG alterations indicative of myocardial ischemia, and in severe circumstances, have been documented to progress to myocardial infarction and sudden cardiac death [2,4–9].

To date, the manifestation of acute 5-FU cardiotoxicity is commonly believed to be a consequence of a direct effect of the drug on the vasculature [2], with both in vitro and in vivo evidence of altered vessel tone [10–12] during or shortly following exposure to 5-FU. However, the long-term consequence that 5-FU could have on the vasculature in cancer survivorship is not well understood. Recent unpublished observations from our laboratory, as well as the published findings of others, has indicated alterations in both NO-mediated vasodilator pathways [11,13] and a rise in arterial stiffness [14] following treatment with 5-FU-based regimens. Not only do such changes have short-term consequences for cardiovascular health, but they also set the stage for

the future development of long-term cardiovascular-related ailments in the years following treatment [15]. Specifically, impaired endothelial function and the onset of arterial stiffening are considered vital contributors to the development of vascular calcification [16]—a well-established predictor of cardiovascular disease and all-cause mortality [17–19]. Indeed, even low levels of coronary artery calcification (CAC, CAC score of 1-10) are associated with nearly a 2-fold greater increase in mortality compared to CAC scores of 0 [20]. Thus, provided the growing in vitro and in vivo evidence for the potential development of critical precursors of arterial calcification following 5-FU treatment, we tested the hypothesis that rat aortic smooth muscle cells (SMC) exposed to 5-FU under both in vivo and in vitro conditions would be more prone to the development of calcium deposits following culture with a calcification inducing, high-phosphate medium, than SMC devoid of 5-FU. To test this hypothesis, we conducted experiments in SMC derived from the aortas of animals treated in vivo with a clinically relevant dose of 5-FU or volume-matched saline. First, SMC isolated from 5-FU and saline-treated animals were incubated in a calcification medium to assess the development of calcium deposits. Follow-up experiments were conducted to determine if the application of 5-FU directly to the cells resulted in the development of calcification in previously untreated SMC. We hope that findings from the present work will provide preliminary evidence for further in vivo investigation into the potential long-term vascular consequences of 5-FU chemotherapy treatment.

Methods

Animals

All procedures performed herein were approved by the Kansas State University Institutional Animal Care and Use Committee and conformed to the National Institutes of Health Guide for the Care and Use of Laboratory Animals. Male Sprague Dawley rats (n=7, 6-8 mo. old, avg. weight = 622 g; Charles River; Wilmington, MA) were housed in a temperature-controlled facility (23°C) on a 12:12-h light-dark cycle. Standard rat chows and water were provided *ab libitum*.

Surgical procedures

Before surgery, animals were first anesthetized with a 5% isoflurane-O_2 mixture (isoflurane vaporizer; Harvard Apparatus; Cambridge, MA) and placed on a heated surgical station (Rodent Surgical Monitor, Indus Instruments; Houston, TX) maintained at 37°C. Surgical procedures were then completed with rats maintained at a 2.5% isofluorane-O_2 mixture. First, an incision was made in the left ventral neck for placement of a left jugular vein catheter (PE-50 tubing) used for continuous infusion of 5-FU chemotherapy or saline. A second catheter was then placed in the caudal artery (PE-10 connected to PE-50 tubing) for continuous blood pressure monitoring (Digi-Med BPA; Micro-Med; Louisville, KY) over the course of the experimental treatment protocol. Upon completion of the catheterization procedures, rats were transitioned from isoflurane to pentobarbital anesthesia by slowly reducing the isoflurane concentration to 0%. For the remainder of the experiment, rats were continuously monitored through palpebral and toe flinch reflexes and supplemented with pentobarbital sodium anesthesia (~16 mg/kg/hr) via the caudal artery as needed.

In vivo 5-fluorouracil (5-FU) or saline administration

Following the completion of surgical procedures, all animals were randomized to receive treatment with either a clinically relevant dose of 5-FU (n=3) or volume-matched saline (n=4) control (CON). In clinical practice, common 5-FU-based regimens such as FOLFOX (Folinic acid, 5-FU, Oxaliplatin) [21], FOLFIRI (Folinic acid, 5-FU, Irinotecan) [22], and FOLFIRINOX (Folinic acid, 5-FU, Irinotecan, Oxaliplatin) [23] often include an intravenous 5-FU bolus of 400 mg/m^2 followed by the initiation of a continuous infusion of 2,400 mg/m^2 delivered for 46 – 72 hours. Thus, we designed a translational rat model of 5-FU cardiotoxicity, using allometric scaling [24] from the doses used in clinical practice, to align our study with the drug delivery methods used clinically. Following the completion of surgical procedures, a slow bolus dose of 50 mg/kg of 5-FU or volume-matched saline was delivered via a jugular catheter using a 10 mL syringe. The jugular catheter was then attached to a programmable syringe pump (Pump 11 Elite, Harvard Apparatus, Holliston, MA) for initiation of a 2h continuous infusion of 265 mg/kg 5-FU or volume matched saline (henceforth referred to as CON).

Isolation of primary SMC

Upon completion of the 2h infusion, all animals were euthanized via thoracotomy followed by heart removal. The thoracic aorta was immediately removed and placed in a sterile 100-mm tissue culture dish (130182, Thermo Scientific, Waltham, MA) filled with ice-cold Dulbecco's Modified Eagle's Medium (DMEM) (30-2001, American Type Culture Collection, Manassas, VA), and transferred to a sterile biological safety cabinet for SMC isolation using a modified aortic explant technique [25]. The aortic tissue was first cleaned of blood and surrounding connective tissue using sterile forceps and micro scissors before transfer to a second 100-mm cell culture dish containing fresh DMEM. The tissue was then cut longitudinally to expose the vessel

lumen while using the blunt end of curved forceps to scrape the intimal layer to remove endothelial cells gently. Fresh DMEM was used to rinse the vessel lumen of remaining adherent cells and debris prior to placing it in a third culture dish with fresh DMEM, 1% penicillin-streptomycin (100 U/ml penicillin, 100 ug/ml Streptomycin) (15140122, Life Technologies, Carlsbad, CA), and 1% glutamine (25030164, Life Technologies) (henceforth referred to as pre-culture medium). Next, while holding the vessel in place with a clean set of forceps, a second set of forceps was used to separate the vessel media (i.e., tunica media) from the adventitia by pressing and pulling the vessel dorsally. Once clear separation of the two layers was achieved, the vessel media was placed in a fourth 100-mm cell culture dish supplemented with pre-culture medium and cut into 3-5 small pieces (~.5 mm^2 each). The dish was then placed in an incubator (37°C/5% CO_2) for 4-6 hours to allow the explants to attach to the cell culture dish. Upon attachment, 3 mL of additional pre-culture medium supplemented with 20% fetal bovine serum (FBS) (S11550, R&D Systems, Minneapolis, MN) (henceforth referred to as 20% growth medium) was added to the dish. Spent growth medium was replaced with 5 mL of fresh 20% growth medium every 48 hours.

Subculture of primary SMC

Once cells began to grow from the aortic tissue explant and reach local confluency (~10 days from initial plating), the cell culture medium and aortic tissue explant were gently removed, leaving the SMC remaining in the dish. The SMC were gently washed with sterile 1x-phosphate-buffered saline (1xPBS) prior to cell collection via incubation with Trypsin EDTA (0.05% trypsin, 0.02% EDTA) for primary cells (PCS-999-003; ATCC). After ~3 minutes of incubation, the trypsin solution was deactivated with equal parts 20% growth medium. The cells were collected and pelleted via centrifugation at 150 x g for 5 minutes. Cells were then counted using

a hemocytometer to calculate appropriate freezing and plating densities for future experiments. All subsequent subculturing was completed in pre-culture medium supplemented with 10% FBS (henceforth referred to as 10% growth medium) in 75 cm^2 tissue culture treated flasks (156499, Thermo Scientific) as needed to obtain sufficient numbers of cells for experiments. During specific calcification experiments (described below), cells were seeded in either 6-well plates (Product ID3516; Corning, Glendale, AZ, USA) (10-20k cells per well) or 100 mm^2 dishes (50-100k cells per dish). Plating densities were selected with consideration of typical SMC doubling times and expected confluency values on the day of the experiment. Cells not presently used for experiments were stored in a liquid nitrogen vapor phase in 2 mL cryovials (368632, Thermo Fisher) suspended in 1.5 mL of 10% growth medium and 7% DMSO. Prior to conducting experiments, select SMC from each group were stained with monoclonal antibodies for α-smooth muscle actin (ab184675, Abcam, Waltham, MA) and DAPI (P36935, Invitrogen, Waltham, MA) and imaged (Axio Observer.A1, Zeiss, Dublin, CA) under 100-400x magnification to ensure high proportion of smooth muscle cells were present in each cell line (**Figure 3.1)**. All cell culture experiments were completed on SMC between passages 4 and 6 using an aseptic technique in a sterile biological safety cabinet with downward-flowing HEPA-filtered air. Surgical tools used in SMC isolation were sterilized using an autoclave, and all cell culture medium components were passed through a vacuum filter (431097, Corning, Glendale, AZ) prior to use.

Figure 3.1 Rat aortic smooth muscle cells stained with smooth muscle actin

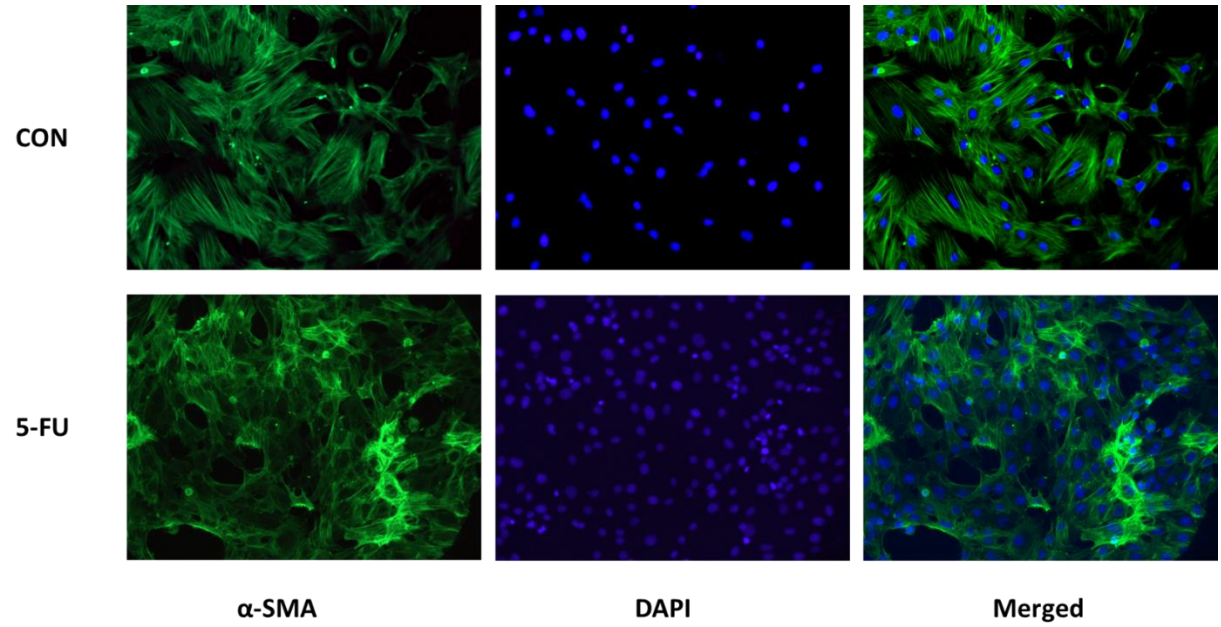

Representative alpha-smooth muscle actin (α-SMA) and nuclear (DAPI) counterstains in rat aortic smooth muscle cells derived from control (top) and 5-FU (bottom) treated Sprague-Dawley rats. SMC were grown on sterile coverslips and fixed with 100% methanol. Cells were imaged at 200x magnification.

Induction of SMC calcification

As demonstrated by others [26–28], SMC calcification was induced via incubation in a calcification medium (10% growth medium in the presence of 3.2 mmol/L inorganic phosphate). Briefly, calcification medium (Calc. M.) or normal growth medium (Grow. M.) was applied to CON and 5-FU cells every 48 hours during standard medium changes over the course of 5- and 8-day time frames. Vascular calcification was assessed using two separate techniques: 1) Alizarin red staining with quantification assay (ab146374, Abcam) and 2) a colorimetric calcium assay (Product ID: 701220, Cayman Chemical, Ann Arbor, MI). Protocols for each method of calcification detection as well as the respective experiments are described below.

Alizarin Red S staining and quantification assay

A graphical summary of this protocol is depicted in **Figure 3.2 (Exp. 1a)**. Alizarin red S (ARS) staining and quantification was completed with slight modifications from the methods described by Gregory et al. [29]. Briefly, ARS reacts with calcium resulting in the formation of calcium complexes which can be first viewed using an inverted microscope and then quantified via extracting the dye and completing an absorbance assay [29]. SMC lines derived from CON (N=3) and 5-FU (N=3) treated animals were seeded in 6-well plates (1 plate with 6 separate wells per cell line) as described above. Following a brief attachment period (24-48h), the 6 wells on each plate were randomly assigned treatment with Grow. M. or Calc. M. (n=3 each). Plates were treated as described above for 5- and 8-day time periods. Upon completion of the designated time frame, culture medium was carefully decanted, and the cell monolayer was washed 3 times with 1xPBS before fixing the cells with 4% formaldehyde. After 15 minutes of incubation at room temperature, the formaldehyde was removed, and the cells were washed an additional 3 times with diH_2O. 1.5 mL of 40 mM ARS was then added to each well and

incubated at 20°C on a plate rocker for 30 minutes. The dye was then removed, and the monolayer was washed 5 times with deionized water. Wells from each dish were imaged using an inverted fluorescent microscope (Axio Observer.A1). Stained cells were then extracted for ARS stain quantification via addition of 800 µL of 10% acetic acid to each well followed by a 30-minute incubation period on a plate rocker at 20°C. Cells were then carefully collected using a sterile cell scraper (70-1180, Biologix, Camarillo, CA) and transferred to a 1.5 µL centrifuge tube. Each tube was vortexed for ~30 seconds, covered in parafilm, and then placed on a microcentrifuge tube dry bath heater (BSH1002, Benchmark, Sayereville, NJ) set to 85°C for 10 minutes. Tubes were then fully cooled on ice for 5 minutes and centrifuged for 15 minutes at 20,000g. 500 µL of the cell mixture was transferred to a fresh 1.5 µL centrifuge tube and gently mixed with 200 µL of 10% ammonium hydroxide to neutralize the acid. 150 µL aliquots from each well were then plated in a 96-well plate to be read on a commercially available microplate reader (accuSkan GO, Thermo Fisher) at 405 nm. Absorbance values were used to calculate ARS concentration in mM using the methods described by Gregory et al. [29]. Absolute ARS concentrations were compared between Grow. M. and Calc. M. conditions within each group at the 5- and 8-day time points to determine differences in calcium deposition. However, given the different cell growth rates in CON and 5-FU derived cells, we also calculated the percent difference in ARS absorbance in Calc. M. relative to Grow. M. condition for a given time point to allow for comparison between the groups (i.e., CON and 5-FU). Samples from each well were completed in duplicate, with cells from 9 total wells compared between NM and CM conditions (n=9 per group) at each time point for both CON and 5FU cells.

Figure 3.2. Graphical representation of the experimental design

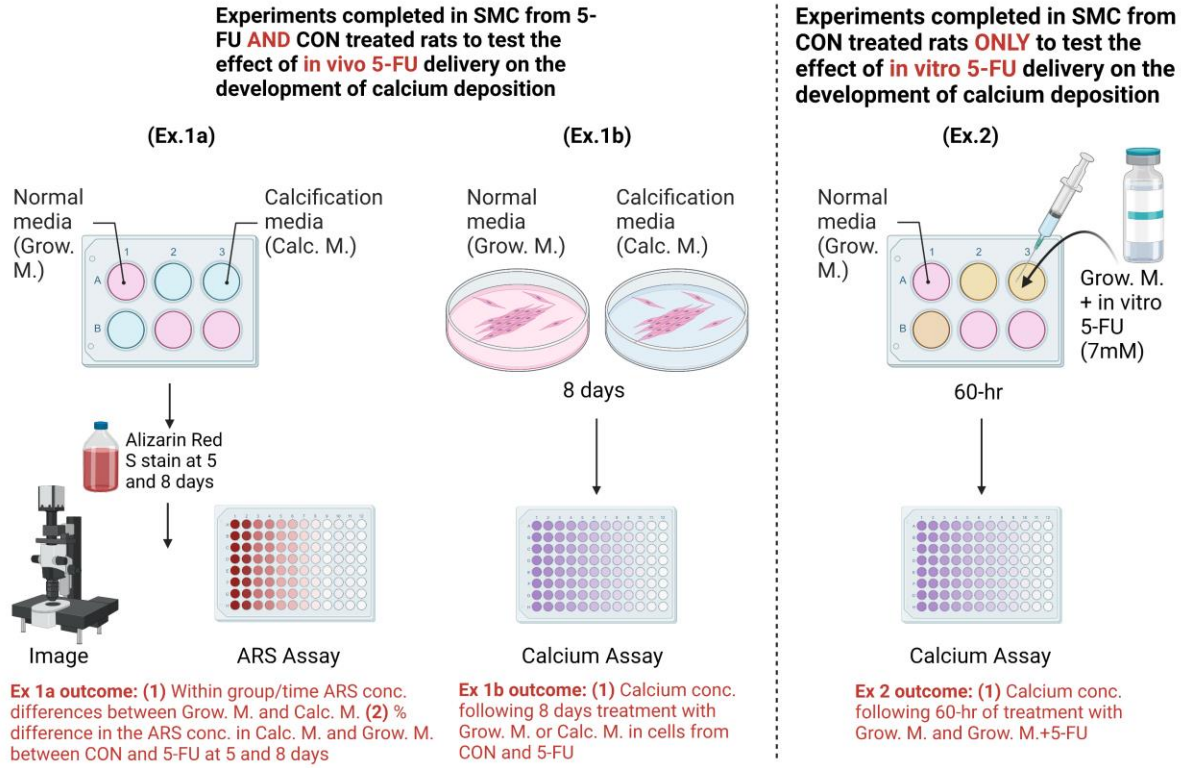

Experimental design with individual experimental outcomes. Figure created with Biorender.com.

Calcium concentration assay

To further compare potential differences in the development of calcification between CON and 5-FU derived SMC, a commercially available calcium quantification assay based on the o-Cresolphthalein-calcium reaction was completed per manufacturer guidelines with slight modifications. Two separate experiments were conducted to better understand the impact of both in vivo and in vitro 5-FU delivery on the development of calcification in SMC. A graphical representation of each of these protocols is depicted in **Figure 3.2 (Ex.1b and Ex.2).** First, experiments were conducted in SMC lines derived from both 5-FU (n=3) and CON (n=3) animals. SMC from each group were seeded in 100 mm^2 culture dishes as described above, with each cell line plated in two separate dishes (12 total dishes, n=3 per group). Following completion of 8-days of treatment with Grow. M. or Calc. M., cells were collected as described above and protein concentrations were determined using a Qubit 2.0 Fluorometer (Life Technologies). The calcium assay was then completed according to manufacturer guidelines while normalizing each sample for total protein to account for potential differences in cell number between the groups. A second experiment was completed in SMC derived from CON cells to test the effect of in vitro 5-FU administration on the development of calcification. Four separate CON cell lines were treated with Grow. M. with or without the addition of 7mM of 5-FU (Grow. M. + 5-FU) for 60h (n=4 cultures per group) to determine if 5-FU alone could stimulate increases in calcium. The assays for both experiments were completed on a commercially available plate reader at 570 nm with all samples completed in duplicate. Absorbance values were used to calculate total calcium concentration in mg/dl according to manufacturer guidelines.

Statistical analysis

All statistical analyses were completed using a commercially available software package (GraphPad Prism 9.5; San Diego, Ca, USA). Differences in ARS concentration between Grow. M. and Calc. M. conditions were compared using independent samples t-tests at each time point for both CON and 5-FU derived SMC. The percent change in ARS concentration in CM relative to the Grow. M. condition was compared between groups using a two-way analysis of variance (2-way ANOVA) with main effects for group (CON and 5-FU) and time point (5 and 8 days). Calcium concentrations using the o-Cresolphthalein-calcium reaction were also compared between groups using a 2-way ANOVA with main effects for group (5-FU and CON) and treatment medium (Grow. M. and Calc. M.). Multiple comparisons were assessed using Šídák's multiple comparisons test as appropriate. To determine whether in vitro administration of 5-FU influenced calcium concentrations in SMC from CON treated animals, cells treated with Calc. M. with and without administration of 7 mM of 5-FU were compared using an independent samples t-test. Statistical significance was set to 0.05 for all tests.

Results

Alizarin Red S

Representative ARS stains of SMC derived from in vivo treated CON and 5-FU animals following 8-days of treatment with Grow. M. and Calc. M. are presented in **Figures 3.3a and 3.4a**, respectively. In cultured SMC derived from CON aortas, ARS concentrations did not differ following 5-days of culture in Grow. M. or Calc. M. (NM = 0.140 ± 0.024 mM ARS, v = 0.142 ± 0.024 mM ARS, P = 0.88) (**Figure 3.3b**). Similarly, no differences in ARS concentration were present between Grow. M. and Calc. M. treated cells following 8 days of treatment (Grow. M. = 0.125 ± 0.028 mM ARS, Calc. M. = 0.121 ± 0.023 mM ARS, P = 0.75) (**Figure 3.3c**) in CON cells.

Figure 3.3. Alizarin Red S staining and assay in cells derived from CON treated animals

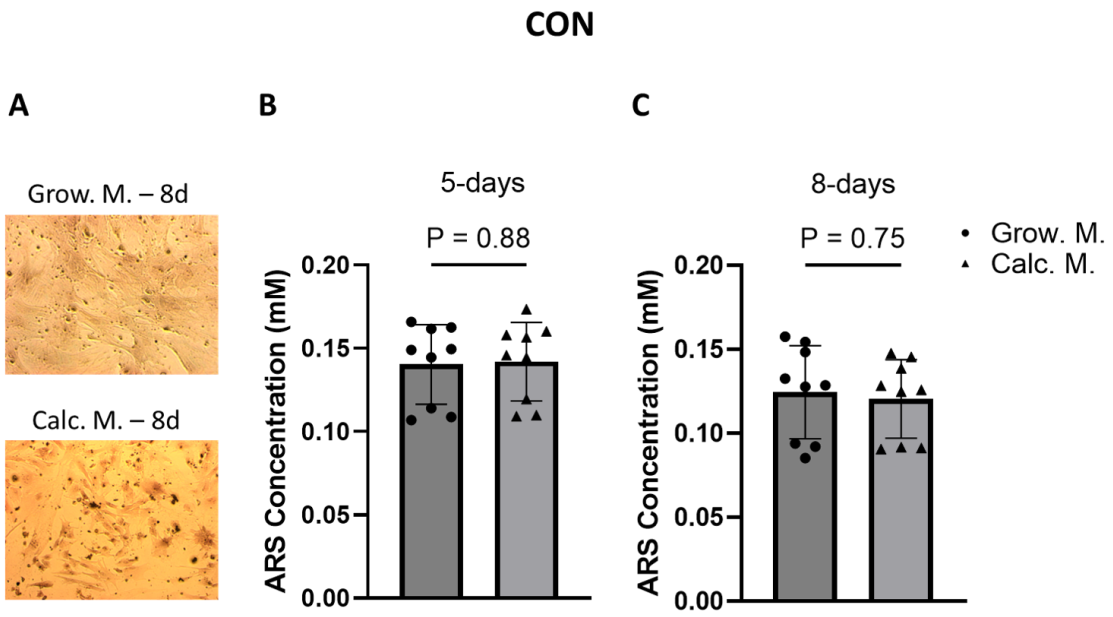

Representative ARS images (A) in cells derived from CON-treated animals at the 8-day timepoint for Grow. M. (top) and Calc. M. (bottom) media treatment conditions. In SMC derived from saline (CON) treated animals, no differences in ARS concentration were detected at the 5- (B) or 8-day (C) time points between Grow. M. and Calc. M.-treated cells. Cell lines from 3 CON and 3 5-FU treated animals were used (3 wells per cell line per condition). All samples were assayed in duplicate. Data were analyzed using independent-samples t-tests. Grow. M. = normal growth media. Calc. M. = calcification media.

Conversely, in SMC derived from 5-FU treated animals, there were significant increases in ARS concentration at the 5- (Grow. M. = 0.084 ± 0.02, Calc. M. = 0.100 ± 0.01, P = 0.02) (**Figure 3.4b**) and 8-day (Grow. M. = 0.082 ± 0.01, Calc. M. = 0.010 ± 0.02, P = 0.007) (**Figure 3.4c**) timepoints suggesting greater calcium deposition in Calc. M. treated cells from 5-FU animals. No significant group x time interaction (P = 0.36) or main effect for time (P = 0.75) was present when comparing the percent difference in ARS concentration from the two media conditions between CON and 5-FU groups, yet a significant main effect was apparent for group (P = < 0.001). Post-hoc analysis revealed no differences between the groups at the 5-day time point (CON: 1.55 ± 7.7%; 5-FU: 20.93 ± 15.4%; P = 0.08). However, at the 8-day time point, 5-FU had a significantly greater percent difference in ARS (CON: -2.34 ± 7.8%; 5-FU: 28.94 ± 33.1%; P = 0.003) than CON, suggesting a greater effect of Calc. M. media in inducing calcium deposition in cells derived from 5-FU treated animals. (**Figure 3.5**).

Figure 3.4. Alizarin red S staining and assay in cells derived from 5-FU treated animals

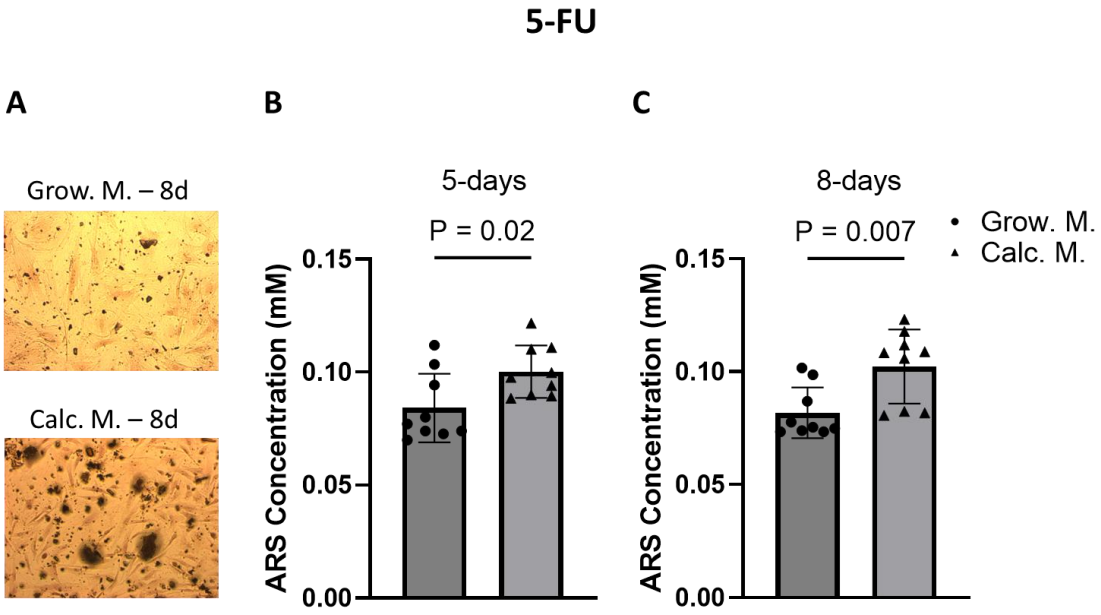

Representative ARS images (A) in cells derived from 5-FU treated animals at the 8-day time point for Grow. M. (top) and Calc. M. (bottom) media treatment conditions. SMC derived from 5-FU treated animals had significantly greater ARS absorbance at 5- (B) and 8-days (C) when treated with Calc. M. compared to Grow. M. n = 9 individual wells per media treatment condition for each time point. Cell lines from 3 CON and 3 5-FU treated animals were used (3 wells per cell line per condition). All samples were assayed in duplicate. Data were analyzed using independent-samples t-tests. Grow. M. = normal growth media. Calc. M. = calcification media.

Figure 3.5. ARS percent change between media conditions in CON and 5-FU derived cells

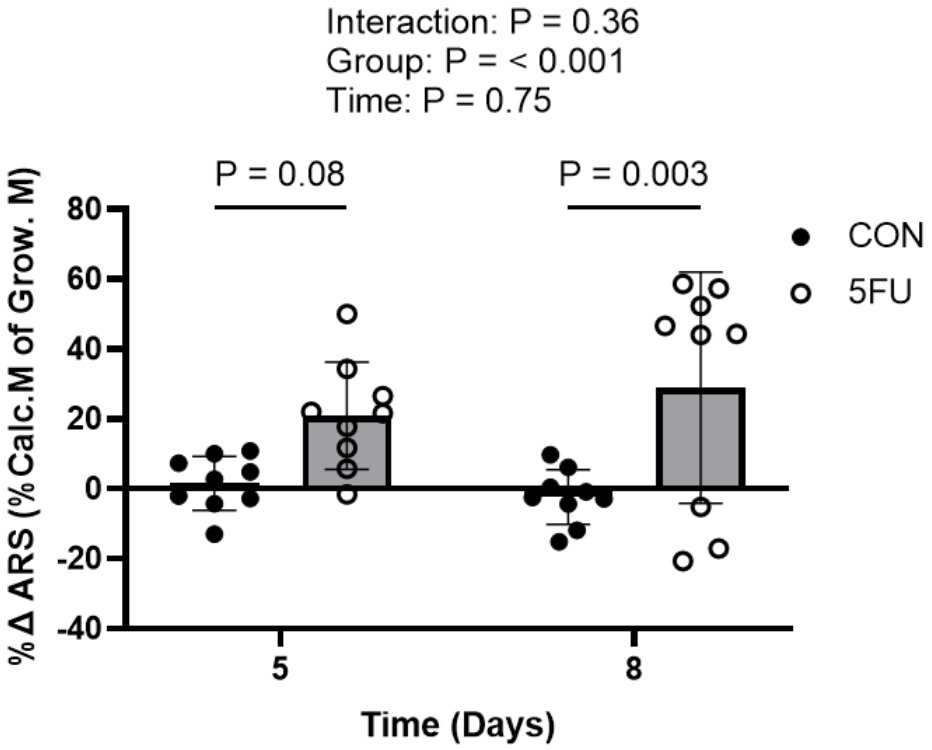

SMC from 5-FU treated animals had a significantly higher percent difference in the ARS concentration between the two media treatment conditions compared to CON cells at the 8-day time point. n = 9 individual wells per media treatment condition for each time point. Cell lines from 3 CON and 3 5-FU treated animals were used (3 wells per cell line per condition). All samples were assayed in duplicate. Data were analyzed using 2-way ANOVA and multiple comparisons with Šidák's multiple comparison test.

Calcium assay

In SMC derived from in vivo treated 5-FU and CON animals, a significant group x treatment medium interaction was present for calcium concentration following 8-days of culture ($P = 0.04$). Post-hoc analyses revealed a significantly higher calcium concentration in 5-FU-derived cells cultured with Calc. M. compared to Grow. M. (Grow. M.: 0.477 ± 0.02 mg/dl, Calc. M.: 1.43 ± 0.40 mg/dl, $P = 0.003$), whereas no significant difference between Calc. M. and Grow. M. was present in CON cells (Grow. M.: 0.674 ± 0.05 mg/dl, Calc. M.: 1.02 ± 0.12 mg/dl, $P = 0.38$). The calcium concentration in 5-FU cells treated with Calc. M. was also significantly higher than that of Grow. M. treated CON cells ($P = 0.01$) (**Figure 3.6**). In addition, CON cells treated in vitro with 7mM of 5-FU for 60 hours had significantly higher calcium concentrations than cells treated with Grow. M. alone (Grow. M.: 0.236 ± 0.04 mg/dl, Grow. M. + 5-FU: 0.335 ± 0.05 mg/dl, $P = 0.02$) (**Figure 3.7**).

Figure 3.6. Calcium concentrations between media conditions in CON and 5-FU derived cells

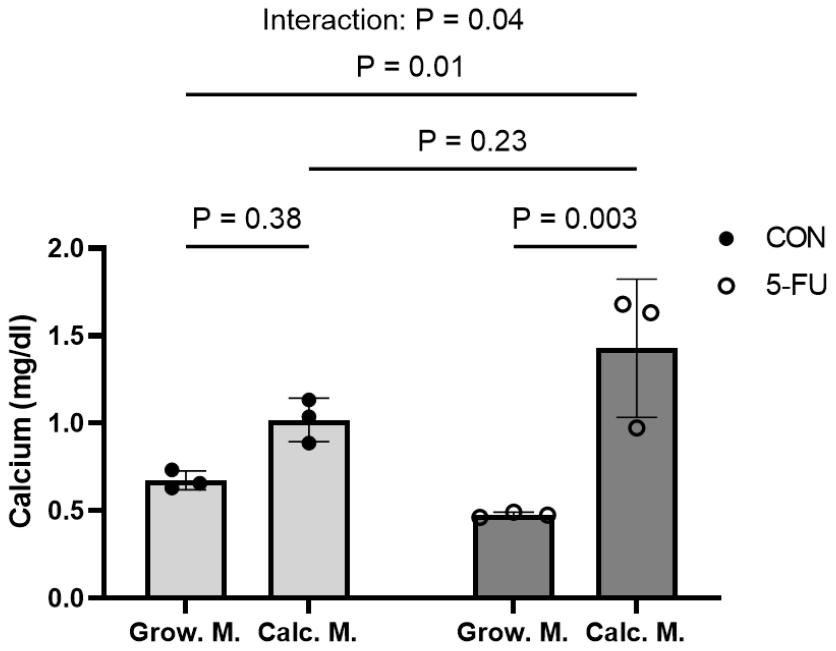

In cells from 5-FU treated animals, there was a significantly higher calcium concentration in Calc. M. treated cells compared to Grow. M. treated cells. This difference in calcium concentration between the treatment mediums was not present in cells derived from CON animals. The calcium concentration in 5-FU cells treated in Calc. M. was also significantly higher than those in CON cells treated with NM Grow. M. All other comparisons failed to reach statistical significance (all P = > 0.05). n = 3 separate cell lines for CON and 5-FU, with one plate from each cell line treated with Grow. M. and Calc. M. conditions. Each plate was assayed in duplicate. Data were analyzed using 2-way ANOVA and multiple comparisons with Šidák's multiple comparison test. Grow. M. = normal growth media. Calc. M. = calcification media.

Figure 3.7. Calcium concentration of CON derived cells following in vitro 5-FU administration

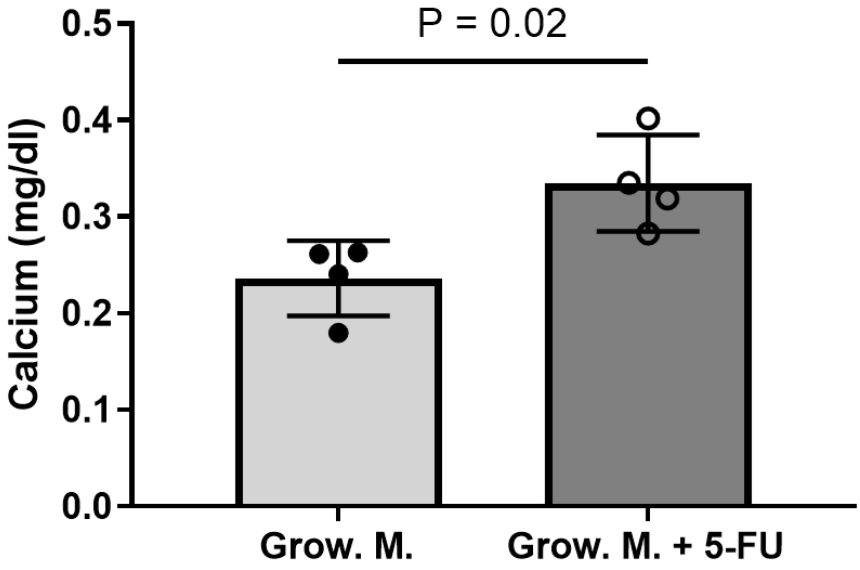

In vitro treatment with 5-FU (7mM) for 60h increases the calcium content in cells derived from saline (CON) treated animals. n = 4 separate CON cell lines completed in duplicate. Data compared using independent-samples t-test. Grow. M. = normal growth media. Grow. M. + 5-FU = normal growth medium with addition of 7 mM 5-FU.

Discussion

The present study aimed to assess the impact of 5-FU—a common chemotherapy agent used in the treatment of cancer—on the development of vascular calcification in a cell culture model of rat aortic smooth muscle cells. Our findings suggest that SMC cultured from the aorta of animals treated with a clinically relevant dose of 5-FU are prone to the development of calcification when cultured in media containing a pathological concentration of inorganic phosphate (e.g., Calc. M.), as assessed by ARS stain concentration and a calcium concentration assay. Interestingly, exposure to Calc. M. did not trigger an increase in calcification in SMC derived from animals who received an in vivo dose of saline (i.e., CON group). To confirm these findings using a different experimental model, SMC cultivated from the aortas of saline-treated animals were cultured with standard growth medium or standard medium supplemented with 7 mM of 5-FU for 60h. Consistent with our other experiments, SMC directly treated with 5-FU had significantly higher calcium levels supporting the hypothesis that 5-FU may induce cellular alterations which result in the onset of smooth muscle cell calcification. Thus, the findings of the present work suggest that SMC exposed to 5-FU under either in vivo or in vitro conditions may be more prone to the development of vascular calcification. These preclinical data highlight the need for additional mechanistic work and long-term patient monitoring to enhance our understanding of how 5-FU chemotherapy may impact vascular function in cancer survivorship.

The onset of calcification has a complex etiology and is considered an actively regulated process involving cellular communication and cascades across multiple layers of the vessel wall [16,30,31]. Specifically, altered redox status coupled with reductions in the bioavailability of NO in the endothelium can trigger a pro-oxidant, inflammatory, and vasoconstrictor-ridden environment leading to a shift towards a more osteogenic and senescent smooth muscle

phenotype and alterations in the surrounding extracellular matrix [16]. Such changes, including reduced calcification inhibitor function, apoptosis of smooth muscle cells, and an increase in proteins involved in mineralization, are considered key steps in the phenotypical switch of smooth muscle cells to a more osteogenic phenotype, the deterioration of the extracellular matrix, and ultimately the development of calcified lesions [31].

In the present study, we induced calcification via the addition of a pathological concentration of inorganic phosphate to the culture media of SMC [26–28]. In SMC isolated from 5-FU treated animals, differences in ARS concentration—a marker of calcium deposition—were apparent following 5- and 8-days of calcification medium treatment. Interestingly, such developments did not occur in SMC derived from CON animals, suggesting that in vivo 5-FU administration may have predisposed SMC to develop a calcification-like phenotype. Further, cells from 5-FU treated animals exhibited higher overall calcium concentrations and a greater percent difference in the ARS absorbance between the Grow. M. and Calc. M. conditions compared to CON cells. Although exploration of the mechanisms involved are beyond the scope of the current study, prior investigations have demonstrated increases in oxidative stress and inflammation [32–35], alterations in eNOS protein content/phosphorylation [13,34], altered cytoskeletal structure [36,37], and induction of senescence and apoptosis [13,32,36] following both in vivo and in vitro treatment of 5-FU. Such cellular alterations are known to assist in the transition of smooth muscle cells from a contractile to a more synthetic phenotype, with the latter being more prone to the development of calcification [38]. Thus, it is conceivable that initiating such processes during the infusion of 5FU may have ‘set the stage’ for the augmented development of calcification to occur when cells were faced with the additional stress of heightened Pi concentrations. Further, it is worth noting that though the phenotype of the SMC cultured herein was not specifically

quantified, our cells do have morphological resemblance (**Figure 1**) to the contractile and synthetic cells presented by Furmanik et al. (see Furmanik et al., Figure 1a) [38]. Specifically, SMC from CON animals had a visually elongated structure typical of contractile smooth muscle cells, whereas 5-FU-derived cells presented with the rhomboid morphology more typical in synthetic smooth muscle cells. However, more work is needed to address whether 5-FU induces these morphological changes and their relationship to the onset of vascular calcification.

A second finding of the present work was that the direct addition of 5-FU to the culture media increases the calcium concentration in SMC as measured by a commercially available calcium assay compared to otherwise untreated cells. This finding suggests that 5-FU may elicit direct cellular alterations that increase intracellular calcium levels. Can and colleagues have demonstrated similar findings—albeit in colon cancer carcinoma cells—in which direct application of 5-FU to the culture medium stimulated an influx of extracellular calcium that played a crucial role in the initiation of the early apoptotic process [39]. However, whether similar pathways are involved in the increased calcium levels demonstrated in the SMC investigated herein is unknown. Furmanik et al. found that overexpression of the reactive oxygen species (ROS) producing enzyme NOX5 increased calcium levels in smooth muscle cells treated with a high-calcium media suggesting ROS-mediated pathways were involved in alterations in cellular calcium concentrations [38]. As alluded to above, 5-FU is associated with increasing levels of ROS and oxidative stress [32,33,40], which can both stimulate greater influx of calcium from the treatment media or its release from intracellular stores [41] as well as drive the cell towards a fate of senescence or apoptosis [42,43] when antioxidant defense systems are overrun. The concentration of 5-FU used in this study (7 mM) is higher than those previously demonstrated to induce ROS in other 5-FU culture models [32,33] and within the range of concentrations that can induce apoptosis

[36]. Thus, future work may build upon our findings by assessing the potential relationship between 5-FU-induced ROS, alterations in cellular calcium homeostasis, and the onset of apoptosis and cellular senescence as precursors to vascular calcification.

To date, there remains a paucity of mechanistic data regarding the relationship of cancer and its associated treatments with the onset of vascular calcification. Much of the early understanding of this topic is derived from epidemiological datasets assessing the differences between CAC scores in patients treated with radiation therapy compared to expected, age-matched scores from the general population. In what is believed to be the first longitudinal analysis of CAC development in a cancer population, Whitlock and colleagues suggest that a cancer diagnosis predisposes subjects to a ~30% greater risk of transitioning from a CAC score of 0 to a score greater than 0, compared to a cancer-free population [44]. Importantly, this finding persisted despite controlling for other key risk factors, suggesting the direct involvement of cancer and/or its associated treatments in the development of calcified lesions. This work is supported by several other smaller prior studies [45,46] but not all [47], which suggests a relationship between prior cancer treatment and elevated CAC scores. As new evidence emerges suggesting relationships between CAC and cancer risk [48] and the development of cardiac events in cancer patients [49], future mechanistic work designed to assess the interplay of cancer and its associated treatments on the overall risk of developing vascular calcification may provide important insight into the long-term vascular consequences of chemotherapies such as 5-FU.

Experimental considerations

There are several experimental considerations germane to interpretation of the present work. First, the in vitro concentrations of 5-FU (7mM) and Pi (3.2 mmol/L) used herein are much higher than the physiological concentrations expected in vivo. Normal concentrations of

serum phosphate are in the range of 1.12 -1.45 mmol/L [50] and can rise to > 2 mmol/L in hyperphosphatemia [51]. Plasma 5-FU levels can vary depending on the regimen and individual patient factors but have been reported between < 1 - 500 µM [52–55]. Importantly, the concentrations used in our experiments are similar to those published by prior preclinical works [10,12,26,36] and our in vivo infusion of 5-FU is reflective of the dosing regimens and concentrations seen in clinical practice. Next, our sample size is relatively small, but consistent with similar in vitro work with SMC calcification [26]. However, given that we did derive SMC from multiple host animals (7 total) as opposed to propagation of cells from a single commercially available cell line, we feel this strengthens our findings and that these results provide valuable preliminary evidence for an effect of 5-FU on the development of smooth muscle cell calcification. Due to noticeable differences in cell number in SMC obtained from in vivo treated 5-FU and saline animals, as well as the need to plate at different seeding densities for time course experiments, we were unable to make direct comparisons for absolute ARS concentration between groups or across time. This is primarily due to our inability to control for cell number via cell counting with a hemocytometer or isolation of protein following ARS staining. That being said, the use of a secondary method of measuring calcium concentrations (i.e., o-Cresolphthalein-calcium assay) did permit protein normalization prior to comparison, and the group response differences noted in the ARS experiments remained apparent. Much of the clinical work on vascular calcification has emphasized CAC scores in the coronary vasculature due to their relationship with all-cause and cardiovascular-related mortality, whereas we employed the use of aortic smooth muscle cells of animal origin. It is worth noting, however, that many of these same relationships persist for aortic calcification, which has also been demonstrated as an independent predictor of cardiovascular disease and mortality [56,57]. Future mechanistic work is needed to understand

whether 5-FU or other cancer treatments impact calcification within the coronary circulation. Lastly, the present study was not designed to address how 5-FU treatment induces vascular calcification mechanistically. We hope that future studies will build upon these findings and enhance our understanding of how 5-FU impacts long-term vascular health. Such investigations may place emphasis on the role of 5-FU-induced alterations in smooth muscle phenotype, increases in ROS production, or endothelium-smooth muscle signaling perturbations which may arise in the face of 5-FU treatment.

Conclusion

Findings from the present work suggest that 5-FU chemotherapy may predispose SMC to the development of vascular calcification. Notably, SMC isolated from rats after completion of a clinically relevant dose of 5-FU were prone to increased calcium content and deposition levels when stressed with a high-phosphate calcification medium for 5-and 8-days. Interestingly, neither the increase in calcium deposition nor calcium content was reciprocated upon high-phosphate treatment in SMC derived from rats treated with saline. Further, when 5-FU was applied directly to previously untreated cells, calcium concentrations were higher than in cells that remained untreated. Taken together, these findings provide preliminary support for smooth muscle cell calcification following 5-FU treatment.

References

1. Siegel, R., Miller, K., Wagle, N. & Jemal, A. Cancer statistics, 2023. *CA Cancer J Clin* **73**, 17–48 (2023).
2. Sara, J. D. *et al.* 5-fluorouracil and cardiotoxicity: a review. *Ther Adv Med Oncol* **10**, 1–18 (2018).
3. Longley, D. B., Harkin, D. P. & Johnston, P. G. 5-Fluorouracil: Mechanisms of action and clinical strategies. *Nature Reviews Cancer* vol. 3 330–338 Preprint at (2003).
4. Dechant, C. *et al.* Acute Reversible Heart Failure Caused by Coronary Vasoconstriction due to Continuous 5-Fluorouracil Combination Chemotherapy. *Case Rep Oncol* **5**, 296–301 (2012).
5. Lestuzzi, C. *et al.* Cardiotoxicity from Capecitabine Chemotherapy: Prospective Study of Incidence at Rest and During Physical Exercise. *Oncologist* **27**, e158–e167 (2022).
6. Dyhl-Polk, A. *et al.* Myocardial Ischemia Induced by 5-Fluorouracil: A Prospective Electrocardiographic and Cardiac Biomarker Study. *Oncologist* **9999**, (2020).
7. Dyhl-Polk, A. *et al.* Incidence and risk markers of 5-fluorouracil and capecitabine cardiotoxicity in patients with colorectal cancer. *Acta Oncol (Madr)* **59**, 475–483 (2020).
8. Polk, A., Vaage-Nilsen, M., Vistisen, K. & Nielsen, D. L. Cardiotoxicity in cancer patients treated with 5-fluorouracil or capecitabine: A systematic review of incidence, manifestations and predisposing factors. *Cancer Treat Rev* **39**, 974–984 (2013).
9. Rezkalla, S. *et al.* Continuous ambulatory ECG monitoring during fluorouracil therapy: A prospective study. *Journal of Clinical Oncology* **7**, 509–514 (1989).
10. Mosseri, M., Fingert, H. J., Varticovski, L., Chokshi, S. & Isner, J. M. In Vitro Evidence That Myocardial Ischemia Resulting from 5-Fluorouracil Chemotherapy Is Due to Protein Kinase C-mediated Vasoconstriction of Vascular Smooth Muscle. *Cancer Res* **53**, (1993).
11. Südhoff, T. *et al.* 5-Fluorouracil induces arterial vasocontractions. *Annals of Oncology* **15**, 661–664 (2004).
12. Hayward, R. *et al.* Training Enhances Vascular Relaxation after Chemotherapy-Induced Vasoconstriction. *Med Sci Sports Exerc* **36**, 428–434 (2004).
13. Altieri, P. *et al.* 5-fluorouracil causes endothelial cell senescence: potential protective role of glucagon-like peptide 1. *Br J Pharmacol* **174**, 3713–3726 (2017).

14. Visvikis, A. *et al.* Cardiotoxic Profile and Arterial Stiffness of Adjuvant Chemotherapy for Colorectal Cancer. *Cancer Manag Res* **12**, 1175 (2020).
15. Widlansky, M. E., Gokce, N., Keaney, J. F. & Vita, J. A. The clinical implications of endothelial dysfunction. *J Am Coll Cardiol* **42**, 1149–1160 (2003).
16. van den Bergh, G., Opdebeeck, B., D'Haese, P. C. & Verhulst, A. The Vicious Cycle of Arterial Stiffness and Arterial Media Calcification. *Trends in Molecular Medicine* vol. 25 1133–1146 (2019).
17. Nasir, K. *et al.* Interplay of coronary artery calcification and traditional risk factors for the prediction of all-cause mortality in asymptomatic individuals. *Circ Cardiovasc Imaging* **5**, 467–473 (2012).
18. Yeboah, J. *et al.* Comparison of Novel Risk Markers for Improvement in Cardiovascular Risk Assessment in Intermediate-Risk Individuals. *JAMA* **308**, 788–795 (2012).
19. O'Malley, P. G., Taylor, A. J., Jackson, J. L., Doherty, T. M. & Detrano, R. C. Prognostic value of coronary electron-beam computed tomography for coronary heart disease events in asymptomatic populations. *Am J Cardiol* **85**, 945–948 (2000).
20. Blaha, M. *et al.* Absence of Coronary Artery Calcification and All-Cause Mortality. *JACC Cardiovasc Imaging* **2**, 692–700 (2009).
21. Cheeseman, S. L. *et al.* A 'modified de Gramont' regimen of fluorouracil, alone and with oxaliplatin, for advanced colorectal cancer. *British Journal of Cancer 2002 87:4* **87**, 393–399 (2002).
22. Petrelli, F. *et al.* FOLFIRI-Bevacizumab As First-Line Chemotherapy in 3500 Patients With Advanced Colorectal Cancer: A Pooled Analysis of 29 Published Trials. *Clin Colorectal Cancer* **12**, 145–151 (2013).
23. Conroy, T. *et al.* FOLFIRINOX versus Gemcitabine for Metastatic Pancreatic Cancer. *New England Journal of Medicine* **364**, 1817–1825 (2011).
24. Nair, A. B. & Jacob, S. A simple practice guide for dose conversion between animals and human. *J Basic Clin Pharm* **7**, 27 (2016).
25. Chi, J. *et al.* Primary Culture of Rat Aortic Vascular Smooth Muscle Cells: A New Method. *Med Sci Monit* **23**, 4014 (2017).
26. Takemura, A. *et al.* Sirtuin 1 Retards Hyperphosphatemia-Induced Calcification of Vascular Smooth Muscle Cells. *Arterioscler Thromb Vasc Biol* **31**, 2054–2062 (2011).

27. Son, B. K. *et al.* Gas6/Axl-PI3K/Akt pathway plays a central role in the effect of statins on inorganic phosphate-induced calcification of vascular smooth muscle cells. *Eur J Pharmacol* **556**, 1–8 (2007).
28. Son, B. K. *et al.* Statins Protect Human Aortic Smooth Muscle Cells From Inorganic Phosphate-Induced Calcification by Restoring Gas6-Axl Survival Pathway. *Circ Res* **98**, 1024–1031 (2006).
29. Gregory, C. A., Gunn, W. G., Peister, A. & Prockop, D. J. An Alizarin red-based assay of mineralization by adherent cells in culture: comparison with cetylpyridinium chloride extraction. *Anal Biochem* **329**, 77–84 (2004).
30. Tesauro, M. *et al.* Arterial ageing: from endothelial dysfunction to vascular calcification. *J Intern Med* **281**, 471–482 (2017).
31. Shanahan, C. M., Crouthamel, M. H., Kapustin, A. & Giachelli, C. M. Arterial Calcification in Chronic Kidney Disease: Key Roles for Calcium and Phosphate. *Circ Res* **109**, 697–711 (2011).
32. Focaccetti, C. *et al.* Effects of 5-fluorouracil on morphology, cell cycle, proliferation, apoptosis, autophagy and ros production in endothelial cells and cardiomyocytes. *PLoS One* **10**, (2015).
33. Lamberti, M. *et al.* 5-Fluorouracil induces apoptosis in rat cardiocytes through intracellular oxidative stress. *Journal of Experimental and Clinical Cancer Research* **31**, 1–8 (2012).
34. Muhammad, R. N., Sallam, N. & El-Abhar, H. S. Activated ROCK/Akt/eNOS and ET-1/ERK pathways in 5-fluorouracil-induced cardiotoxicity: modulation by simvastatin. *Sci Rep* **10**, 14693 (2020).
35. Güçlü, O., Doğanlar, O., Yüksel, V. & Doğanlar, Z. B. FOLFIRI-Mediated Toxicity in Human Aortic Smooth Muscle Cells and Possible Amelioration with Curcumin and Quercetin. *Cardiovasc Toxicol* **20**, 139–154 (2020).
36. Filgueiras, M. de C., Morrot, A., Soares, P. M. G., Costa, M. L. & Mermelstein, C. Effects of 5-Fluorouracil in Nuclear and Cellular Morphology, Proliferation, Cell Cycle, Apoptosis, Cytoskeletal and Caveolar Distribution in Primary Cultures of Smooth Muscle Cells. *PLoS One* **8**, e63177 (2013).

37. Gordon, S. R., Climie, M. & Hitt, A. L. 5-fluorouracil interferes with actin organization, stress fiber formation and cell migration in corneal endothelial cells during wound repair along the natural basement membrane. *Cell Motil Cytoskeleton* **62**, 244–258 (2005).
38. Furmanik, M. *et al.* Reactive Oxygen-Forming Nox5 Links Vascular Smooth Muscle Cell Phenotypic Switching and Extracellular Vesicle-Mediated Vascular Calcification. *Circ Res* **127**, 911–927 (2020).
39. Can, G., Akpinar, B., Baran, Y., Zhivotovsky, B. & Olsson, M. 5-Fluorouracil signaling through a calcium–calmodulin-dependent pathway is required for p53 activation and apoptosis in colon carcinoma cells. *Oncogene 2013 32:38* **32**, 4529–4538 (2012).
40. Durak, İ., Karaayvaz, M., Kavutcu, M., Büyükkoçak, S. & Öztürk, H. S. Reduced antioxidant defense capacity in myocardial tissue from guinea pigs treated with 5-Fluorouracil. **59**, 585–589 (2010).
41. Roveri, A. *et al.* Effect of hydrogen peroxide on calcium homeostasis in smooth muscle cells. *Arch Biochem Biophys* **297**, 265–270 (1992).
42. Tsai, I. C. *et al.* Reactive oxygen species derived from NADPH oxidase 1 and mitochondria mediate angiotensin II-induced smooth muscle cell senescence. *J Mol Cell Cardiol* **98**, 18–27 (2016).
43. Koike, S. *et al.* Advanced Glycation End-Products Induce Apoptosis of Vascular Smooth Muscle Cells: A Mechanism for Vascular Calcification. *International Journal of Molecular Sciences 2016, Vol. 17, Page 1567* **17**, 1567 (2016).
44. Whitlock, M. C. *et al.* Cancer and Its Association With the Development of Coronary Artery Calcification: An Assessment From the Multi-Ethnic Study of Atherosclerosis. *J Am Heart Assoc* **4**, (2015).
45. Rademaker, J. *et al.* Coronary Artery Disease After Radiation Therapy for Hodgkin's Lymphoma: Coronary CT Angiography Findings and Calcium Scores in Nine Asymptomatic Patients. **191**, 32–37 (2012).
46. Andersen, R. *et al.* Relation of coronary artery calcium score to premature coronary artery disease in survivors >15 years of Hodgkin's lymphoma. *Am J Cardiol* **105**, 149–152 (2010).

47. Tjessem, K. H. *et al.* Coronary calcium score in 12-year breast cancer survivors after adjuvant radiotherapy with low to moderate heart exposure - Relationship to cardiac radiation dose and cardiovascular risk factors. *Radiother Oncol* **114**, 328–334 (2015).
48. Dzaye, O. *et al.* Coronary artery calcium is associated with increased risk for lung and colorectal cancer in men and women: the Multi-Ethnic Study of Atherosclerosis (MESA). *Eur Heart J Cardiovasc Imaging* **23**, 708–716 (2022).
49. Phillips, W. J. *et al.* Comparison of Framingham risk score and chest-CT identified coronary artery calcification in breast cancer patients to predict cardiovascular events. *Int J Cardiol* **289**, 138–143 (2019).
50. Bansal, V. K. Serum Inorganic Phosphorus. *Clinical Methods: The History, Physical, and Laboratory Examinations* (1990).
51. Rudolph, E. H. & Gonin, J. M. Disorders of phosphorus metabolism. in *Nephrology Secrets* (eds. Lerma, E. & Nissenson, A.) 551–559 (Mosby, 2012).
52. Findlay, M. P. N. *et al.* Measurement of plasma 5-fluorouracil by high-performance liquid chromatography with comparison of results to tissue drug levels observed using in vivo 19F magnetic resonance spectroscopy in patients on a protracted venous infusion with or without interferon-alpha. *Ann Oncol* **7**, 47–53 (1996).
53. Takimoto, C. H. *et al.* High inter- and intrapatient variation in 5-fluorouracil plasma concentrations during a prolonged drug infusion. *Clin Cancer Res* **5**, 1347–1352 (1999).
54. Casale, F. *et al.* Plasma concentrations of 5-fluorouracil and its metabolites in colon cancer patients. *Pharmacol Res* **50**, 173–179 (2004).
55. Büchel, B. *et al.* LC-MS/MS method for simultaneous analysis of uracil, 5,6-dihydrouracil, 5-fluorouracil and 5-fluoro-5,6-dihydrouracil in human plasma for therapeutic drug monitoring and toxicity prediction in cancer patients. *Biomedical Chromatography* **27**, 7–16 (2013).
56. Witteman, J. C. M., Kok, F. J., van Saase, J. L. C. M. & Valkenburg, H. A. Aortic calcification as a predictor of cardiovascular mortality. *The Lancet* **328**, 1120–1122 (1986).
57. Wilson, P. W. F. *et al.* Abdominal Aortic Calcific Deposits Are an Important Predictor of Vascular Morbidity and Mortality. *Circulation* **103**, 1529–1534 (2001).

Chapter 4 - The efficacy of an acute exercise preconditioning protocol on the prevention of 5-fluorouracil cardiotoxicity

Abstract

Background: 5-fluorouracil (5-FU) chemotherapy is one of the most common chemotherapeutic agents used in cancer treatment, yet its use is often associated with the onset of severe cardiotoxicity. To date, there remains a paucity of data regarding the mechanisms driving these cardiovascular maladaptations and modalities to alleviate their occurrence. Thus, the present study aimed to test the effect of an acute exercise preconditioning protocol on the prevention of left ventricular and vascular maladaptations in a pre-clinical rodent model in response to a clinically relevant 5-FU dosing regimen. Moreover, we aimed to identify potential signaling pathways for future study via completion of reverse phase protein analysis of cardiac and aortic tissue. We hypothesized that 5-FU treatment would induce left ventricular and vascular alterations and that 4 days of exercise preconditioning would prevent these adverse side effects. **Methods:** Male, Sprague-Dawley rats (6-8 weeks of age) were randomized to 1 of 4 groups: sedentary control (SEDCON), sedentary 5-FU (SED5FU), exercise control (EXCON) or exercise 5-FU (EX5FU). Rats either remained sedentary or completed a 4-day treadmill preconditioning protocol (20-25 min, 20 m/min, 5% grade) with the final bout ending ~ 1-hr before treatment with a clinically relevant dose of 5-FU (50 mg/kg bolus + 265 mg/kg 2-hr infusion) or volume matched saline. Echocardiographic indices of left ventricular function and measurements of aortic pulse wave velocity (PWV; a clinical marker of arterial stiffness) were completed at baseline and in the final moments of the 2-hr infusion. Inflammatory gene expression and reverse phase protein analysis (RPPA) were conducted on myocardial and aortic tissue lysate upon completion of the experimental protocol. **Results:** 5-FU did not induce significant changes in left

ventricular function or myocardial inflammatory gene expression. PWV increased significantly from baseline to the 2-hr time point in SED5FU (BL: 396 ± 39 cm/s; 2-hr: 452 ± 54 cm/s; P = 0.002), but not SEDCON (BL: 417 ± 55 cm/s; 2-hr: 392 ± 64 cm/s; P=0.35), EXCON (BL: 408 ± 35 cm/s; 2-hr: 410 ± 46 cm/s; P > 0.99), or EX5FU (BL: 398 ± 13 cm/s; 2-hr: 417± 23 cm/s; P = 0.67). This resulted in significantly higher absolute PWV at 2-hr (SED5FU: 452 ± 54 cm/s; SEDCON: 392 ± 64 cm/s; P = 0.03) as well as greater changes from baseline to 2-hr (SED5FU: 14.5 ± 10.9%; SEDCON: -5.3 ± 15.7%; P = 0.002) in SED5FU compared to SEDCON. Importantly, EX5FU did not present with any significant increases in PWV or differences with SEDCON (all p > 0.05). RPPA analysis of aortic tissue from SEDCON and SED5FU identified several differentially expressed proteins involved in focal adhesion and cytoskeletal regulation pathways. **Conclusion:** Findings from this study provide support for a protective effect of moderate-intensity exercise preconditioning on the development of 5-FU-induced vascular alterations. Investigations in human patients and future mechanistic studies assessing the potential contributions of focal adhesion and cytoskeletal alterations during 5-FU treatment may be helpful in further delineating factors contributing to the development and prevention of 5-FU cardiotoxicity.

Introduction

Since first synthesized by Heidelberger and colleagues in 1957 [1], 5-fluorouracil (5-FU) chemotherapy has remained a cornerstone of numerous gastrointestinal, breast, and head/neck cancer treatment regimens. While this longevity speaks to its effectiveness as an anticancer agent, 5-FU has also gained notoriety for its unfortunate association with treatment-induced cardiotoxicity—most frequently manifesting as severe angina with or without ECG alterations that arise during or shortly following cessation of treatment [2]. For many chemotherapies (i.e., anthracyclines), the emphasis has been placed on the prevention of long-term cardiovascular sequelae, which arise in the decades following treatment. Yet, the greatest obstacle regarding 5-FU cardiotoxicity remains mitigation of the more acute side effects, which can lead to disruption of preferred treatment regimens in as many as 1 of every 13 patients [3]. A heightened understanding of the mechanisms responsible for these side effects and the development of modalities to alleviate their occurrence are critical steps in ensuring patients can continue to sustain treatment with ideal therapeutic regimens.

Though the precise mechanisms responsible for 5-FU cardiotoxicity remain elusive, leading theories include direct myocardial damage and myocardial ischemia secondary to 5-FU-induced vascular endothelial and smooth muscle dysfunction. In vivo evidence in human patients broadly supports the latter, as alterations in coronary vasoreactivity have been evidenced in case reports [4,5] and peripheral vascular abnormalities in experimental studies [6]. In addition, recent unpublished findings from our group suggest reduced cutaneous microvascular reactivity in response to endothelial-dependent stimuli in patients with cancer immediately following treatment with 5-FU when compared to matched, non-cancer controls. This parallels the prior preclinical models, which have suggested 5-FU may have a direct effect on both the myocardium

[7–10] and vasculature [11–17] with reports of cellular and tissue morphology [7,8,13,14,18,19], inflammation [9,20], impaired cellular redox and oxidative stress [8,9,21,22], and alterations in vasodilator/constrictor proteins [9,12,15] frequent throughout the literature. However, while these works have undoubtedly shaped our current understanding of the mechanisms driving 5-FU cardiotoxicity, most have employed dosing regimens dissimilar (e.g., intraperitoneal drug delivery) to those seen in clinical practice, potentially limiting the translatability of these findings to the clinical setting.

Given the frequent use and importance of 5-FU as a first-line cancer treatment, strategies to alleviate or prevent its cardiotoxic side effects have been of recent interest. Most notably, pharmacological therapy with nitrates or calcium channel blockers has yielded mixed findings [6,23–25], and these treatments are typically only administered after a patient experiences adverse treatment-related side effects. However, preclinical models investigating the cardiotoxicity of other anticancer agents (e.g., anthracyclines) have demonstrated the efficacy of short-term aerobic exercise preconditioning to prevent chemotherapy-induced cardiovascular maladaptation [26–29]. Such studies have largely found that acute exercise is able to maintain mitochondrial function and offset deleterious increases in oxidative stress that are induced by chemotherapy treatment [26–29]. Given that 5-FU has been demonstrated to induce similar changes in redox signaling [8,9,22], it is conceivable that exercise prior to the receipt of treatment may provide similar cardioprotective effects. Thus, we tested the hypothesis that a clinically relevant infusion of 5-FU would cause alterations in the cardiovascular function of sedentary Sprague-Dawley rats but not those who completed an acute exercise preconditioning protocol in the days preceding 5-FU treatment.

Methods

Animals

All procedures performed herein were approved by the Kansas State University Institutional Animal Care and Use Committee and conformed to the National Institutes of Health Guide for the Care and Use of Laboratory Animals. Male Sprague Dawley rats (n=38, 6-8 mo. old, ~670 g; Charles River; Wilmington, MA) were used for this study. All rodents were housed in a temperature-controlled facility (23°C) on a 12:12-h light-dark cycle with standard rat chow and water provided *ab libitum*.

Exercise preconditioning

The week before the experimental protocol, all rats were habituated to treadmill exercise on a custom-built motor-driven treadmill for <5 min/day at 15 m/min (0% incline) for three days. Rats were then randomized to exercise (n=18) and sedentary groups (n=20). Then, 3-days before 5-FU or saline treatment, exercise animals began a 4-day acute exercise preconditioning program. Briefly, rats ran on a motorized treadmill at 20 m/min (5% grade) for 20-25 min/day, with the final exercise bout commencing ~ 1-hr before receipt of 5-FU or saline treatment. Based on the prior work of others, we anticipate this exercise intensity to be ~65% VO_2max [30].

Surgical procedures

Approximately 30-min following completion of the final exercise bout, rats were first anesthetized with a 5% isoflurane-O_2 mixture (isoflurane vaporizer; Harvard Apparatus; Cambridge, MA) and subsequently maintained on 2.5% isofluorane-O_2 on a heated surgical station (Rodent Surgical Monitor, Indus Instruments; Houston, TX) maintained at 37°C. An incision was made at the left ventral neck to expose the left jugular vein for catheterization (PE-50 polyethylene tubing, Becton Dickson, Sparks, MD) to administer 5-FU or saline. A second

catheter (PE-10 connected to PE-50) was placed in the caudal artery for continuous blood pressure monitoring. Following the insertion of both catheters, rats were transitioned from isoflurane to pentobarbital sodium anesthesia by slowly reducing and ultimately terminating the isoflurane concentration. Pentobarbital sodium anesthesia was supplemented as needed (~16 mg/kg/hr via caudal artery) for the remainder of the experiment as determined by responses to palpebral and toe flinch reflexes.

5-fluorouracil (5-FU) or saline administration

Animals were randomized to receive treatment with 5-FU (n=19) or volume-matched saline (n=19), resulting in a total of four experimental groups: sedentary saline control (SEDCON, n=10), sedentary 5-FU (SED5FU, n=10) exercise saline control (EXCON, n=9), and exercise 5-FU (EX5FU, n=9). Historically, preclinical animal models of 5-FU cardiotoxicity have utilized either intraperitoneal or bolus injections to study the impact of 5-FU on cardiovascular function. However, this differs from more common drug delivery methods used in clinical settings where 5-FU containing regimens (e.g., FOLFOX, FOLFIRINOX) often comprise a single bolus dose of 5-FU (400 mg/m^2) followed by the initiation of a continuous infusion of 5-FU (2400 mg/m^2) delivered over 48h [31,32]. Thus, aligning our study with the clinical drug delivery methods, we designed a translational rat model of 5-FU cardiotoxicity using allometric scaling from the human doses of 400 mg/m^2 and 2400 mg/m^2 [33]. Following the completion of surgical procedures and collection of baseline measurements (see below), a bolus dose of 50 mg/kg 5-FU or volume-matched saline was delivered via the jugular catheter using a 10 mL syringe. The jugular catheter was then attached to a programmable syringe pump (Pump 11 Elite; Harvard Apparatus; Holliston, MA) for initiation of a 2-hour continuous infusion of 265 mg/kg 5-FU or volume-matched saline. As described below, cardiovascular measurements of

cardiac and vascular function were made before and in the final moments of 5-FU/saline administration.

Echocardiographic evaluation of left ventricular function

Transthoracic echocardiography measures of left ventricular function were performed at baseline and 2-hr timepoints using a commercially available two-dimensional ultrasound system (Logiq e; GE Medical Systems; Milwaukee, WI) as previously demonstrated by our group [34–36]. Briefly, following the removal of hair from the chest (Nair, Johnson & Johnson, New Brunswick, NJ), two-dimensional guided M-mode images were collected at the level of the mitral leaflets in the parasternal short axis view using a 22-MHz linear transducer (GE L10-22-RS, GE Medical Systems). Images were stored on an offline storage device for future measurement of LV dimensions and posterior wall thickness, which were subsequently used to estimate LV volumes using the Teichhholz formula [37] within the manufacturer's imaging analysis software. Images were collected over three continuous cardiac cycles immediately before administration of the bolus treatment (baseline) and at the end of the 2-hour infusion (2-hr).

Hemodynamic variables

Heart rate (HR) and mean arterial blood pressure (MAP) were continuously monitored over the duration of the protocol using a commercially available blood pressure monitor (Digi-Med BPA; Micro-Med; Louisville, KY) with analog output to a laboratory computer via a multifunction data acquisition device (NI USB 6211, National Instruments, Austin, TX). Data were sampled at 1,000 Hz and recorded for offline analysis using commercially available software (LabVIEW version 10.0f2, National Instruments). 8-10 minutes of HR and MAP were collected, and the mean calculated at baseline and 2-hr time points. HR and stroke volume (SV; determined from echocardiography) were used to calculate cardiac output (Q).

Doppler pulse wave velocity

Measurements of aortic pulse wave velocity (PWV)—an established marker of arterial stiffness [38] —were made at baseline and in the final minutes of 2-hr infusion using a commercially available Doppler flow velocity system (Indus Instruments; Houston, TX). Rats were positioned supine, and each paw was fitted with external needle electrodes for the collection of ECG. Two Doppler probes connected to a pulsed Doppler system transceiver were used to attain simultaneous Doppler spectrograms from the descending and abdominal aorta. Briefly, one probe was placed along the abdominal midline for the attainment of abdominal aorta flow velocity and held in place by a micro-positioner. The second probe was held to the right of the sternum near the base of the upper left limb to capture descending aorta velocity traveling away from the probe. Images were captured simultaneously and time aligned with ECG for offline analyses using manufacturer software. The distance between probes (mm) was measured immediately following the obtainment of the image. PWV was calculated as follows: PWV = distance between probe tips (mm) / (time from R wave to the abdominal aorta – time from R wave to aortic arch) (ms) and reported in cm/s.

Tissue collection

After completing the 2-hr measurements, all animals were euthanized via thoracotomy followed by heart removal. The heart and aorta were promptly dissected, cleaned in ice-cold saline, weighed, and snap-frozen in liquid nitrogen before storage at -80°C for future analyses.

Reverse transcriptase polymerase chain reaction (RT-PCR)

Tissue samples from the left ventricle (~5 mg) were placed in 2 mL bead mill tubes containing 0.5 g of 1.4 mm ceramic beads, 350 µL lysis buffer (740934.500; Macherey-Nagel; Allentown, PA), and 3.5 µL of β-mercaptoethanol and homogenized for ~ 90 seconds at 5m/s

using a mini homogenizer (Bead Mill 4, Fisherbrand; Pittsburgh, PA). Sample lysate was then used to obtain total protein and mRNA from a Nucleospin RNA/Protein mini kit (item #: 740933.250; Macherey-Nagel) according to manufacturer guidelines and stored at -80°C for future analyses.

Left ventricular RNA isolates were used to synthesize complementary DNA (cDNA) using a High-Capacity RNA-to-cDNA Kit (Item #: 4387406; Applied Biosystems; Bedford, MA) per manufacturer instructions. cDNA was then used to determine inflammatory marker gene expression in reverse transcriptase polymerase chain reaction (RT-PCR) experiments using TaqMan gene assays specific for tumor necrosis factor (TNF) (assay ID: Rn99999017_m1) and Interleukin 1β (IL1B) (assay ID: Rn00580432_m1). All samples were completed in duplicate on 96-well TaqMan Plates in a QuantStudio 3 RT-PCR System (Applied Biosystems) using Beta-2 microglobulin (B2m) (assay ID: Rn00560865_m1) as an endogenous control. Differences in gene expression between conditions were analyzed using the comparative threshold (ΔΔCT) method.

Reverse phase protein analysis

Exploratory reverse phase protein analysis (RPPA) was conducted at the MD Anderson Cancer Center Proteomics Core Facility as described by others [39] to identify potential protein targets altered by 5-FU treatment. Briefly, pooled group samples of aortic (~2 mg per animal, n=4 rats per group) and cardiac (~5 mg per animal, n=4 rats per group) tissue were homogenized in RPPA lysis buffer consisting of 1% Triton X-100, 50 mM HEPES (pH 7.4), 150 mM NaCl, 1.5 mM MgCl2, and 1 mM EGTA supplemented with protease (05056489001, Roche, Basel, Switzerland) and phosphatase (04906837001, Roche) inhibitor cocktails using a bead mill homogenizer. Protein concentration was determined via Bradford assay, and each sample was

subsequently adjusted to 1.5 µg/µl using lysis buffer. Sample lysate was then denatured with 1% SDS (1/10 volume β-mercaptoethanol) and diluted 2-fold in 5 serial dilutions. The serially diluted lysates were spotted onto nitrocellulose-coated slides (Grace Bio-Labs, Bend, OR) and arrayed using an Asuhon 2470 arrayer (Aushon Biosystems, Billerica, MA). Samples were probed for 423 primary antibodies involved in cancer related signaling pathways, and mean net intensities of spots from each antibody were used to determine relative protein levels using the RPPASPACE curve fitting method developed by the MD Anderson Cancer Center Department of Bioinformatics and Computational Biology. These values were normalized for sample loading differences and converted to linear and median-centered values for use in functional network analyses.

Protein networks and functional enrichment analysis

RPPA proteins with a 1.5-fold or greater difference between linear values for SEDCON and SED5FU and/or SED5FU and EX5FU were imported into Cytoscape (version 3.9.1) [40] and used to create protein interaction networks. In addition, functional pathway enrichment analyses were conducted using STRING (Version 11.5; string-db.org) [41] to explore pathways that may be involved in 5-FU cardiotoxicity.

Upon uploading proteins of interest into STRING, a protein interaction network is constructed, comprising two primary components: nodes and edges. Nodes represent the uploaded proteins, while edges (lines connecting various nodes) represent possible functional associations between connected proteins based on a variety of available evidence (e.g., established pathway frameworks such as KEGG or Reactome Pathways, text mining publications, etc.) [42]. The evidence-based confidence of a given interaction between two proteins is symbolized by the thickness of an edge, with thicker edges implying a higher confidence level

for a functional relationship between two proteins (scale of 0.0 – 1.0). For these experiments, minimum confidence was set to medium (confidence score ≥ 0.4). Based on these interactions, STRING computes a protein-protein interaction (PPI) enrichment p-value. A score of $P \leq 0.05$ indicates that the uploaded proteins have a greater number of interactions amongst the group than what would otherwise be expected for a random group of proteins of the same number and degree distribution from the genome (i.e., network has significantly more interactions than expected at random). Functional enrichment analyses were conducted by STRING (hypergeometric tests against the genome [41]) to determine potential biological pathways which contain the proteins expressed in our sample. Given the high volume of pathway overlap, the selection of pathways reported and discussed herein was based on a combination of scores provided by STRING (false discovery rate and strength scores) as well as consideration of how a given pathway relates to the functional in vivo measurements made during the present investigation.

Data analysis

All statistical analyses were completed using a commercially available software package (GraphPad Prism 9.5.0; San Diego, Ca, USA). Echocardiographic and hemodynamic variables, as well as aortic pulse wave velocity, were assessed via two-way analysis of variance (2-way ANOVA) with main effects for group (SEDCON, SED5FU, EXCON, EX5FU) and time (baseline, 2-hours). When appropriate, multiple comparisons were completed using Šídák's multiple comparisons test. Differences in gene expression and body mass were assessed using one-way ANOVA or Welch's ANOVA test for data with equal and unequal variance, respectively. RPPA data were included in individual network analyses when the expression of proteins between SEDCON and SED5FU or SED5FU and EX5FU differed by at least 1.5-fold.

Functional enrichment pathways from the KEGG database were only reported if the false discovery rate (FDR) was $P < 0.05$. All data are presented as mean ± standard deviation unless otherwise stated. Statistical significance was set at 0.05.

Results

A total of 38 rats were used in this study. Three rats died during the surgical procedures, and thus findings from a total sample of 35 rats (SEDCON: n=9; SED5FU: n=10, EXCON: n=8; EX5FU: n=8) are reported herein. There were no differences in body mass between the groups (SEDCON: 642 ± 41 g; SED5FU: 637 ± 87 g; EXCON: 728 ± 119 g; EX5FU: 685 ± 87 g; P = 0.13).

Echocardiographic measurements

Echocardiographic measurements were conducted to assess how 5-FU may directly impact myocardial function and the potential cardioprotective role of exercise preconditioning. A representative image captured during M-mode transthoracic echocardiography is presented in **Figure 4.1,** while group means for individual measurements are reported in **Table 4.1**. There were no significant group × time interactions for echocardiography variables (all P > 0.05). Similarly, no significant main effects for the group were detected (all P > 0.05). There was no significant main effect for time on end-diastolic volume (EDV) (P = 0.06) or stroke volume (SV) (P = 0.96); however, end-systolic volume (ESV) (P = < 0.001) and fractional shortening (FS) (P = < 0.001) did change significantly over the course of the 2-hour infusion (**Figure 4.2 a-d**). Post hoc analyses revealed a significant increase in ESV for SEDCON (P = 0.01), SED5FU (P = 0.01), and EX5FU (P = 0.007), but not for CONEX (P = 0.47) over the course of the 2-hour infusion (**Figure 4.2a**). Similarly, FS was reduced from baseline to 2 hours in SEDCON (P = < 0.001), SED5FU (P = 0.04), and EX5FU (P = < 0.001), while no changes were apparent for EXCON (P = 0.20) (**Figure 4.2d**).

Figure 4.1. Representative ultrasound image of the rat left ventricle

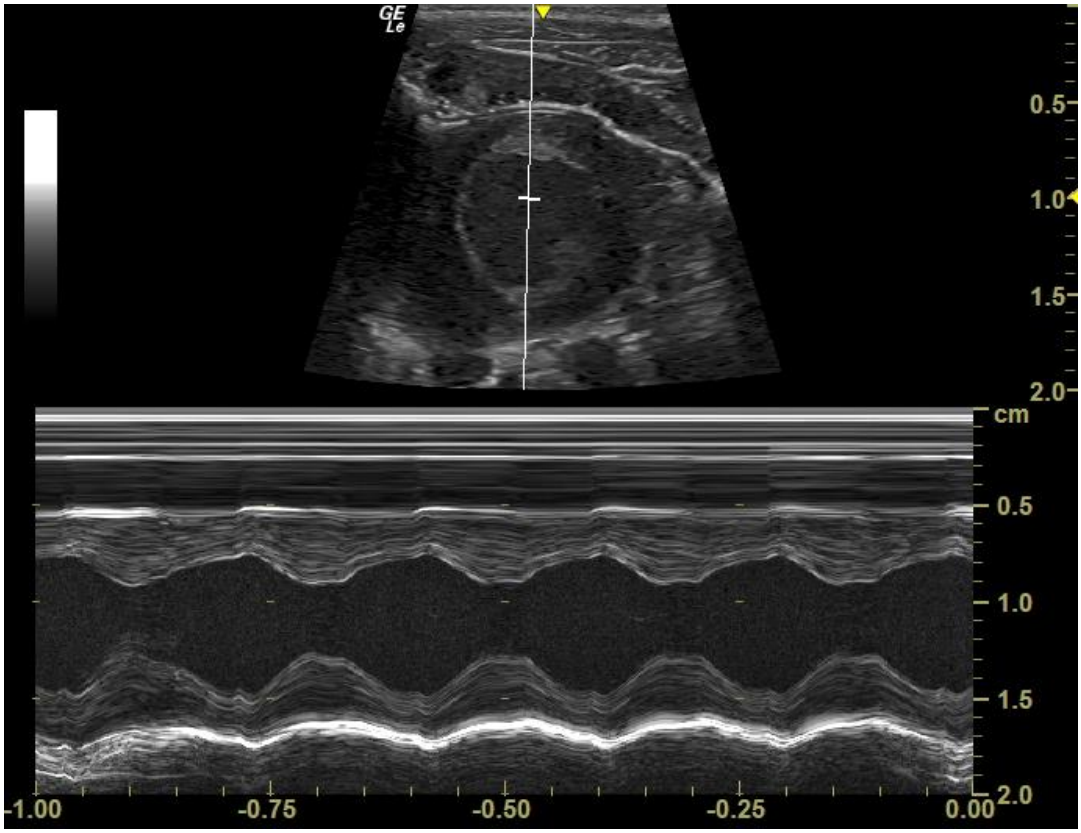

A representative two-dimensional, M-mode ultrasound image of the rat left ventricle. Images were taken at the level of the papillary muscle in the parasternal short axis view.

Figure 4.2. Effect of 5-FU infusion on left ventricular variables

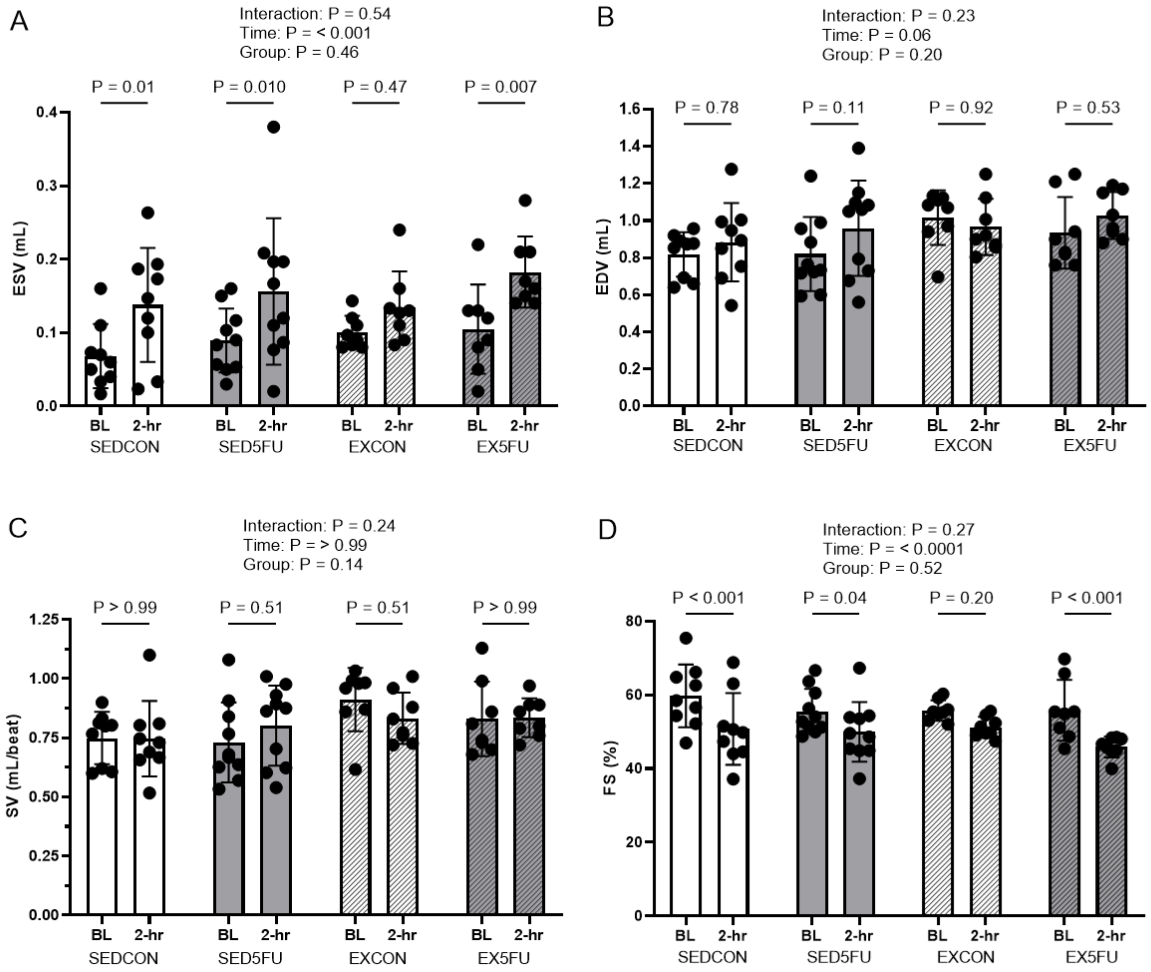

Left ventricular variables. **A)** A significant main effect for time was present for ESV. There was a significant increase in ESV from BL to 2-hr in all groups aside from EXCON. **B)** EDV was not significantly altered for any of the groups from BL to 2-hr. **C)** SV was not changed over the course of the infusion for any of the 4 groups. **D)** There was a significant effect of time on FS. FS was significantly reduced in all groups aside from EXCON over the course of the 2-hr infusion. EXCON n = 9, SED5FU n = 10, EXCON n = 8, EX5FU = 8. Data analyzed using 2-way repeated measures ANOVA.

Table 4.1. Mean data for echocardiographic and hemodynamic variables

	Sedentary Control (CON) n=9		Sedentary 5-FU (5-FU) n=10		Exercise Control (CEX) n=8		Exercise 5-FU (FEX) n=8	
	Baseline	2-hr	Baseline	2-hr	Baseline	2-hr	Baseline	2-hr
ESV (mL)	0.07±0.04	0.14±0.08*	0.09±0.04	0.16±0.10**	0.10±0.02	0.13±0.05	0.10±0.06	0.18±0.05**
EDV (mL)	0.82±0.12	0.88±0.21	0.82±0.20	0.96±0.26	1.02±0.15	0.97±0.15	0.92±0.19	1.03±0.13
SV (mL/kg)	0.75±0.11	0.75±0.16	0.73±0.17	0.80±0.17	0.91±0.13	0.83±0.11	0.82±0.15	0.84±0.08
FS (%)	59.8±8.5	50.8±9.7†	55.5±6.1	50.0±8.1*	55.8±2.8	50.9±3.5	57.3±8.9	45.9±2.8†
MAP (mmHg)	78±12	86±21	81±9	87±10	76±15	85±24	76±10	84±23
HR (BPM)	323±26	326±28	321±31	314±29	316±28	308±33	319±57	329±14
Q (mL/min)	243.0±49.0	245.6±68.3	234.9±61.0	250.7±52.7	286.3±33.3	256.7±46.2	264.6±70.9	274.6±25.3

Abbreviations: ESV, End systolic volume; EDV, End diastolic volume; SV, Stroke volume; FS, Fractional shortening; MAP, Mean arterial pressure; HR, Heart rate; Q, Cardiac output. * P≤0.05 baseline to post; ** P≤0.01 baseline to post; † P≤0.001 baseline to post.

Hemodynamic variables

Mean values for hemodynamic variables for all groups and time points are presented in **Table 4.1**. There was no significant group × time interaction for MAP (P = 0.99), HR (p = 0.78), or Q (P = 0.44). HR did not differ between the groups (P = 0.70), nor did it change significantly from baseline to 2 hours (P = > 0.99). Similarly, Q was not different between the groups (P = 0.36) and did not change over the course of the infusion (P = 0.98). MAP did not differ between groups (P=0.90) but increased significantly over the course of the 2-hour infusion (P = 0.01). However, multiple comparisons did not individually reveal an increase for any of the groups (SEDCON: P = 0.54; SED5FU: P = 0 .69; EXCON: P = 0.58; EX5FU: P = 0.57).

Aortic pulse wave velocity (PWV)

To gain insight into the potential effects 5-FU may have on the vasculature, PWV measurements were conducted at baseline (BL) and near completion of the infusion (2-hr). A significant group × time interaction was present for PWV (P = 0.004). Interestingly, PWV increased significantly from baseline to the 2-hr time point in SED5FU (BL: 396 ± 39 cm/s; 2-hr: 452 ± 54 cm/s; P = 0.004) but not in SEDCON (BL: 417 ± 55 cm/s; 2-hr: 392 ± 64 cm/s; P=0.35), EXCON (BL: 408 ± 35 cm/s; 2-hr: 410 ± 46 cm/s; P = > 0.99), or EX5FU (BL: 398 ± 13 cm/s; 2-hr: 417 ± 23 cm/s; P = 0.67) (**Figure 4.3a**). There were no differences between any of the groups at baseline (all P > 0.05); however, 5-FU had a significantly greater PWV than SEDCON at the 2-hr time point (SED5FU: 452 ± 54 cm/s; SEDCON: 392 ± 64 cm/s; P = 0.03). No other comparisons between groups at the 2-hr time point reached statistical significance. When PWV was compared as a percent change from baseline, SED5FU had a significantly greater change than SEDCON (SED5FU: 14.5 ± 10.9%; SEDCON: -5.3 ± 15.7%; P = 0.002) (**Figure 4.3b**). All other comparisons failed to reach statistical significance.

Figure 4.3. Effect of 5-FU infusion on aortic pulse wave velocity

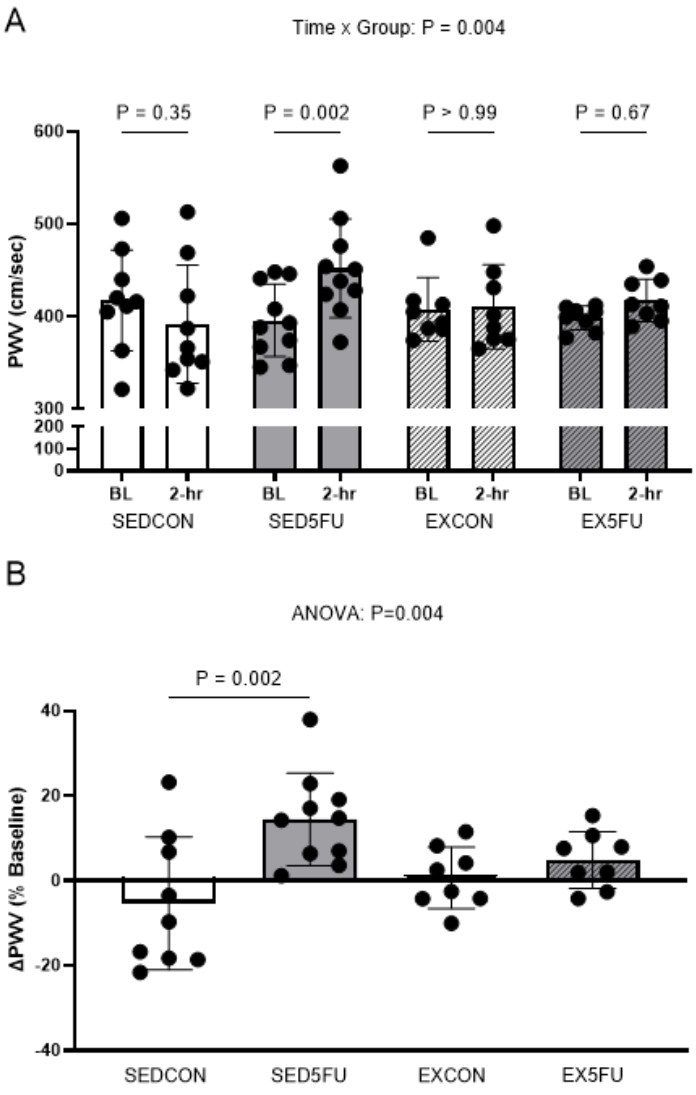

Aortic pulse wave velocity**. A)** PWV significantly increases in SED5FU but not in SEDCON, EXCON, or EX5FU suggesting acute exercise may dampen the effect of 5FU on the vasculature. **B)** SED5FU had a significantly higher change in PWV from baseline to the 2-hour time point than SEDCON. No other comparisons achieved statistical significance. Data analyzed using 2-way repeated measures ANOVA (A) and one-way ANOVA (B). EXCON n = 9, SED5FU n = 10, EXCON n = 8, EX5FU = 8.

Left ventricular inflammatory gene expression

While no functional differences in cardiac parameters were apparent between groups, RT-PCR was performed on a subset of left ventricular homogenates to determine potential subclinical alterations in inflammatory gene expression following 5-FU treatment. Both the group means ($P = 0.04$) and variances ($P = <0.0001$) were significantly different main effects between the groups for TNF gene expression (SEDCON: 1.18 ± 0.52 a.u; SED5FU 2.27 ± 2.09 a.u; EXCON 0.43 ± 0.49 a.u; EX5FU: 0.82 ± 0.15 a.u.), however, no individual group differences were revealed upon post hoc comparison (**Figure 4.4a**). In addition, no significant difference in IL1B gene expression was present between the groups (SEDCON: 1.24 ± 0.84 a.u; SED5FU 0.81 ± 0.37 a.u; EXCON 0.57 ± 0.49 a.u; EX5FU: 1.23 ± 0.25 a.u.; $P = 0.14$) (**Figure 4.4b**).

Figure 4.4. Left ventricular inflammatory gene expression

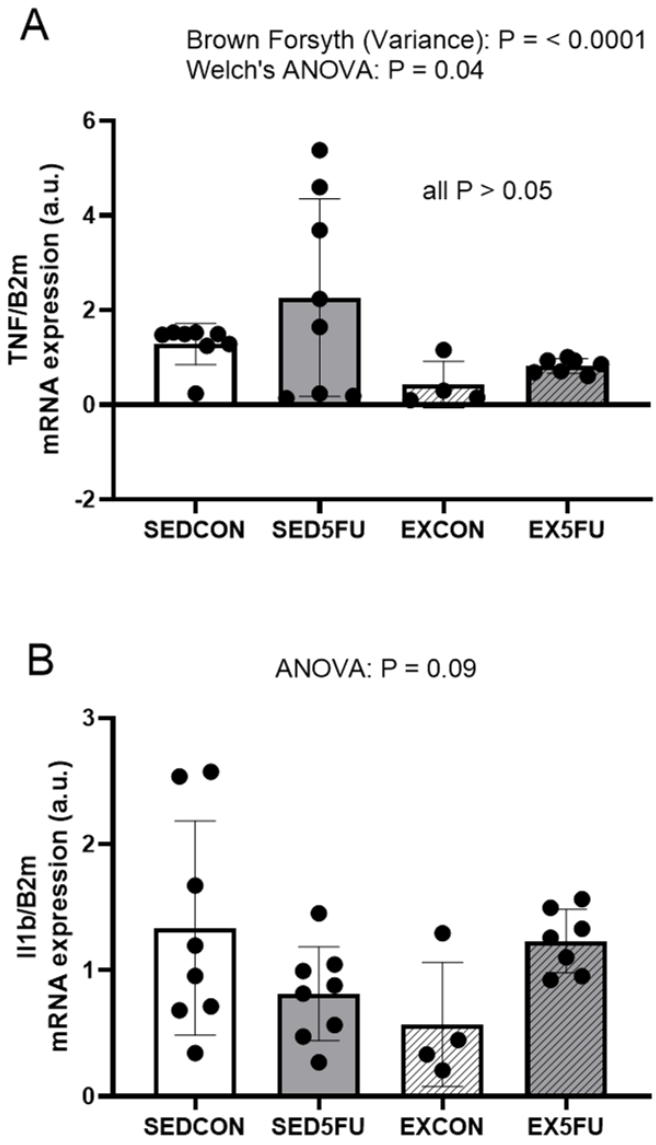

Left ventricular gene expression. No differences were apparent in **(A)** TNF or **(B)** Il1b gene expression between the groups. Interestingly, TNF gene expression had significant differences in variance between the groups. Data were analyzed using Welch's ANOVA (A) and One-way ANOVA (B). In addition, variance was assessed using the Brown Forsyth test. (SEDCON n=8, SED5FU n =8, EXCON n=4 EX5FU n=7).

RPPA and network analyses

Left ventricular and aortic lysates were probed with 423 individual antibodies. In left ventricular tissue, 4 proteins expressed at least a 1.5-fold difference between SEDCON and SED5FU (actual edges: 2; edges expected: 0; PPI = 0.03) (**Figure. 4.5a**). Functional enrichment analysis identified three significant KEGG Pathways: Fluid shear stress and atherosclerosis (pathway: rno05418; strength: 2.1, FDR = 0.0003), autophagy (pathway: rno04140; strength: 1.94; FDR: 0.034), and focal adhesion (pathway: rno04510; strength: 1.79; FDR: 0.04). 14 proteins had at least a 1.5-fold difference between SED5FU and EX5FU (actual edges:16, expected edges: 6, PPI = 0.0007). One of these proteins was differentially expressed under both conditions (i.e., SEDCON vs SED5FU and SEDFU vs EX5FU) (**Figure 4.5b**).

Figure 4.5. Protein network and functional enrichment analysis of left ventricular tissue

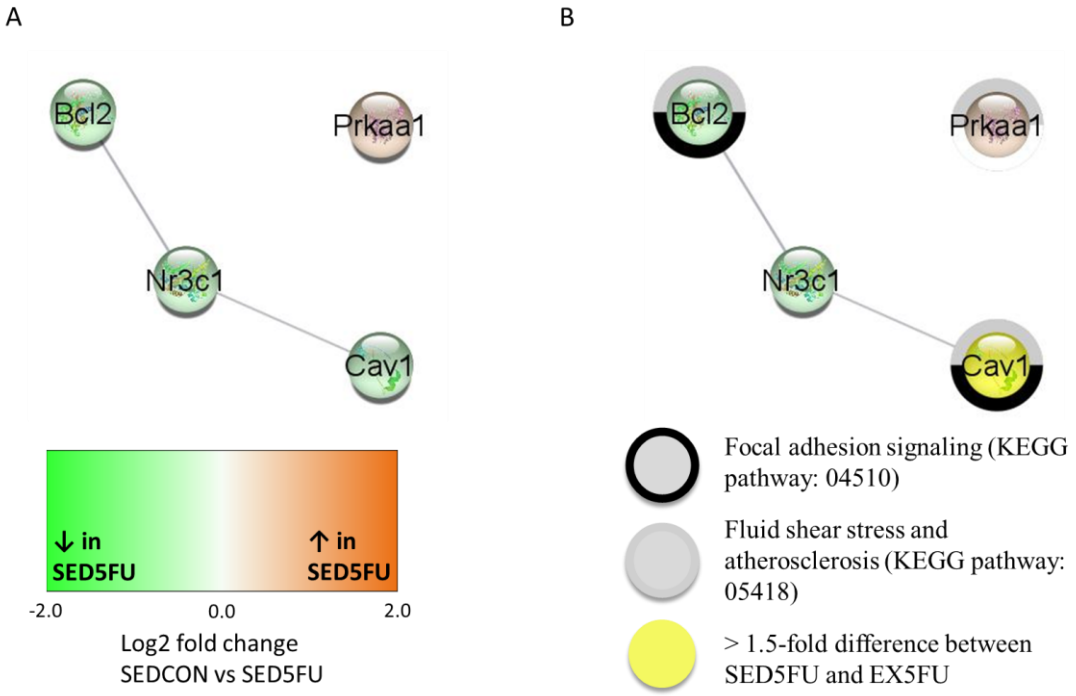

Protein network and functional enrichment analysis of left ventricular tissue. **A.** 4 proteins were differentially expressed by at least 1.5-fold between SEDCON and SED5FU. Nodes are labeled by the gene name for each protein and the color intensity indicates the direction of the Log2 fold change in SED5FU relative to SEDCON (e.g., green = ↓ in SED5FU relative to SEDCON; red = ↑ SED5FU relative to SEDCON). Edges are the lines connecting each node with the thickness of each line denoting the level of confidence that the STRING software has for an interaction between two proteins based on the available evidence (e.g., experiments, text mining, databases, etc.). **B.** Upon completion of functional enrichment, this network was determined to have a significant amount of interactions (PPI = 0.03). Proteins involved in select pathways deemed significant following functional enrichment analysis are denoted by colored outlines. KEGG identifiers for each pathway are included in parentheses. There was one protein differentially expressed (> 1.5-fold) between SED5FU and SEDCON and SED5FU and EX5FU, which is denoted by the yellow highlight. n = 4 pooled left ventricular lysates per group. The gene abbreviations above represent the following proteins: Bcl2 = B-cell lymphoma 2; Cav1 = Caveolin1; Nr3c1 = nuclear receptor subfamily 3 group c member 1; Protein kinase AMP-activated catalytic subunit alpha 1 phosphorylated at threonine 172.

Interestingly, 18 proteins were differentially expressed at least 1.5-fold in aortic tissue between SEDCON and SED5FU (actual edges: 21; expected edges: 8; PPI: 0.0002) (**Figure 4.6a).** Furthermore, functional enrichment revealed 26 KEGG pathways with an FDR of <0.05 and 5 pathways involving at least 5 of our identified proteins. Of specific interest to the in vivo findings of the present study are pathways involving focal adhesion (pathway: rno04510; strength: 1.53; FDR: 0.00005) and regulation of the actin cytoskeleton (pathway: rno04810; strength: 1.49; FDR: 0.00005). In addition, SED5FU and EX5FU had 11 proteins with at least a 1.5-fold difference in expression (actual edges: 4, expected edges: 1, PPI = 0.02) —4 of which were also altered during the sedentary comparison (**Figure 4.6b**). Again, this resulted in the return of 18 significant KEGG pathways, including focal adhesion signaling (pathway: rno04510; strength: 1.52; FDR: 0.03).

Figure 4.6. Protein network and functional enrichment analysis of aortic tissue

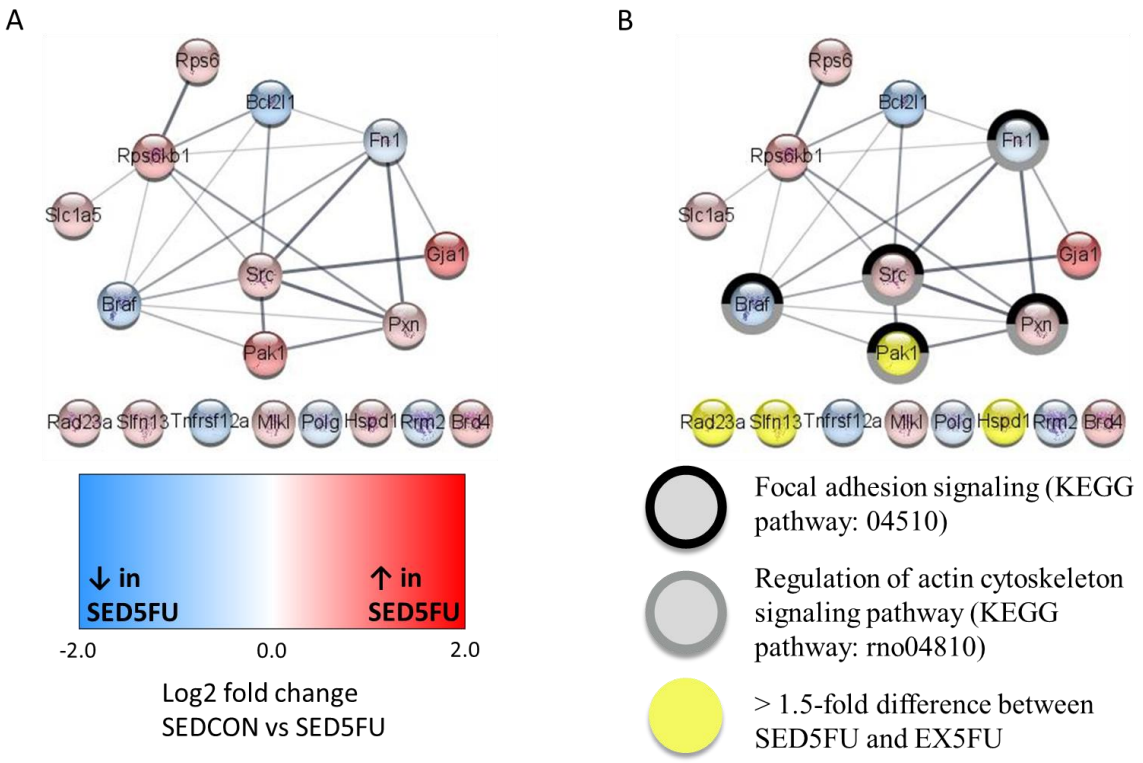

Protein network and functional enrichment analysis of aortic tissue. **A.** 18 proteins were differentially expressed by at least 1.5-fold between SEDCON and SED5FU. Nodes are labeled by the gene name for each protein and the color intensity indicates the direction of the Log2 fold change in SED5FU relative to SEDCON (e.g., blue = ↓ in SED5FU relative to SEDCON; red = ↑ SED5FU relative to SEDCON). Edges are the lines connecting each node with the thickness of each line denoting the level of confidence that the STRING software has for an interaction between two proteins based on the available evidence (e.g., experiments, text mining, databases, etc.). **B.** Upon completion of functional enrichment, this network was determined to have a significant amount of interactions present (PPI = 0.00019). Proteins involved in select pathways deemed significant by functional enrichment analysis are denoted by colored outlines. KEGG identifiers for each pathway are included in parentheses. There were four proteins differentially expressed (> 1.5-fold) between SED5FU and SEDCON and SED5FU and EX5FU, which are denoted by the yellow highlight. n = 4 pooled aortic lysates per group. The gene abbreviations above represent the following proteins: Bcl1 = B-cell lymphoma-extra large; Braf = serine/threonine-protein kinase B-Raf; Brd4 = Bromodomain-containing protein 4; Fn1 = Fibronectin-1; Gja1 = Connexin 43; Hspd1 = Heat shock protein family D member 1; Mlkl = mixed lineage kinase domain like pseudokinase; Pak1 = P21 (RAC1) activated kinase 1; Pxn = Paxillin; Polg = DNA polymerase gamma, catalytic subunit; Rad23a = Rad23a homolog A nucleotide excision repair protein; Rps6 = Ribosomal protein S6 phosphorylated at serine 235/236; Rps6kb1 = Ribosomal protein S6 kinase beta-1 phosphorylated at threonine 389; Rrm2 = ribonucleotide reductase regulatory subunit M2; Slc1a5 = Solute carrier family 1 member 5; Slfn13 = Schlafen 13; Src = SRC proto-oncogene, non-receptor tyrosine kinase phosphorylated at tyrosine 527; Tnfrsf12a = TNF receptor superfamily member 12A.

Discussion

The present study aimed to assess the efficacy of an acute exercise preconditioning protocol in preventing 5-FU-induced cardiotoxicity. In agreement with others, our findings suggest that cardiovascular maladaptation caused by 5-FU seemingly arises from alterations in vascular function. Specifically, while 5-FU induced no apparent changes in echocardiographic indices of left ventricular function, PWV increased over the 2-hr infusion in SED5FU while remaining unchanged in the other groups. Furthermore, this increase resulted in significantly higher PWV at the 2-hr time point in SED5FU compared to SEDCON despite the absence of differences in MAP, SV, Q, or EDV. Notably, these increases in PWV were not apparent in animals treated with 5-FU following 4-days of moderate-intensity treadmill running. This suggests that acute exercise training in the days preceding treatment may prevent the onset of 5-FU-induced vascular alterations. In addition, RPPA and functional enrichment analysis revealed several differentially expressed aortic proteins in SEDCON and SED5FU tissue lysates which were subsequently determined to be involved in focal adhesion and cytoskeletal regulation—two pathways known to contribute to arterial stiffening [43,44]. Taken together, we interpret these findings to suggest that short-term aerobic preconditioning before 5-FU treatment may alleviate some of the adverse vascular consequences associated with 5-FU chemotherapy and that the development of such vascular alterations may involve changes to focal adhesion and/or cytoskeletal regulation pathways. As such, the present work offers initial insight into potential pathways involved in the onset of 5-FU-induced vascular alterations and provides preclinical support for the use of exercise as a modality to prevent the development of 5-FU cardiotoxicity.

Despite continued advances in cancer care, 5-FU chemotherapy has remained a central component of numerous cancer treatment regimens for over 60 years [45,46]. However, a serious yet

often underreported [47,48] consequence of 5-FU is the onset of acute cardiotoxicities that arise during or shortly following cessation of treatment [2,49,50]. A heightened understanding of the mechanisms in which 5-FU cardiotoxicity develops and the identification of mitigating modalities will help ensure patients receive the preferred treatment regimen without increased risk of cardiovascular maladaptation. While preclinical studies have played a significant role in growing the current understanding of these mechanisms, prior works have exclusively employed bolus (20 sec. to 10 minutes) [10,13,14,17,51] or intraperitoneal [7,9,21,52] dosing models, while many clinical 5-FU based regimens (e.g., FOLFOX, FOLFIRINOX, FOLFIRI) incorporate a continuous infusion of 5-FU delivered over 46 hours [31,32,53,54]. This prolonged exposure to 5-FU has been associated with greater treatment efficacy (49,50) and heightened rates of cardiotoxicity compared to bolus injection alone [55]. Thus, we designed a preclinical dosing model incorporating a continuous infusion of 5-FU to more closely align our study with the methods of delivery most commonly seen in the clinical setting.

Importantly, this approach did not detect differences in left ventricular function between the 5-FU treated and saline control. This is in agreeance with the findings of Zhang and colleagues, who found no differences in FS between a control group and rats receiving 5 consecutive daily doses of either 25 or 50 mg/kg of 5-FU via intraperitoneal injection [7]. Clinically, reductions in left ventricular function secondary to 5-FU are seemingly rare in large scale studies but have been reported in several clinical case reports [56–58]. It is worth noting, however, that increases in ESV and reductions in FS were apparent in all of our experimental groups—with changes in 3 groups reaching statistical significance for ESV and FS alike over the course of the 2-hr infusion. These alterations are seemingly independent of 5-FU and may be a consequence of prolonged use of pentobarbital anesthesia, as reductions in FS have been noted

over the course of 3-hr of pentobarbital anesthesia in dogs [59]. Notably, despite statistically significant reductions, the FS values reported herein remain well above those seen in our rat model of heart failure (FS = ~20-26%) [34,35,60,61] and are consistent with previously published values in healthy rats [34,35,60–62].

Numerous preclinical works have reported perturbations in cellular/organellular structure [8], inflammatory signaling [9], and oxidative damage [9,22] in myocardial tissue/cell culture following 5-FU exposure. This differs from the present study's findings in that we could not detect individual group differences in the gene expression of the inflammatory markers TNF or IL1B in left ventricular tissue lysate. However, it is worth noting that TNF gene expression presented significant variability between the groups, seemingly driven by the SED5FU group. These findings partially agree with those recently demonstrated by Barary and colleagues who also report a lack of difference in TNF gene expression following a 125 mg/kg ip injection of 5-FU [52]. Interestingly, the Baray et al. findings also appear to have differences in TNF sample variance—especially in the 5-FU group—although group means and standard deviations were not reported. Others have found an increase in TNF gene and/or TNF-α protein levels following 5-FU exposure in myocardial tissue [63] and macrophages [64], as well as the induction of other prominent inflammatory mediators such as ERK/MAPK [9,64] and COX-2 [9]. Interestingly, our RPPA analysis revealed just 4 differentially expressed proteins (i.e., > 1.5-fold difference between SEDCON and SED5FU) in left ventricular lysate, resulting in the detection of only 3 significant KEGG pathways upon completion of functional enrichment analysis. These pathways included focal adhesions, autophagy, and atherosclerosis and fluid shear stress. Focaccetti and colleagues have previously demonstrated increased autophagy in cultured cardiomyocytes that was preventable when treated with a reactive oxygen species (ROS) scavenger suggesting a role for oxidative

stress in subclinical indices of 5-FU induced cardiac myocyte damage [8]. Though not investigated herein, ROS and oxidative stress are a regularly reported consequence of 5-FU treatment in various experimental models and tissue types [8,9,21,22] and have also been implicated in the onset of atherosclerosis, potentially via alterations in shear stress [65], and the activation of focal adhesion proteins [66]. Future work investigating the contribution of these subclinical molecular alterations and pathways in cardiac tissue (and the small arterioles within) and how they contribute to the onset of 5-FU-mediated cardiotoxicity is warranted.

The most prevalent theory of 5-FU cardiotoxicity suggests the materialization of side effects because of a direct impact of the drug on the vasculature. In agreeance with this notion, we demonstrate increases in PWV in SED5FU over the 2-hr infusion that SEDCON, EXCON, or EX5FU did not reciprocate, despite a lack of difference in hemodynamic variables known to influence PWV. SED5FU also presented with significantly higher PWV at the 2-hr time point and as a change from baseline compared to SEDCON. Notably, PWV was higher at 2-hr than baseline in all 10 SED5FU animals. To our knowledge, others have yet to investigate changes in PWV following a single cycle of 5-FU. Our group has previously demonstrated a relationship between anticancer therapy and arterial stiffness [67,68], as well as an association between an index of arterial stiffness and cardiovascular/cancer mortality in some cancer populations [69], thus highlighting the importance of this measurement throughout cancer survivorship. Visvikis and colleagues recently found a ~10% increase in the PWV of patients with colorectal cancer upon completing 6-12 cycles of 5-FU-based chemotherapy regimens [70]. The mechanisms responsible for these vascular alterations are incompletely understood but appear to involve a complex array of signaling events spanning several layers of the vessel wall. Specifically, 5-FU has been demonstrated to have deleterious effects on numerous components of the endothelium and

smooth muscle, including the induction of senescence and/or apoptosis [8,12], increases in oxidative stress and/or inflammation [8,9], alterations in the actin cytoskeleton [18,19], and modification of vasodilator/vasoconstrictor proteins [9,12]. Studies in both aortic rings [11,71] and human patients [6,72] have shown arterial vasoconstriction following exposure to 5-FU. The ex vivo findings of Mosseri and colleagues suggest this vasoconstrictor effect arises via endothelium-independent, PKC-mediated pathways [11]. However, critical differences between in vivo and ex vivo preparations, including how the drug first encounters a given cell type (i.e., bloodstream to endothelium to smooth muscle vs. diffusion from a bath) as well as the potential effect of high local drug concentrations in ex vitro preparations warrant consideration before translating these ex vivo findings to the clinical setting.

Though the pathways mentioned above were not investigated herein, RPPA revealed 18 differentially expressed proteins with at least a 1.5-fold difference between SEDCON and SED5FU. This resulted in detection of 26 significant KEGG pathways upon completion of functional enrichment analysis. Of particular interest to our in vivo findings of altered PWV were pathways involving focal adhesion signaling and regulation of the actin cytoskeleton, as both have previously been implicated in the modulation of vessel contractile responses and stiffness [43,73]. Specifically, focal adhesions play a critical role in the structure of the vascular wall by acting as a bridge between the actin cytoskeleton and the extracellular matrix [44,74]. Focal adhesion signaling is modified in response to a myriad of intra-and extracellular stimuli, including alterations in shear stress [75,76], exposure to vasoactive peptides [77,78], and changes to the actin cytoskeleton [79,80]. In addition, 5-FU treatment has been associated with increased endothelin-1 [9,81,82] and alterations to the actin cytoskeleton [18,19]. Thus, 5-FU-induced activation of these cellular events could set the stage for increased focal adhesion signaling and ultimately

increased vascular stiffness. Saphirstein and colleagues have previously demonstrated that stimulation of aortic rings with phenylephrine can increase focal adhesion linkage to the extracellular matrix resulting in increased contractility and stiffness. Importantly, these findings were subsequently diminished with pharmacological inhibition of the key focal adhesion proteins focal adhesion kinase and proto-oncogene tyrosine-protein kinase Src (Src) [43]. Future work to assess changes in focal adhesion and cytoskeletal regulatory pathways following exposure to 5-FU may provide key insight into the underlying mechanisms of 5-FU-induced vascular alterations.

Another critical finding of this work is the protective effect of pre-treatment moderate-intensity exercise on changes in PWV in response to 5-FU treatment. Indeed, the significant increase in PWV, apparent in SED5FU over the 2-hr infusion, was not reciprocated in EX5FU. Similarly, the absolute PWV was not different between EX5FU and SEDCON at the 2-hr time point, nor were there differences between the groups when comparing the change in PWV from baseline. We interpret these findings to suggest that 4 bouts of exercise preconditioning may induce stimuli capable of offsetting the adverse vascular consequences of 5-FU treatment. Though findings from the current study cannot provide complete insight into the exact mechanisms for this apparent vasculo-protective effect, RPPA analysis again revealed several differentially expressed proteins between SED5FU and EX5FU involved in focal adhesion signaling and this represents an intriguing future experimental direction. The efficacy of acute exercise preconditioning has previously been demonstrated in preventing cardiotoxicity induced by anthracycline chemotherapy in rodents [26,28,83] and human patients [84] with a specific focus on left ventricular function. To our knowledge, only Hayward and colleagues have assessed the potential vasculo-protective effects of exercise on 5-FU mediated vasoconstriction, albeit

through a longitudinal training program (4-6 weeks) and ex vivo experimental model. Their work suggests improved acetylcholine vasodilation in 5-FU pre-constricted aortic rings isolated from exercise-trained (20-25 m/min, 5 d/w, 8-wks) rats noting increased aortic content of eNOS as a potential mechanism for this improvement. Interestingly, though it did not reach statistical significance, the authors observed a consistent 30% reduction in the 5-FU-induced tension of aortic rings from exercised animals compared to controls.

Limitations

The following experimental considerations are pertinent to interpreting the present study's findings. First, a key component of our work included using a novel preclinical dosing regimen designed to reflect 5-FU delivery methods used in clinical practice. To perform this protocol, animals remained under pentobarbital anesthesia for approximately 150 – 180 minutes. Such prolonged periods of pentobarbital anesthesia can result in alterations in cardiac parameters (as discussed above) that should be considered in the interpretation of our findings. However, pentobarbital has been demonstrated to have a lesser impact on cardiovascular function than other commonly used anesthetics (e.g., isoflurane, ketamine/xylazine), and cardiovascular alterations may be both dose and species-dependent [85]. Future work in which the use of an anesthetic is minimized during the infusion through the use of implantable infusion pumps should be considered. Second, the animals used in the present study were free of cancer, as is common in most studies of chemotherapy-induced cardiotoxicity [7,9,13,14,17,26–28]. It is possible that this could affect the metabolism of 5-FU differently than in tumor-bearing animals and/or patients with cancer. To our knowledge, differences in 5-FU metabolism in tumor-bearing vs non-tumor bearing animals have yet to be studied. However, the inclusion of tumor-bearing animals in future investigations of 5-FU cardiotoxicity is a critical step in improving the

translatability of preclinical animal models of cardiotoxicity. Similarly, 5-FU is regularly delivered alongside several other chemotherapy drugs (e.g., leucovorin, oxaliplatin, bevacizumab, etc.) to improve cancer treatment efficacy. Several of these drugs have been suggested to increase the incidence of 5-FU-induced cardiotoxicity [86,87]. While the focus of the current study was to better understand the impact of 5-FU alone, future works may seek to include other treatments regularly delivered alongside 5-FU to better understand the mechanisms of specific treatment regimens (e.g., FOLFOX, FOLFIRINOX). Lastly, the present study has not assessed individual proteins (i.e., via western blot) involved with the signaling pathways determined by functional enrichment analyses and thus cannot provide definitive answers regarding the proteins and signaling involved in the onset of 5-FU-induced cardiotoxicity. However, identifying these pathways using RPPA in conjunction with STRING provides an intriguing rationale and starting point for future investigations to uncover the mechanisms of 5-FU-induced cardiotoxicity.

Conclusion

The present work sought to test the effects of an acute exercise preconditioning protocol on preventing cardiovascular maladaptation in response to a clinically relevant dose of 5-FU chemotherapy. Our findings suggest that a single cycle of 5-FU induces increases in aortic PWV, but not reductions in left ventricular function. Importantly, these alterations in PWV were negated in exercised rats, implying that four 20-minute bouts of moderate-intensity exercise in the days immediately preceding treatment may prevent the onset of the cardiotoxic effects of 5-FU. Furthermore, functional enrichment analysis of differentially expressed proteins between sedentary 5-FU and control animals point to focal adhesion and cytoskeletal regulation signaling pathways as potential contributors to the onset of 5-FU-induced changes in vascular function.

Future works aimed at better understanding the role of these pathways, as well as the efficacy of exercise preconditioning programs in the prevention of 5-FU-induced vascular changes in human patients, may play a critical role in improved understanding of the mechanisms driving 5-FU cardiotoxicity and the development of modalities to alleviate its occurrence.

References

1. Heidelberger, C. *et al.* Fluorinated pyrimidines, a new class of tumour-inhibitory compounds. *Nature* **179**, 663–666 (1957).
2. Sara, J. D. *et al.* 5-fluorouracil and cardiotoxicity: a review. *Ther Adv Med Oncol* **10**, 1–18 (2018).
3. Jin, X., Bai, Y., Gao, · Lan & Wu, · Shikai. Incidence of and risk factors for cardiotoxicity after fluorouracil-based chemotherapy in locally advanced or metastatic gastric cancer patients. *Cancer Chemother Pharmacol* **84**, 599–607 (2019).
4. Shoemaker, L. K., Arora, U. & Rocha Lima, C. M. S. 5-Fluorouracil–Induced Coronary Vasospasm. **11**, 46–49 (2017).
5. Luwaert, R., Descamps, O., Majois, F., Chaudron, JM. & Beauduin, M. Coronary artery spasm induced by 5-fluorouracil. *Eur Heart J* **12**, 468–470 (1991).
6. Südhoff, T. *et al.* 5-Fluorouracil induces arterial vasocontractions. *Annals of Oncology* **15**, 661–664 (2004).
7. Zhang, D. & Ma, J. Mitochondrial Dynamics in Rat Heart Induced by 5-Fluorouracil. *Med Sci Monit* **24**, 6666 (2018).
8. Focaccetti, C. *et al.* Effects of 5-fluorouracil on morphology, cell cycle, proliferation, apoptosis, autophagy and ros production in endothelial cells and cardiomyocytes. *PLoS One* **10**, (2015).
9. Muhammad, R. N., Sallam, N. & El-Abhar, H. S. Activated ROCK/Akt/eNOS and ET-1/ERK pathways in 5-fluorouracil-induced cardiotoxicity: modulation by simvastatin. *Sci Rep* **10**, 14693 (2020).
10. Tsibiribil, P. *et al.* Cardiac lesions induced by 5-uorouracil in the rabbit. *Hum Exp Toxicol* **25**, 305–309 (2006).
11. Mosseri, M., Fingert, H. J., Varticovski, L., Chokshi, S. & Isner, J. M. In Vitro Evidence That Myocardial Ischemia Resulting from 5-Fluorouracil Chemotherapy Is Due to Protein Kinase C-mediated Vasoconstriction of Vascular Smooth Muscle. *Cancer Res* **53**, (1993).
12. Altieri, P. *et al.* 5-fluorouracil causes endothelial cell senescence: potential protective role of glucagon-like peptide 1. *Br J Pharmacol* **174**, 3713–3726 (2017).
13. Kinhult, S., Albertsson, M., Eskilsson, J. & Cwikiel, M. Effects of probucol on endothelial damage by 5-fluorouracil. *Acta Oncol (Madr)* **42**, 304–308 (2003).

14. Kinhult, S., Albertsson, M., Eskilsson, J. & Cwikiel, M. Antithrombotic treatment in protection against thrombogenic effects of 5-fluorouracil on vascular endothelium: A scanning microscopy evaluation. *Scanning* **23**, 1–8 (2001).
15. Gajalakshmi, P. *et al.* Breast cancer drugs dampen vascular functions by interfering with nitric oxide signaling in endothelium. *Toxicol Appl Pharmacol* **269**, 121–131 (2013).
16. Cwikiel, M., Eskilsson, J., Albertsson, M. & Stavenow, L. The influence of 5-fluorouracil and methotrexate on vascular endothelium. An experimental study using endothelial cells in the culture. *Annals of Oncology* **7**, 731–737 (1996).
17. Cwikiel, M., Eskilsson, J., Wieslander, J., Stjernquist, M. & Albertsson, M. The appearance of endothelium in small arteries after treatment with 5-fluorouracil. An electron microscopic study of late effects in rabbits - PubMed. *Scanning Microsc.* **10**, 805–819 (1996).
18. Filgueiras, M. de C., Morrot, A., Soares, P. M. G., Costa, M. L. & Mermelstein, C. Effects of 5-Fluorouracil in Nuclear and Cellular Morphology, Proliferation, Cell Cycle, Apoptosis, Cytoskeletal and Caveolar Distribution in Primary Cultures of Smooth Muscle Cells. *PLoS One* **8**, e63177 (2013).
19. Gordon, S. R., Climie, M. & Hitt, A. L. 5-fluorouracil interferes with actin organization, stress fiber formation and cell migration in corneal endothelial cells during wound repair along the natural basement membrane. *Cell Motil Cytoskeleton* **62**, 244–258 (2005).
20. Elsea, C. R., Roberts, D. A., Druker, B. J. & Wood, L. J. Inhibition of p38 MAPK suppresses inflammatory cytokine induction by etoposide, 5-fluorouracil, and doxorubicin without affecting tumoricidal activity. *PLoS One* **3**, e2355 (2008).
21. Durak, İ., Karaayvaz, M., Kavutcu, M., Büyükkoçak, S. & Öztürk, H. S. Reduced antioxidant defense capacity in myocardial tissue from guinea pigs treated with 5-Fluorouracil. **59**, 585–589 (2010).
22. Lamberti, M. *et al.* 5-Fluorouracil induces apoptosis in rat cardiocytes through intracellular oxidative stress. *Journal of Experimental and Clinical Cancer Research* **31**, 1–8 (2012).
23. Zafar, A. *et al.* The efficacy and safety of cardio-protective therapy in patients with 5-FU (Fluorouracil)-associated coronary vasospasm. *PLoS One* **17**, e0265767 (2022).

24. Patel, B. *et al.* 5-Fluorouracil Cardiotoxicity: Left Ventricular Dysfunction and Effect of Coronary Vasodilators. *Am J Med Sci* **294**, 238–243 (1987).
25. Eskilsson, J. & Albertsson, M. Failure of Preventing 5-Fluorouracil Cardiotoxicity by Prophylactic Treatment with Verapamil. **29**, 1001–1003 (2009).
26. Kavazis, A. N., Smuder, A. J., Min, K., Tümer, N. & Powers, S. K. Short-term exercise training protects against doxorubicin-induced cardiac mitochondrial damage independent of HSP72. *American Journal of Physiology-Heart and Circulatory Physiology* **299**, H1515–H1524 (2010).
27. Kavazis, A. N., Smuder, A. J. & Powers, S. K. Effects of short-term endurance exercise training on acute doxorubicin-induced FoxO transcription in cardiac and skeletal muscle. *J Appl Physiol* **117**, 223–230 (2014).
28. Ascensão, A. *et al.* Acute exercise protects against calcium-induced cardiac mitochondrial permeability transition pore opening in doxorubicin-treated rats. *Clin Sci* **120**, 37–49 (2011).
29. Wonders, K. Y., Hydock, D. S., Schneider, C. M. & Hayward, R. Acute Exercise Protects Against Doxorubicin Cardiotoxicity. **7**, 147–154 (2008).
30. Bedford, T. G., Tipton, C. M., Wilson, N. C., Oppliger, R. A. & Gisolfi, C. v. Maximum oxygen consumption of rats and its changes with various experimental procedures. *J Appl Physiol Respir Environ Exerc Physiol* **47**, 1278–1283 (1979).
31. Cheeseman, S. L. *et al.* A 'modified de Gramont' regimen of fluorouracil, alone and with oxaliplatin, for advanced colorectal cancer. *British Journal of Cancer 2002 87:4* **87**, 393–399 (2002).
32. Conroy, T. *et al.* FOLFIRINOX versus Gemcitabine for Metastatic Pancreatic Cancer. *New England Journal of Medicine* **364**, 1817–1825 (2011).
33. Nair, A. B. & Jacob, S. A simple practice guide for dose conversion between animals and human. *J Basic Clin Pharm* **7**, 27 (2016).
34. Butenas, A. L. E. *et al.* Thromboxane A2 receptors contribute to the exaggerated exercise pressor reflex in male rats with heart failure. *Physiol Rep* **9**, e15052 (2021).
35. Butenas, A. L. E. *et al.* Exaggerated sympathetic and cardiovascular responses to dynamic mechanoreflex activation in rats with heart failure: role of endoperoxide 4 and thromboxane A2 receptors. *Auton Neurosci* **232**, 102784 (2021).

36. Baumfalk, D. R. *et al.* Effects of prostate cancer and exercise training on left ventricular function and cardiac and skeletal muscle mass. *J Appl Physiol* **126**, 668–680 (2018).
37. Teichholz, L., Kreulen, T., Herman, M. & Gorlin, R. Problems in echocardiographic volume determinations: echocardiographic-angiographic correlations in the presence or absence of asynergy. *Am. J. Card.* **37**, 7–11 (1976).
38. Laurent, S. *et al.* Expert consensus document on arterial stiffness: methodological issues and clinical applications. *Eur Heart J* **27**, 2588–2605 (2006).
39. Tibes, R. *et al.* Reverse phase protein array: validation of a novel proteomic technology and utility for analysis of primary leukemia specimens and hematopoietic stem cells. *Mol Cancer Ther* **5**, 2512–2521 (2006).
40. Shannon, P. *et al.* Cytoscape: A Software Environment for Integrated Models of Biomolecular Interaction Networks. *Genome Res* **13**, 2498–2504 (2003).
41. Szklarczyk, D. *et al.* The STRING database in 2021: customizable protein-protein networks, and functional characterization of user-uploaded gene/measurement sets. *Nucleic Acids Res* **49**, D605–D612 (2021).
42. Szklarczyk, D. *et al.* STRING v10: protein–protein interaction networks, integrated over the tree of life. *Nucleic Acids Res* **43**, D447–D452 (2015).
43. Saphirstein, R. J. *et al.* The Focal Adhesion: A Regulated Component of Aortic Stiffness. *PLoS One* **8**, e62461 (2013).
44. Ribeiro-Silva, J. C., Miyakawa, A. A. & Krieger, J. E. Focal adhesion signaling: vascular smooth muscle cell contractility beyond calcium mechanisms. *Clin Sci* **135**, 1189–1207 (2021).
45. Ansfield, F. J., Schroeder, J. M. & Curreri, A. R. Five Years Clinical Experience with 5-Fluorouracil. *JAMA* **181**, 295–299 (1962).
46. Gustavsson, B. *et al.* A review of the evolution of systemic chemotherapy in the management of colorectal cancer. *Clin Colorectal Cancer* **14**, 1–10 (2015).
47. Lestuzzi, C. *et al.* Effort myocardial ischemia during chemotherapy with 5-fluorouracil: an underestimated risk. *Annals of Oncology* **25**, 1059–1064 (2014).
48. Lestuzzi, C. *et al.* Fluoropyrimidine-Associated Cardiotoxicity: Probably Not So Rare As It Seems. *Oncologist* **25**, e1254–e1254 (2020).

49. Polk, A., Vaage-Nilsen, M., Vistisen, K. & Nielsen, D. L. Cardiotoxicity in cancer patients treated with 5-fluorouracil or capecitabine: A systematic review of incidence, manifestations and predisposing factors. *Cancer Treat Rev* **39**, 974–984 (2013).
50. Polk, A., Vistisen, K., Vaage-Nilsen, M. & Nielsen, D. L. A systematic review of the pathophysiology of 5-fluorouracil-induced cardiotoxicity. *BMC Pharmacol Toxicol* **15**, 1–11 (2014).
51. Matsubara, I., Kamiya, J. & Imai, S. Cardiotoxic effects of 5-fluorouracil in the guinea pig. *The Japanese Journal of Pharmacology* **30**, 871–879 (1980).
52. Barary, M. *et al.* The effect of propolis on 5-fluorouracil-induced cardiac toxicity in rats. *Scientific Reports* **12**, 1–16 (2022).
53. Akdeniz, N. *et al.* The comparison of FOLFOX regimens with different doses of 5-FU for the adjuvant treatment of colorectal cancer: a multicenter study. *Int J Colorectal Dis* **36**, 1311–1319 (2021).
54. Petrelli, F. *et al.* FOLFIRI-Bevacizumab As First-Line Chemotherapy in 3500 Patients With Advanced Colorectal Cancer: A Pooled Analysis of 29 Published Trials. *Clin Colorectal Cancer* **12**, 145–151 (2013).
55. Saif, M. W., Shah, M. M. & Shah, A. R. Fluoropyrimidine-associated cardiotoxicity: revisited. **8**, 191–202 (2009).
56. Allison, J. D., Tanavin, T., Yang, Y., Birnbaum, G. & Khalid, U. Various Manifestations of 5-Fluorouracil Cardiotoxicity: A Multicenter Case Series and Review of Literature. *Cardiovasc Toxicol* **20**, 437–442 (2020).
57. Chaudary, S., Song, S. Y. T. & Jaski, B. E. Profound, yet reversible, heart failure secondary to 5-fluorouracil. *Am J Med* **85**, 454–456 (1988).
58. Dechant, C. *et al.* Acute Reversible Heart Failure Caused by Coronary Vasoconstriction due to Continuous 5-Fluorouracil Combination Chemotherapy. *Case Rep Oncol* **5**, 296–301 (2012).
59. Lang, R. M. *et al.* A time-course study of the effects of pentobarbital, fentanyl, and morphine chloralose on myocardial mechanics. **73**, 143–150 (1992).
60. Butenas, A. L. E. *et al.* No effect of endoperoxide 4 or thromboxane A2 receptor blockade on static mechanoreflex activation in rats with heart failure. *Exp Physiol* **105**, 1840–1854 (2020).

61. Craig, J. C. *et al.* Central and peripheral factors mechanistically linked to exercise intolerance in heart failure with reduced ejection fraction. *Am J Physiol Heart Circ Physiol* **317**, H434–H444 (2019).
62. Pawlush, D. G., Moore, R. L., Musch, T. I. & Davidson, W. R. Echocardiographic evaluation of size, function, and mass of normal and hypertrophied rat ventricles. *J Appl Physiol* **74**, 2598–2605 (1993).
63. Arafah, A. *et al.* Myricetin (3,3′,4′,5,5′,7-Hexahydroxyflavone) Prevents 5-Fluorouracil-Induced Cardiotoxicity. *ACS Omega* **7**, 4514–4524 (2022).
64. Elsea, C. R., Roberts, D. A., Druker, B. J. & Wood, L. J. Inhibition of p38 MAPK Suppresses Inflammatory Cytokine Induction by Etoposide, 5-Fluorouracil, and Doxorubicin without Affecting Tumoricidal Activity. *PLoS One* **3**, e2355 (2008).
65. Harrison, D., Griendling, K. K., Landmesser, U., Hornig, B. & Drexler, H. Role of oxidative stress in atherosclerosis. *Am J Cardiol* **91**, 7–11 (2003).
66. Usatyuk, P. v. & Natarajan, V. Regulation of reactive oxygen species-induced endothelial cell-cell and cell-matrix contacts by focal adhesion kinase and adherens junction proteins. *Am J Physiol Lung Cell Mol Physiol* **289**, 999–1010 (2005).
67. Parr, S. K. *et al.* Anticancer Therapy–Related Increases in Arterial Stiffness: A Systematic Review and Meta-Analysis. *J Am Heart Assoc* **9**, (2020).
68. Frye, J. N. *et al.* Vascular and autonomic changes in adult cancer patients receiving anticancer chemotherapy. *J Appl Physiol* **125**, 198–204 (2018).
69. Parr, S. K., Steele, C. C., Hammond, S. T., Turpin, V. R. G. & Ade, C. J. Arterial stiffness is associated with cardiovascular and cancer mortality in cancer patients: Insight from NHANESIII. *Int J Cardiol Hypertens* **9**, 100085 (2021).
70. Visvikis, A. *et al.* Cardiotoxic Profile and Arterial Stiffness of Adjuvant Chemotherapy for Colorectal Cancer. *Cancer Manag Res* **12**, 1175 (2020).
71. Hayward, R. *et al.* Training Enhances Vascular Relaxation after Chemotherapy-Induced Vasoconstriction. *Med Sci Sports Exerc* **36**, 428–434 (2004).
72. Salepci, T. *et al.* 5-Fluorouracil induces arterial vasoconstrictions but does not increase angiotensin II levels. *Med Oncol* **27**, 416–420 (2010).
73. Qiu, H. *et al.* Short Communication: Vascular Smooth Muscle Cell Stiffness As a Mechanism for Increased Aortic Stiffness With Aging. *Circ Res* **107**, 615–619 (2010).

74. Ciobanasu, C., Faivre, B. & le Clainche, C. Integrating actin dynamics, mechanotransduction and integrin activation: The multiple functions of actin binding proteins in focal adhesions. *Eur J Cell Biol* **92**, 339–348 (2013).
75. Li, S. *et al.* Fluid Shear Stress Activation of Focal Adhesion Kinase. *Journal of Biological Chemistry* **272**, 30455–30462 (1997).
76. Mott, R. E. & Helmke, B. P. Mapping the dynamics of shear stress-induced structural changes in endothelial cells. *Am J Physiol Cell Physiol* **293**, 1616–1626 (2007).
77. Daher, Z., Noël, J. & Claing, A. Endothelin-1 promotes migration of endothelial cells through the activation of ARF6 and the regulation of FAK activity. *Cell Signal* **20**, 2256–2265 (2008).
78. Turner, C. E., Pietras, K. M., Taylor, D. S. & Molloy, C. J. Angiotensin II stimulation of rapid paxillin tyrosine phosphorylation correlates with the formation of focal adhesions in rat aortic smooth muscle cells. *J Cell Sci* **108**, 333–342 (1995).
79. Balaban, N. Q. *et al.* Force and focal adhesion assembly: a close relationship studied using elastic micropatterned substrates. *Nature Cell Biology 2001 3:5* **3**, 466–472 (2001).
80. Corne, T. D. J. *et al.* Deregulation of focal adhesion formation and cytoskeletal tension due to loss of A-type lamins. *Cell Adh Migr* **11**, 447–463 (2017).
81. Porta, C., Moroni, M., Ferrari, S. & Nastasi, G. Endothelin-1 and 5-fluorouracil-induced cardiotoxicity. *Neoplasma* **45**, 81–82 (1998).
82. Thyss, A. *et al.* Very high endothelin plasma levels in patients with 5-FU cardiotoxicity. *Annals of Oncology* **3**, 88 (1992).
83. Wonders, K. Y., Hydock, D. S., Schneider, C. M. & Hayward, R. Acute exercise protects against doxorubicin cardiotoxicity. *Integr Cancer Ther* **7**, 147–154 (2008).
84. Kirkham, A. A. *et al.* Protective effects of acute exercise prior to doxorubicin on cardiac function of breast cancer patients: A proof-of-concept RCT. *Int J Cardiol* **245**, 263–270 (2017).
85. Stein, A. B. *et al.* Effects of anesthesia on echocardiographic assessment of left ventricular structure and function in rats. *Basic Res Cardiol* **102**, 28–41 (2007).
86. Abdel-Rahman, O. 5-Fluorouracil-related Cardiotoxicity; Findings From Five Randomized Studies of 5-Fluorouracil-based Regimens in Metastatic Colorectal Cancer. *Clin Colorectal Cancer* **18**, 58–63 (2019).

87. Kosmas, C. *et al.* Cardiotoxicity of fluoropyrimidines in different schedules of administration: A prospective study. *J Cancer Res Clin Oncol* **134**, 75–82 (2008).

Chapter 5 - Conclusion

5-fluorouracil (5-FU) chemotherapy has been a key component of several gastrointestinal, head/neck, and breast cancer treatment regimens since the early 1960s. Despite frequent use and high efficacy in the treatment of malignant disease, 5-FU is associated with severe cardiovascular side effects which often limit its utility. In the present dissertation, our aim was to take a 'clinic to culture approach' to better understanding 5-FU chemotherapy induced cardiotoxicity with a specific focus on how this drug impacts the vasculature. To do this, we allowed our initial studies in human patients to guide our subsequent experiments in preclinical cell culture and animal models with hopes that these latter studies can inspire future investigations in the clinical setting.

In chapter 2, we tested the hypothesis that patients undergoing treatment for cancer with 5-FU-based chemotherapy regimens would present with impairments in cutaneous microvascular reactivity compared to matched controls. Our primary finding was that patients undergoing 5-FU chemotherapy have significant impairments in cutaneous microvascular responses to local skin heating—a process largely mediated by endothelium-derived nitric oxide production. This finding was supported by the inability of the nitric oxide synthase inhibitor L-NAME to reduce the cutaneous microvascular vasodilator response in 5-FU patients, despite successfully doing so in controls. Follow up experiments in human endothelial cell culture confirmed reductions in eNOS gene expression following in vitro treatment with 5-FU. Findings from this study suggested perturbations along the eNOS-nitric oxide vasodilator pathway in patients undergoing treatment with 5-FU based chemotherapy regimens and provide a foundation for future experiments into how this pathway may be involved in the symptoms experienced by patients in the clinical setting.

Given that alterations in endothelial function are a known precursor to long-term vascular maladies such as vascular calcification, in chapter 3, we sought to determine whether 5-FU exposure stimulated increases in calcium deposition in aortic smooth muscle cells. Using an established aortic explant technique, we cultured aortic smooth muscle cells from rats following completion of a continuous infusion of 5-FU chemotherapy. We found that cells derived from 5-FU treated rats were prone to the development of calcium deposition following 5 and 8 days of culture in a calcification media despite seeing no effect of the media in cells derived from saline treated animals. To test this finding in a second model, we exposed cells derived from saline rats to 5-FU in vitro, finding an increase in calcium concentration compared to cells that remained untreated. These findings suggest that 5-FU exposure—whether in vivo or in vitro—may predispose smooth muscle cells to the development of a calcified phenotype. These preclinical data highlight the need for additional mechanistic studies and long-term patient monitoring to improve our understanding of how 5-FU chemotherapy may impact vascular function in cancer survivorship.

The paucity of data regarding modalities to prevent and alleviate the development of 5-FU cardiotoxicity inspired us to test the effects of an acute exercise preconditioning program on the prevention of 5-FU cardiotoxicity in rats. In chapter 4, we monitored changes in cardiac and vascular function prior to and following completion of a clinically relevant dose of 5-FU or volume matched saline in sedentary or prior exercised rats. Despite finding no direct effect of 5-FU on left ventricular function, sedentary rats treated with 5-FU presented with a significant increase in aortic pulse wave velocity—a clinical measure of aortic stiffness—over the course of the 2-hour infusion. Importantly, this change in pulse wave velocity was not apparent in either of the saline control groups or the 5-FU group undergoing pretreatment exercise preconditioning.

Reverse phase protein analysis of aortic tissue lysate revealed alterations in proteins involved in focal adhesion and cytoskeletal regulation following 5-FU treatment providing an interesting future direction for exploration of the mechanisms involved in the development of 5-FU induced vascular alterations. Findings from this study provide preclinical support for the use of exercise preconditioning as a potential non-pharmacological modality to prevent the onset of 5-FU cardiotoxicity.

Taken together, findings from the present dissertation offer preclinical insight into potential mechanisms involved in the development of 5-FU cardiotoxicity as well as a modality to prevent its occurrence. We feel these studies provide an important foundation for future work focused on the precise involvement of these pathways in the coronary circulation as well as translation of exercise preconditioning to the clinical setting.

Appendix A - Curriculum vitae

Curriculum Vitae

Stephen T. Hammond, M.S.

Doctoral Student, Kansas State University

Manhattan, KS, USA

Email: sthammond1@k-state.edu

Education

Ph.D. Kansas State University, Kinesiology – Physiology — Aug. 2018 - present

M.S. Eastern Michigan University, Exercise Physiology — December 2017

Thesis Title: An in depth look into the running economy of male and female runners at absolute and relative speeds: Can stance time or angular kinematics explain economy differences between sexes?

GPA: 3.89

B.S. Wingate University, Sports Science – Sport Management — May 2014

Minor: Psychology

GPA: 3.67

Academic and Industry Appointments

Kansas State University — Aug. 2018 – present

College of Health and Human Sciences

Graduate Teaching and Research Assistant – Kinesiology

Appalachian State University — Aug. 2017 – July 2018

North Carolina Research Campus ASU Human Performance Laboratory

Research Technician

STRYD — July 2016 – May 2017

Exercise Physiologist

Eastern Michigan University — Aug. 2014 – 2017

School of Health and Human Performance

Graduate Teaching and Research Assistant – Exercise Physiology

Research Support **Awarded: $27,702**

Extramural Support **Awarded: $6,495**

Kansas Academy of Sciences 2/2021

Graduate Student Research Grant

Title: *Vascular dysfunction in cancer patients receiving 5-Fluorouracil chemotherapy: A role for eNOS?*

Total costs: $1,500

Status: **Awarded**

American College of Sports Medicine 1/2021

Doctoral Student Research Grant

Title: *The efficacy of an acute exercise protocol for alleviation of 5-Fluorouracil chemotherapy induced cardiotoxicity*

Total Costs: $4,995

Status: **Awarded**

National Aeronautics and Space Association 12/2020

HRP Grant Augmentation Proposal

Title: *Sexual dimorphism in the spatial heterogeneity of muscle O_2 transport: Implications for astronaut exercise capacity and EVA performance*

Total Costs: $26,941

Status: Not awarded

Intramural Support **Awarded: $21,207**

Johnson Cancer Research Center Spring 2022

Graduate Cancer Research Award

Title: *5-Fluorouracil cardiotoxicity: Mechanisms and modalities for improved cancer outcomes*

Total costs: $7,500

Status: **Awarded**

Johnson Cancer Research Center 10/2021

Helen L. Graves Heart Research Award

Title: *The intersection of cancer and thromboembolism: A role for eNOS?*

Total costs: $4,722

Status: **Awarded**

Johnson Cancer Research Center Spring 2021

Graduate Cancer Research Award

Title: *Vascular dysfunction in cancer patients receiving 5-Fluorouracil chemotherapy: Implications for cancer-specific outcomes*

Total costs: $5,000

Status: **Awarded**

Johnson Cancer Research Center Spring 2020

Graduate Cancer Research Award

Title: *Understanding 5-Fluorouracil chemotherapy-related toxicity and its potential impact on cancer outcomes*

Total costs: $3,985

Status: **Awarded**

Teaching Experience

Kansas State University

KIN 603: Cardiovascular Physiology – Guest Lecturer – "Coronary Circulation" 12-21-21

KIN 603: Cardiovascular Physiology – Guest Lecturer – "Reactive Hyperemia and Lower Body Negative Pressure" – 10-19-21

KIN 220: Biobehavioral Basis of Physical Activity – Teaching Assistant (Laboratory Lecturer) – (12 sections)

KIN 336: Physiology of Exercise – Teaching Assistant (Laboratory Lecturer) – (3 sections)

KIN 360: Anatomy and Physiology - Teaching Assistant (Laboratory Lecturer) – (5 sections)

KIN 310: Meas. and Res. in Kines. - Teaching Assistant (Laboratory Lecturer) – (1 section)

Eastern Michigan University

SPMD 300: Physiology of Exercise – Teaching Assistant (Laboratory Lecturer) – (6 sections)

SPMD 410: Laboratory Techniques of Human Performance – Teaching Assistant – (3 sections)

SPMD 554: Biomechanics of Performance – Teaching Assistant – (2 sections)

Professional Memberships

Kansas Academy of Science 2021 – present

American Physiological Society 2018 – present

American College of Sports Medicine 2015 – present

North Carolina Alliance for Athletics, Health, Physical Education, Recreation, Dance, and Sport Management 2013 – 2014

Reviewing Activities

Cancer Medicine 2023 –

American Journal of Physiology: Heart and Circulatory Physiology 2023 –

Medicine & Science in Sports & Exercise 2022 –

International Journal of Cardiology 2021 –

Supportive Care in Cancer 2020 –

Awards and Honors

American Physiological Society CV Section *Physiological Reports* Award ($125) 2022

KSU RSCAD Forum Top Research Poster ($200) 2022

KSU GSC Travel Award ($450) 2022

Capitol Graduate Research Summit BioKansas Award Winner ($100) 2021

Kansas State University Research in the State Winner ($250) 2020

KSU Kinesiology Dept. Outstanding Graduate Student Leadership Award 2020

KSU GSC Travel Award ($500) 2021

KSU CHHS Travel Award ($800) 2019 - 2022

KSU GSC Travel Award ($400) 2019

Research featured on WIBW Topeka television station 2019

Eastern Michigan University Exercise Physiology Graduate Student of the Year 2016

Capital One Academic All–America 3rd team 2014

Wingate University Sports Management Outstanding Student Award 2014

United States Track & Field and Cross-Country Coaches Association All-Academic Team – five-time honoree 2011 – 2014

Peer Reviewed Publications * denotes co- first authors

11. *Turpin, VRT., *Lovoy, GM., Parr, SK., Hammond, ST., Post, HK., Caldwell, JT., Banister, HR., Scheurmann, B., Coldburn, TD., and Ade, CJ. (2022). Inorganic Nitrate Supplementation Improves Diastolic Function and the O2 cost of low-intensity exercise in Cancer Survivors treated Anticancer Chemotherapy. *Supportive Care in Cancer*.

10. Ade, CJ., Dockery, L., Holman, LL., Walter, AC., Benbrook, DM., Vesely, SK., **Hammond, ST**., and

Moore, KN. (2022). Prognostic biomarkers of primary cytoreductive surgery complications and delays in adjuvant chemotherapy in older ovarian cancer patients. *Nutrition and Cancer.*

9. Butenas, ALE., Rollins, KS., Parr, SK., Hammond, ST., Ade, CJ., Hageman, KS., Musch, TI., and Copp, SW. (2022). Novel Role for Acid Sensing Ion Channel Subtype 1a in Evoking the Exercise Pressor Reflex in Rats with Heart Failure. *J. Physiol.*

8. Ade, CJ., Turpin, VRG., Parr, SK**., Hammond, ST**., White, ZJ., Weber, RE., Schulze, KM., Colburn, TD., and Poole, DC. (2021). Does Wearing a facemask decrease arterial blood oxygenation and impair exercise tolerance? *Respiratory Physiology and Neurobiology*, *294*, 103765.

7. Butenas, ALE., Rollins, KS., Williams, AC., Parr, SK., **Hammond, ST**., Ade, CJ., Hageman, KS., Musch, TI., and Copp, SW. (2021). Thromboxane A_2 Receptors Contribute to the Exaggerated Pressor Reflex in Male Rats with Heart Failure. *Physiological Reports,9(*18), e15052.

6. Hammer, SM., **Hammond, ST**., Parr, S.K., Alexander, AM., Turpin, VRG., White, ZJ., Didier, KD., Barstow, TJ., Ade, CJ. (2021). Influence of muscular contraction on vascular conductance during exercise above versus below critical power. *Respiratory Physiology and Neurobiology*, 103718.

5. Parr, SK., Steele, CC., **Hammond, ST**., Turpin, VRG., and Ade, CA. Increased Arterial Stiffness as Measured by Peripheral Pulse Pressure is Associated with Increased Risk of All-Cause and Cardiovascular Mortality in Cancer Patients: Data from NHANES III. (2021). *International Journal of Cardiology Hypertension*, *9*, 100085.

4. Banister, HR., **Hammond, ST**., Parr, SK., Turpin, VRG., Treinen, S., Bell, MJ., and Ade, CA. (2021). Lower cutaneous endothelial-dependent microvascular reactivity in adult breast cancer patients receiving radiation therapy. *Cardio-Oncology*, *7*(1), 1-8.

3. Butenas, ALE., Rollins, KS., Williams, AC., Parr, SK., **Hammond, ST**., Ade, CJ., Hageman, KS., Musch, TI., and Copp, SW. (2020). Exaggerated sympathetic and cardiovascular responses to dynamic mechanoreflex activation in rats with heart failure: role of endoperoxide 4 and thromboxane A2 receptors. *Autonomic Neuroscience: Basic and Clinical, 232,* 102784.

2. Butenas, ALE., Rollins, KS., Matney, JE.,Williams, AC., Kleweno, TE., Parr, SK, **Hammond, ST**., Ade, CJ., Hageman, KS., Musch, TI., Copp, SW. (2020). No Effect of Endoperoxide 4 or Thromboxane A2 receptor inhibition on Static Mechanoreflex Activation in Rats with Heart Failure. *Experimental Physiology*, 1-15.

1. Caldwell, JT., Sutterfield, SL., Post, HK., Lovoy, GM., Banister, HR., Turpin, VRG., Colburn, TD., **Hammond, ST.**, Copp, SW., and Ade, CJ. (2020). Impact of high sodium intake on blood pressur e and functional sympatholysis during rhythmic handgrip exercise. *Appl Physiol Nutr Metab* (6), 613-620.

Manuscripts in Preparation or Revi

5. Hammond, ST., Baumfalk, DR., Parr, SK., Butenas, ALE., Behnke, BJ., Hashmi, MH., McGrath, V., Ade, CJ. Impaired Endothelium-Dependent Microvascular Reactivity with 5-Fluorouracil Chemotherapy: A Case for eNOS Dysfunction. *Manuscript in preparation*.

4. Post, HK., Lovoy, GM., Caldwell, JT., **Hammond, ST**., Sutterfield, SL., Banister, HR., and Ade, CJ. Strain rate Imaging Demonstrates Reduced Cardiac Function in Cancer Patients Treated with Androgen

Deprivation Therapy. *Manuscript in preparation*.

3. Ade, CJ., **Hammond, ST**., Bello, NM., Barstow, TJ., Lichar, DE., and Downs, ME. (2022). Development of operational tools for determination of fitness requirements for exploration tasks. *Manuscript in preparation.*

2. White, Z., Parr, SK., **Hammond, ST**., Turpin, VRT., and Ade, CJ. (2022) Central arterial stiffness is associated with cognitive decline and cardiovascular disease manifestation. *Manuscript in preparation*.

1. Turpin, VRG., Parr, SK., **Hammond, ST**., Tickner, P., White, ZJ., Goerl, KV., and Ade, CJ. SARS-CoV-2 cardiac and pulmonary involvement during the convalescent phase of COVID-2019 Infection in competitive student athletes. Manuscript in review at *Physiology Reports*.

Published Abstracts

19. Parr, SK., Scheuermann, BC., **Hammond, ST**., and Ade, CJ. (2023). Non-invasive Aortic Pulse Wave Velocity Is Related To Gold Standard Carotid-femoral Pulse Wave Velocity: Implications For Monitoring Large Artery Stiffness In The Clinic. *Stroke*. (54): ATP99. [Abstract].

18. Scheuermann, BC., Colburn, TD., Parr, SK., Kunkel, ON., **Hammond, ST**., Rosenkranz, SK., and Ade, CJ. (2023). Carotid Distension and Remodeling Is Associated with The Aorta-Carotid Stiffness Gradient. *Stroke*. (54): AWP137-AWP137. [Abstract].

17. Butenas, ALE, Rollins, KS, Williams, AC., Parr, SK., **Hammond, ST**., Ade, CJ., Hagerman, KS., Musch, TI., and Copp, SW. Mechanisms of Mechanoreflex Activation in Rats with Heart Failure: Possible Mechanosensory Role of ASIC1a. *Medicine & Science in Sports & Exercise.* [Abstract].

16. Hammond, ST., Baumfalk, DR., Horn, AG., Kunkel, OK., Parr, SK, Coburn, TD., Schadler, KL., Ade, CJ., Behnke, BJ. (2022). Acute exercise in 5-Fluorouracil cardiotoxicity: Effects on cardiac function and reverse phase protein analysis. *The FASEB Journal.* [Abstract].

15. Baumfalk, DR., **Hammond, ST**., Horn, AG., Kunkel, OK., Parr, SK, Schadler, KL., Ade, CJ., Behnke, BJ. (2022). Effects of Exercise on Aortic Stiffness Associated with 5-Flurouracil in Rats. *The FASEB Journal.* [Abstract].

14. Parr, SK., Smith, JR., **Hammond, ST.,** Sutterfield, SL., and Ade, CJ. (2022). Cutaneous Microvascular Endothelial Function: Effects of Sex and Menopause Stage. *The FASEB Journal.* [Abstract].

13. Butenas, ALE., Parr, SK., **Hammond, ST**., Ade, CJ., Hageman, KS., Much, TI., and Copp, SW. (2022). Protein Kinase C Epsilon Contributes to the Exaggerated Mechanoreflex in Rats with Heart Failure. *The FASEB Journal.* [Abstract].

12. White, ZJ., Parr, SK., Turpin, VRT., **Hammond ST** and Ade, CA**.** Central arterial stiffness is associated with cognitive decline and cardiovascular disease manifestation in cancer survivors in the Framingham Heart Study. *Circulation.* [Abstract].

11. Butenas, ALE., Rollins, KS., Williams, AC., Parr, SK., **Hammond, ST**., Musch, TI., Copp, SW. (2021). The role played by ASIC1a in the Exercise Pressor Reflex in Rats with Heart Failure. *The American Autonomic Society.* [Abstract].

10. Hammond, ST., Parr, SK., Hilgenfeld, EG., Turpin, VRG., White, ZJ., and Ade, CJ. (2021). Cutaneous Microvascular Impairment in 5-Fluorouracil Treated Cancer Patients. *The FASEB Journal.* [Abstract].

9. Parr, SK., **Hammond, ST**., Baumfalk, DR., Kunkel, ON., Behnke, BJ., and Ade, CJ. (2021). 5-Fluorouracil Induces Vascular Calcification in Rat Aortic Smooth Muscle Cells. *The FASEB Journal.* [Abstract].

8. Butenas, ALE., Rollins, KS., Williams, AC., **Hammond, ST**., Musch, TI., Copp, SW. (2021). Thromboxane A_2 Receptors Contribute to the Exaggerated Exercise Pressor Reflex in Rats with Heart Failure. *The FASEB Journal.* [Abstract].

7. Hammond, ST., Parr, SK., Hilgenfeld, EG., Turpin, VRG., and Ade, CJ. (2020). Microvascular responses following 5-Fluorouracil chemotherapy administration. *The FASEB Journal*. [Abstract].

6. Parr, S.K., **Hammond, ST.**, Baumfalk, DR., Kunkel, ON., Behnke, BJ., and Ade, CJ. (2020). Protein Kinase C activity is increased in human coronary smooth muscle cells following exposure to 5-Fluorouracil chemotherapy. *The FASEB Journal*. [Abstract].

5. Turpin, V.R.G., Parr, S.K., **Hammond, ST.**, Ade, CJ. (2020). Therapeutic Role of Dietary Nitrates on Cardiorespiratory Function in Cancer Survivors. *The FASEB Journal*. [Abstract].

4. Hammond, ST., Caldwell, J.T., Sutterfield, S.L., Post, H.K., Lovoy, GM., Banister, HR., Turpin, VRG., Colburn, TD., Copp, SW., and Ade, CJ. (2019). Dietary salt intake exaggerates arterial blood pressure during exercise in healthy normotensive adults. *The FASEB Journal*. [Abstract].

3. Banister, H.R., Sutterfield, S.L., Turpin, V.R.G., Parr, S.K., **Hammond, ST**., Ade, C.J. (2019). Effects of radiation on cutaneous microvascular function in the intact human circulation. *The FASEB Journal*. [Abstract].

2. Hammond, ST., Lindsay, T.R., and McGregor, S.J. (2018). Does stance time predict running economy at relative speeds in highly trained distance runners? *American College of Sports Medicine.* [Abstract].

1. Hammond, ST., McGregor, S.J., and Lindsay, T. (2015). Differences in acceleration, stride lengths, and stance time between trained and untrained low BMI individuals. *American College of Sports Medicine.* [Abstract].

Oral Presentations

9. Kansas State University Cancer Fighters, Manhattan, KS (Virtual), 30 March 2023. "From clinic to culture: Improving our understanding of cancer associated cardiotoxicity"

8. Medical College of Wisconsin Cardiovascular Center ATVB Seminar Series, Milwaukee, WI, 6 June 2022. "5-Fluorouracil Cardiotoxicity: From Clinic to Culture"

7. Experimental Biology Annual Meeting, Exercise and Cancer Care: From the Bench to the Clinic Symposium, Philadelphia, PA, 5 April 2022. "Acute exercise in 5-Fluorouracil cardiotoxicity: Effects on cardiac function and reverse phase protein analysis."

6. Kansas Academy of Sciences Annual Meeting, Sterling College, 2 April 2022. "The role of exercise in prevention of 5-Fluorouracil chemotherapy induced cardiotoxicity."

5. Capitol Graduate Research Summit, Topeka, KS (Virtual), 2 February 2021. "Skin blood vessel responses following 5-Fluorouracil chemotherapy administration."

4. Research and the State Competition, Kansas State University (Virtual), 23 October 2020. "Skin blood vessel responses following 5-Fluorouracil chemotherapy administration."

3. American College of Sports Medicine - Michigan Chapter Annual Meeting, Gaylord, MI, February 2017. "The effect of select gait variables and axial accelerations on the running economy of highly trained athletes."

2. American College of Sports Medicine - Michigan Chapter Annual Meeting, Gaylord, MI, February 2016. "Validity of an approach using two defined – distance running trials for determination of critical speed."

1. American College of Sports Medicine - Michigan Chapter Annual Meeting, Gaylord, MI, February 2015. "Differences in acceleration, stride lengths, and stance time between trained and untrained low BMI individuals."